Characterisation of glutamate-gated chloride channel receptors in the parasitic nematode haemonchus contortus

Cheeseman, Catherine Louise

Award date:
2001

Awarding institution:
University of Bath

CHARACTERISATION OF GLUTAMATE-GATED CHLORIDE CHANNEL RECEPTORS IN THE PARASITIC NEMATODE *HAEMONCHUS CONTORTUS*

submitted by Catherine Louise Cheeseman

for the degree of PhD

of the University of Bath

2001

ProQuest LLC
789 East Eisenhower Parkway
P.O. Box 1346
Ann Arbor, MI 48106-1346

"Well in our country," said Alice, still panting a little, "you'd generally get to somewhere else – if you ran very fast for a long time, as we've been doing."
"A slow sort of country!" said the Queen. "Now, *here*, you see, it takes all the running *you* can do, to keep in the same place. If you want to get somewhere else, you must run at least twice as fast as that!"

Through the Looking Glass and What Alice Found There
Lewis Carroll, 1871

Summary

The avermectin and milbemycin (AM) class of anthelmintics constitutes a significant part of the anthelmintic market and experiments on model organisms (*Caenorhabditis elegans*) suggest that they exert their nematocidal effect by irreversibly binding to, and opening, glutamate-gated chloride channels (GluCl). Prior to this study, three genes encoding four GluCl subunits, with high levels of identity to their *C.elegans* orthologues, had been identified from the parasitic nematode *Haemonchus contortus.* Only two full-length cDNAs were available, however, and there had been no published tests of the ability of the AM to interact with recombinant GluCl from parasites. The aim of this thesis was to further the understanding of *H.contortus* GluCl receptors by cloning additional subunits and studying their pharmacology in a mammalian expression system.

Northern blot analysis was used in this investigation to confirm that the GluCl subunits HG2 and HG3 are the product of an alternatively spliced gene and are expressed at similar levels in *H.contortus* eggs. RT-PCR was employed to amplify full-length HG2 and HG5 cDNAs from *H.contortus* eggs. HG5 cDNA was also amplified from ivermectin-resistant adult *H.contortus* and a comparison with wild-type indicated no coding differences.

Gene transfer into mammalian cells was selected as a tool to analyse the expression of the GluCl subunits *in vitro.* The production of stable cell lines expressing either HG3 or HG4 polypeptides was attempted. The transcription of the GluCl subunit RNA was apparent, but protein was not detected. Each of the four *H.contortus* GluCl subunits was therefore transiently expressed in COS-7 cells. As predicted by functional data from the *C.elegans* orthologues, the HG2 and HG4 subunits failed to bind [^{3}H] ivermectin. The HG3 and HG5 subunits bound [^{3}H] ivermectin with high affinity; the K_ds were 70 +/- 16 pM and 26 +/- 12 pM respectively. A variety of avermectin derivatives competed for the ivermectin-binding site with differing affinities, but none was as effective as ivermectin. No interaction was seen between GABA, glutamate, fipronil or picrotoxin and [^{3}H] ivermectin binding. The affinity of [^{3}H] ivermectin binding to *H.contortus* L3 larval membrane preparations was re-examined and found to be 70 +/- 7 pM.

The ivermectin-binding capacity of the GluCl subunits appears to be conserved across species, however the repertoire and relative importance of those subunits may vary. It is probable that the native receptor is heteromeric; this is supported by recent localisation studies, and co-expression of subunits may result in different pharmacology.

Contents

1 Introduction 1

1.1 Phylum Nematoda 1

1.1.1 Anatomy 1

1.1.2 Classification 3

1.1.3 Caenorhabditis elegans 6

1.1.4 Parasitic nematodes 7

1.1.4.1 Animal parasites 7

1.1.4.1.1 *Haemonchus contortus* 9

1.2 Control of parasitic nematodes 11

1.2.1 Biological control 11

1.2.2 Vaccines 12

1.2.3 Chemical control 14

1.2.3.1 Benzamidazoles 15

1.2.3.2 Piperazine 16

1.2.3.3 Imidathiazoles and tetrahydropyrimidines 17

1.2.3.4 Avermectins and milbemycins 19

1.2.4 Anthelmintic resistance 25

1.3 Neurobiology 29

1.3.1 The anatomy of the nervous system 29

1.3.2 Neurotransmission 31

1.3.2.1 GABA 31

1.3.2.2 Acetylcholine 32

1.3.2.3 Glutamic acid 33

1.3.3 Neurotransmitter receptors 34

1.3.3.1 Vertebrate ligand-gated ion channels 34

1.3.3.2 Nematode ligand-gated ion channels 36

1.3.3.2.1 GABA receptor 37

1.3.3.2.2 Nicotinic acetylcholine receptor 38

1.3.3.2.3 Glutamate-gated chloride channel receptor 40

1.4 Aims of this research 44

2 Materials and Methods 46

2.1 General materials 46

2.1.1 Molecular biology reagents 46
2.1.1.1 Enzymes 46
2.1.2 General buffer compositions 47
2.1.3 Microbiological reagents 47
2.1.3.1 Bacterial culture media....47
2.1.3.2 Bacterial strains and plasmids 48
2.1.4 Cell culture reagents 48
2.1.5 Immunocytochemistry reagents 48
2.1.6 Radioligand binding....49
2.1.7 Western blotting and immunodetection....49
2.2 Methods 49
2.2.1 General molecular biology methods....49
2.2.1.1 Agarose gel electrophoresis....49
2.2.1.2 Purification of DNA from agarose gels 50
2.2.1.3 Restriction endonuclease digestion of DNA....50
2.2.1.4 Phenol/chloroform extraction and ethanol precipitation of DNA 50
2.2.1.5 Ligation of DNA....51
2.2.1.6 Preparation of *E.coli* competent cells....51
2.2.1.7 Transformation of competent cells 51
2.2.1.8 Small scale preparation of plasmid DNA....51
2.2.1.9 Large-scale plasmid preparations using the Qiagen Plasmid Maxikit....52
2.2.2 Production of mRNA from *Haemonchus contortus* 53
2.2.2.1 Isolation and purification of *H.contortus* eggs 53
2.2.2.2 Isolation of adult *H.contortus*....54
2.2.2.3 Isolation of total RNA from *H.contortus* adults and eggs....54
2.2.2.4 Quantitation of RNA solutions 56
2.2.2.5 Purification of mRNA....56
2.2.3 Northern blot analysis 57
2.2.3.1 Labelling RNA with Digoxigenin (DIG) labeled UTP mix 58
2.2.3.1.1 Estimation of yield of DIG-labelled RNA....59
2.2.3.2 Denaturing formaldehyde gel electrophoresis....60
2.2.3.3 Northern transfer 60

2.2.3.4 Hybridisation and detection of Northern blot 60
2.2.4 Amplification of cDNA 61
2.2.4.1 Oligonucleotide production.....61
2.2.4.2 Reverse transcription polymerase chain reaction.....62
2.2.4.2.1 Titan™ RT-PCR system 62
2.2.4.2.2 Access RT-PCR system.....63
2.2.4.3 Blunt-ending PCR products.....63
2.2.5 Cloning of PCR products.....64
2.2.5.1 Sequencing of clones.....64
2.2.6 Cell culture methods 65
2.2.6.1 Maintenance of L929 mouse fibroblast cells and COS 7 primate kidney fibroblast cells.....65
2.2.6.1.1 Preparation of cells for storage in liquid nitrogen 65
2.2.6.1.2 Re-establishment of frozen cells 65
2.2.6.2 Establishment of stable cell lines 65
2.2.6.2.1 Optimisation of G418 selection 65
2.2.6.2.2 Transfection of L929 mouse fibroblast cells.....65
2.2.6.2.3 Isolation of total RNA from cultured cells 66
2.2.6.2.4 Transcription of cRNA.....67
2.2.6.3 Transient expression in COS 7 cells 67
2.2.6.3.1 Transfection of COS 7 cells.....67
2.2.7 Immunofluorescence.....68
2.2.8 Membrane preparation.....68
2.2.8.1 Preparation of membranes from cultured cells.....68
2.2.8.2 Membrane preparations from *H.contortus* L3-stage larvae....69
2.2.8.3 Quantitation of protein in membrane preparations 69
2.2.9 Radioligand binding.....70
2.2.9.1 Binding of [^{3}H] ivermectin to membrane preparations 70
2.2.9.2 Radioligand binding data analysis.....70
2.2.10 Protein analysis.....71
2.2.10.1 SDS-Polyacrylamide gel electrophoresis 71
2.2.10.1.1 Western blotting and immunodetection 72
2.2.10.1.1.1 Electrophoretic transfer to nitrocellulose 72

2.2.10.1.1.2 Immunoprobing and detection 73
3 Molecular analysis of *Haemonchus contortus* Glutamate-gated Chloride Channels 74
3.1 Results 75
3.1.1 Expression of HG2 and HG3 mRNA in *H.contortus* eggs 75
3.1.1.1 Northern blot probe design and production 76
3.1.1.2 *H.contortus* Northern Blot 78
3.1.2 Amplification and cloning of HG2 cDNA 80
3.1.2.1 HG2 cDNA amplification 80
3.2.2.2 Cloning and sequence analysis of HG2 cDNA 81
3.1.3 Amplification and cloning of HG5 cDNA 84
3.1.3.1 HG5 cDNA amplification 84
3.1.3.2 Cloning and sequence analysis of HG5 cDNA 85
3.1.4 Amplification and cloning of HG5 cDNA from ivermectin resistant H.contortus 88
3.1.4.1 Amplification of HG5 cDNA from ivermectin-resistant *H.contortus* 88
3.1.4.2 Cloning and sequence analysis of HG5 from ivermectin-resistant *H.contortus* adults 91
3.2 Discussion 93
4 Stable expression of inhibitory glutamate receptor subunits in a mammalian cell line 99
4.1 Results 100
4.1.1 Attempted construction of an HG3 cell line 100
4.1.1.1 Sub-cloning HG3 for expression in mammalian cells 100
4.1.1.2 Sensitivity of L929 mouse fibroblast cells to the antibiotic G418 102
4.1.1.3 Transfection and selection of L929 cells 103
4.1.2 Analysis of HG3 transformed L929 cells 103
4.1.2.1 RT-PCR amplification of partial HG3 cDNA 103
4.1.2.2 Investigation of HG3 protein expression in transformed L929 cells 105
4.1.2.2.1 Radioligand binding 105
4.1.2.2.2 Western blotting 106

4.1.3 Attempted construction of an HG4 cell line 106
4.1.4 Analysis of HG4 transformed L929 cells 106
4.1.4.1 RT-PCR amplification of partial HG4 cDNA 106
4.1.4.2 Investigation of HG4 protein expression in transformed L929 cells 107
4.2 Discussion 108
5 Pharmacology of glutamate-gated chloride channels 110
5.1 Results 111
5.1.1 Transient expression and analysis of HG2 in COS 7 cells 111
5.1.1.1 Subcloning HG2 cDNA for expression in mammalian cells 111
5.1.1.2 Transfection and harvesting of COS 7 cells 113
5.1.1.3 Analysis of expressed protein 113
5.1.1.3.1 Radioligand binding 113
5.1.1.3.2 Western Blotting 113
5.1.2 Transient expression and analysis of HG3 in COS 7 cells 114
5.1.2.1 Radioligand binding 114
5.1.2.1.1 Saturation and competition analysis of [^{3}H] ivermectin binding 115
5.1.2.1.2 Pharmacology of [^{3}H] ivermectin binding 117
5.1.3 Transient expression and analysis of HG4 in COS 7 cells 119
5.1.3.1 Analysis of expressed protein 119
5.1.3.1.1 Radioligand binding 119
5.1.3.1.2 Immunofluorescence microscopy 119
5.1.4 Transient expression and analysis of HG5 in COS 7 cells 120
5.1.4.1 Subcloning HG5 cDNA for expression in mammalian cells 120
5.1.4.2 Radioligand binding 122
5.1.4.2.1 Saturation and competition analysis of [^{3}H] ivermectin binding 123
5.1.4.2.2 Pharmacology of the recombinant HG5 ivermectin-binding site 125
5.1.5 Ivermectin binding to *H.contortus* membranes 126
5.2 Discussion 128
6 Conclusions 135
7 References 137

Appendices I
Acknowledgements VII
Abbreviations VIII
Publications X

List of Figures

Figure 1 Schematic diagram of general nematode morphology.....2
Figure 2a A cladogram representing the "traditional" nematode classification4
Figure 2b Phylogenetic classification of Nematoda.....5
Figure 3 *H.contortus* attached to host abomasums.....9
Figure 4 Life cycle of the sheep parasite *Haemonchus contortus*.....10
Figure 5 The chemical structures of commonly used benzamidazoles.....15
Figure 6 The chemical structure of piperazine.....17
Figure 7 The chemical structures of some nicotinic anthelmintics.....18
Figure 8 Structure of some of the avermectins and milbemycins.....20
Figure 9 The *Ascaris* nervous system.....30
Figure 10 Model of a cys-loop ligand-gated ion channel.....35
Figure 11 The *unc-49* gene arrangement.....37
Figure 12 Alternative splicing of *gbr-2*.....43
Figure 13 Isolation apparatus for *H.contortus* adults.....55
Figure 14 *gbr-2* probe design.....76
Figure 15 Restriction endonuclease digestion of HG3 intracellular loop from pCRBlunt.....77
Figure 16 Spot test to estimate the concentration of the HG3 RNA probe....77
Figure 17 *H.contortus* egg RNA.....78
Figure 18 Ethidium bromide stained total RNA following denaturing 0.7% (w/v) agarose formaldehyde gel electrophoresis.....79
Figure 19 Northern blot analysis of *H.contortus* gbr2 mRNAs.....79
Figure 20 Schematic of primer design strategy for amplification of full length HG2 cDNA.....80
Figure 21 Amplification of full length HG2 cDNA from *H.contortus* eggs' mRNA.....81
Figure 22 Restriction endonuclease digestion of recombinant pCRBlunt.....82
Figure 23 Alignment of RT-PCR amplified HG2 clones.....82
Figure 24 Alignment of the HG2 amino acid sequence available on the EMBL database (accession number Y14233) and RT-PCR amplified HG2.....83

Figure 25 Amplification of HG5 full length cDNA from *H.contortus* eggs' mRNA 85
Figure 26 Analysis of recombinant pCRBlunt by restriction endonuclease digestion 85
Figure 27 Alignment of HG5 cDNA amplified by RT-PCR 86
Figure 28 Alignment of available HG5 (Hcgluclα) amino acid sequences 88
Figure 29 Total RNA extracted from IVR *H.contortus* eggs 89
Figure 30 Amplification of HG5 from IVR *H.contortus* adults 89
Figure 31 Amplification of HG5 from IVR *H.contortus* adults 90
Figure 32 Restriction endonuclease digestion of recombinant pCRBlunt 91
Figure 33 Alignment of HG5 clones amplified from IVR adult *H.contortus* 92
Figure 34 Alignment of consensus HG5 sequences from IVS and IVR *H.contortus* 93
Figure 35 Restriction endonuclease digestion of recombinant pBluescript II 101
Figure 36 Analysis of recombinant pcDNA3 by restriction digestion 101
Figure 37 Sensitivity of L929 cells to the antibiotic G418 102
Figure 38 Total RNA from transformed L929 clones 103
Figure 39 RT-PCR amplification of partial HG3 cDNA from transfected L929 cells 104
Figure 40 Western blot analysis of transformed L929 cell membranes 106
Figure 41 RT-PCR amplification of partial HG4 cDNA from transformed L929 cells 107
Figure 42 Restriction endonuclease digestion of recombinant pCRBlunt ... 112
Figure 44 Western blot analysis of HG2 transfected COS 7 cell membranes 114
Figure 45 [^{3}H] ivermectin binding to membrane preparations from COS 7 cells transiently expressing HG3 115
Figure 46 Saturation of membranes from COS 7 cells transiently expressing HG3 with [^{3}H] ivermectin 116
Figure 47 Competition between [^{3}H] ivermectin and unlabelled ivermectin for their binding sites on membranes from COS 7 cells transiently expressing HG3 117

Figure 48 Competition for [^{3}H] ivermectin binding by different avermectins 118
Figure 49 Expression of epitope-tagged HG4 in COS 7 cells 120
Figure 50 Removal of HG5 cDNA from the plasmid pCRBlunt 121
Figure 51 Restriction endonuclease digestion of recombinant pcDNA3 121
Figure 52 [^{3}H] ivermectin binding to membrane preparations from COS 7 cells transiently expressing HG5 123
Figure 53 Saturation of membranes from COS 7 cells transiently expressing HG5 with [^{3}H] ivermectin 124
Figure 54 Competition between [^{3}H] ivermectin and unlabelled ivermectin for their binding sites on membranes from COS 7 cells transiently expressing HG5 124
Figure 55 Competition for [^{3}H] ivermectin binding by different avermectins 125
Figure 56 Saturation curve of [^{3}H] ivermectin binding to P2 membranes from *H.contortus* L3 stage larvae 127

List of Tables

Table 1 Affinity of various avermectins for the ivermectin-binding site of recombinant HG3 as measured by competition with [^{3}H] ivermectin.....118
Table 2 Affinity of various avermectins for the ivermectin-binding site of recombinant HG5 as measured by competition with [^{3}H] ivermectin.....126
Table 3 [^{3}H] ivermectin binding to recombinant GluCl subunits and *H.contortus* L3 larvae 127
Table 4 Pharmacology of *C.elegans* and *H.contortus* GluCl subunits 131

1. Introduction

1.1 Phylum Nematoda

The name "Nematoda" originates from the Greek nema (thread) eidos (form) and the members of this phylum are one of the most successful groups of animals. There are over twenty thousand documented nematode species, the actual number is estimated to be over 40,000 (Blaxter 1998a), living in a diverse range of habitats including the sea, fresh-water and soil and as very successful parasites of plants and animals. Almost all are unsegmented, spindle-shaped, roundworms with bilateral symmetry, but their life-cycles vary enormously; ranging from very simple and direct to extremely complicated with the utilisation of a number of hosts (Whitfield, 1993). Most share a highly conserved developmental sequence, however, involving dioecious adults, although some are hermaphrodite, producing fertile eggs which hatch to L1 larvae. These then develop through three more larval stages before sexual maturity is reached. Between larval stages, the juvenile sheds its cuticle and there is an increase in body size. Under conditions of reduced food, an additional stage, the non-developing dauer, is formed at the second larval moult. The dauer larvae store food reserves and can survive adverse conditions for many months. When food becomes available, they moult to normal L4 larvae.

1.1.1 Anatomy

Nematodes share a common anatomical structure (figure 1) of two concentric tubes, the body wall and the gut, separated by the pseudocoelom. The body wall is composed of the cuticle, hypodermis and musculature. The multi-layer, non-cellular cuticle covers the body and is overlaid with a carbohydrate-rich surface coat that may be important in evasion of the host immune response in parasitic species. Surface invaginations of the body wall are also lined with cuticle (Whitfield, 1993). The somatic musculature is similar in structure to vertebrate striated muscle and insect flight muscle, A H and I bands are present and Z are absent, but the rows of filaments are

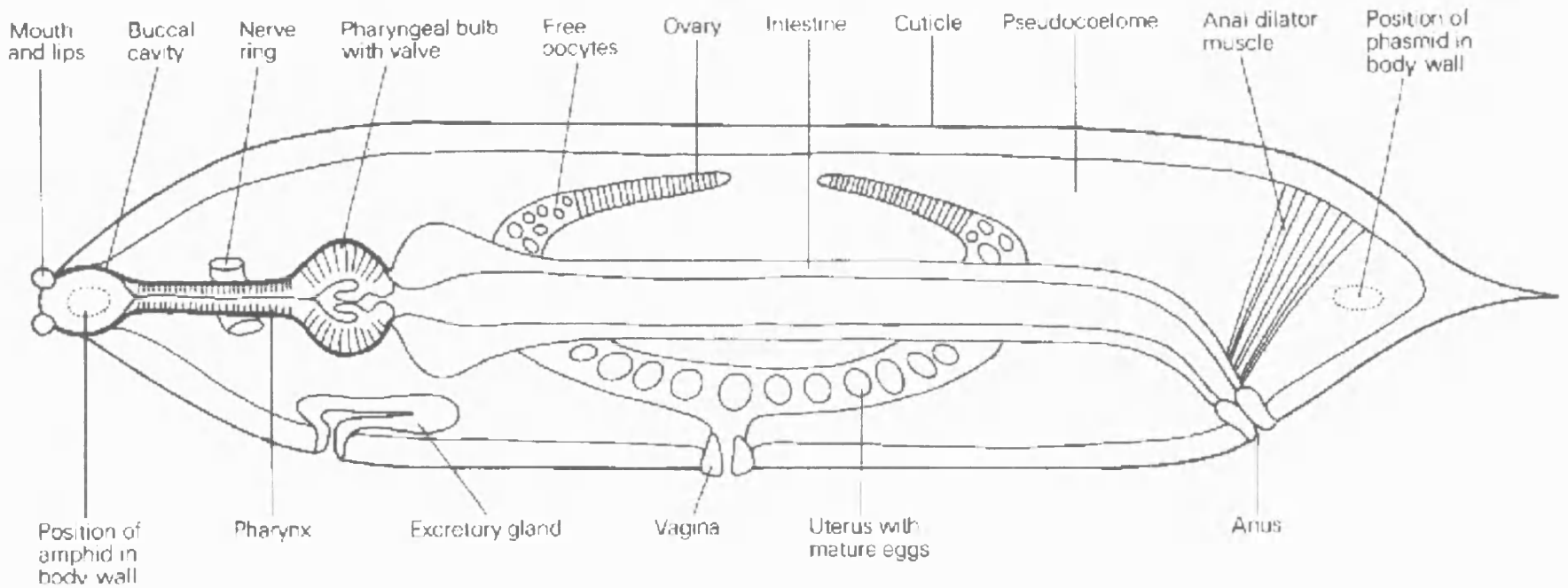

Figure 1 Schematic diagram of general nematode morphology (Whitfield, 1993).

offset. The neuromuscular processes are unlike those found in other animals, in that they run from muscles to nerves. The body wall encloses a fluid-filled cavity, the pseudocoelom, and these act together as an hydrostatic skeleton. The musculature is composed only of longitudinal strands and therefore movement is achieved by a co-ordinated sinusoidal wave of muscular contraction operating against internal hydrostatic pressure. Contraction is in the dorso-ventral plane and each muscle is connected only to its own nerve cord, i.e. dorsal muscle synapses with dorsal nerve cord, allowing contraction of one muscle while the other relaxes (Chappell, 1993; Martin *et al.,* 1996). Nematodes have a complete digestive system with an anterior mouth and an anus near the posterior tip. The buccal cavity is between the mouth and pharynx and is very variable between species and an important taxonomic tool. Pharynxes also vary considerably between orders and species and this can largely be correlated with feeding habits. The pharynx is a pumping organ that sucks food into the alimentary canal and forces it into the intestine. This highly muscular, cuticle-lined device is cylindrical with one or more enlargements (bulbs). Rapid contraction of the buccal muscle and anterior pharyngeal muscle causes the mouth to open and dilates the anterior of the pharynx, sucking in food. The high hydrostatic pressure in the pseudocoel closes the mouth and oesophageal lumen when the muscles relax. Food passes down the pharynx by waves of muscle contraction extending towards the posterior of the worm until the intestine is reached. The intestine extends from the pharynx to the rectum. It is non-muscular and food is pushed towards the rectum as the pharynx pumps in more food. When the anus opens, hydrostatic pressure causes defecation.

1.1.2 Classification

The most frequently used system of classification of nematodes is based on morphological traits such as structure of the pharynx or host specificity. Figure 2a indicates the traditional division of the phylum into two classes, Secernentea and Adenophorea based on the presence or absence of causal sense glands (Dorris *et al.*, 1999). However, as phasmids are often difficult to detect this division is not entirely satisfactory.

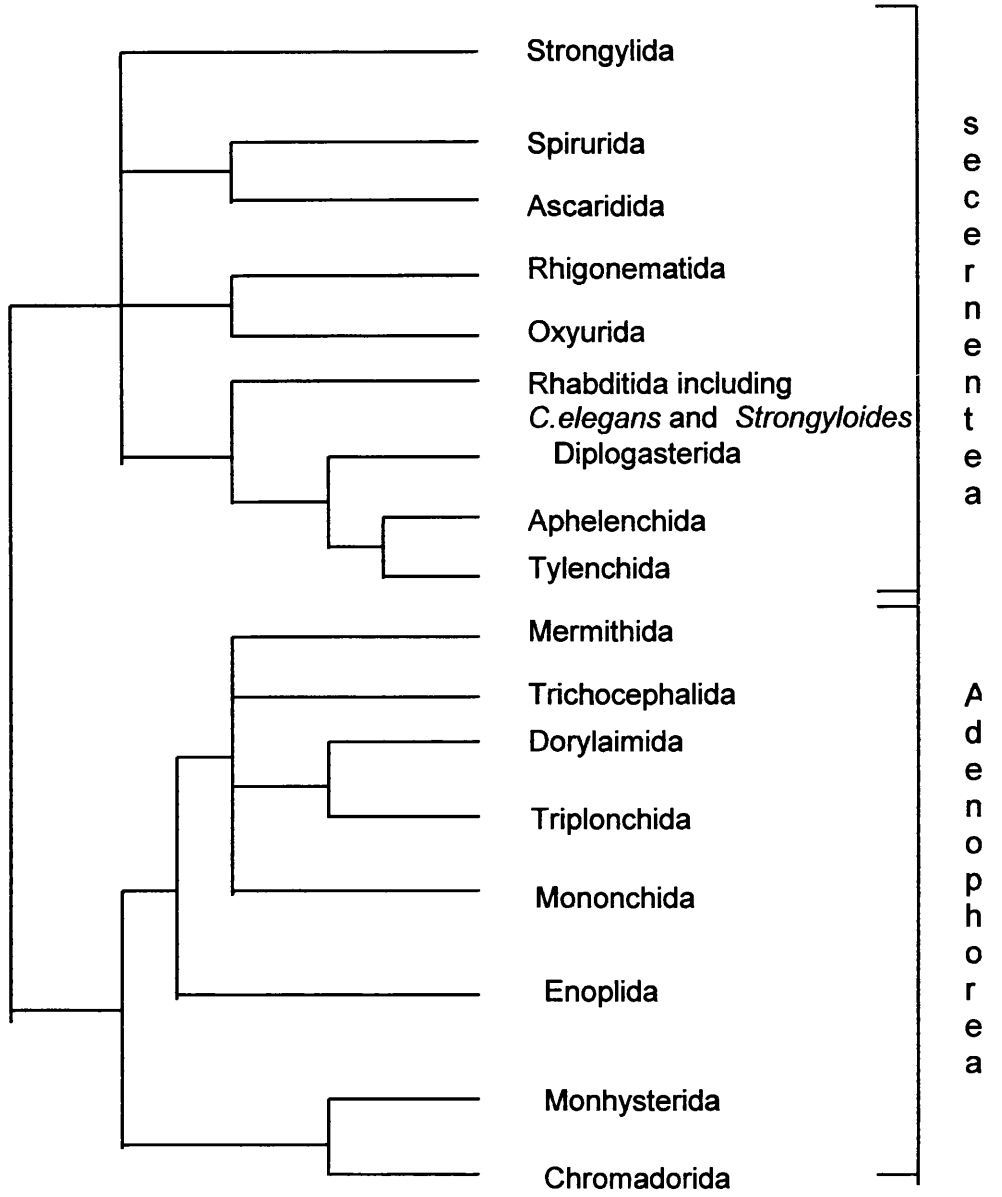

Figure 2a A cladogram representing the "traditional" nematode classification. Species are divided into two classes, Secernentea and Adenophorea, depending on the presence or absence of phasmids. From Dorris *et al.*, 1999.

Advances in molecular techniques have allowed an alternative method of classification to evolve. This phylogenetic analysis questions the original classification system, as the Secernentea appear to have evolved from

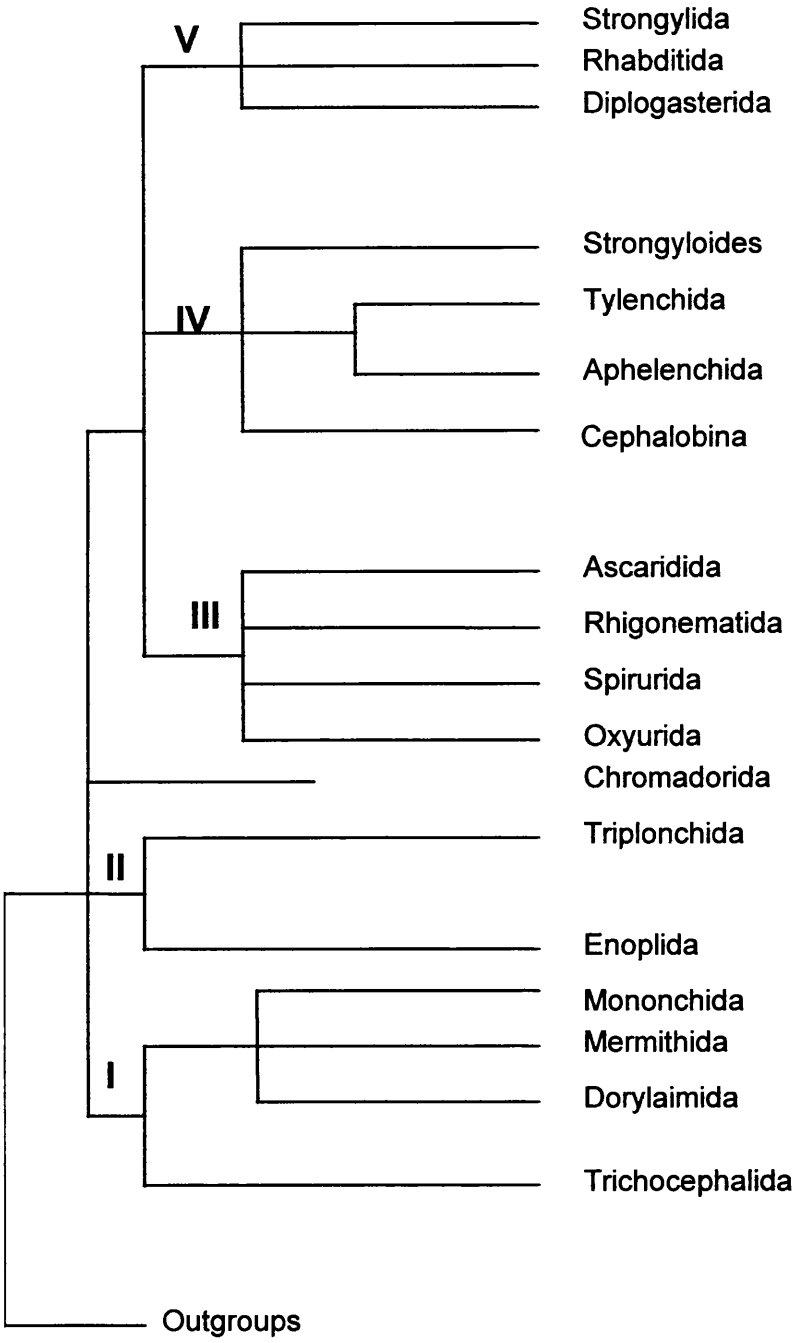

Figure 2b Phylogenetic classification of Nematoda. Five major clades are identified (I-V) by analysis of small subunit rRNA or rDNA. Adapted from Blaxter, 1998.

Adenophorea (figure 2b). Blaxter *et al.* (1998) discuss phylogenetic characterisation using small subunit rRNA and small subunit rDNA. Molecular phylogenic analysis allows the comparison of all taxa with a single defined measurement and is claimed to be a more "natural" classification system (Dorris *et al.*, 1999; Blaxter *et al.,* 1998). Although there are a number of similarities shown by the two classification systems, significant differences are also seen. Due to constraints of culturing parasitic species, free-living counterparts are often used for initial characterisation. The choice of classification method may therefore dictate how indicative the model will be of the parasitic species (Nielsen, 1998). For example, when using the original, morphological method of classification, the free-living nematode *Caenorhabditis elegans* appeared closely related to *Strongyloides sp.,* but when the phylogenetic method was used it was apparent that *Panagrellus sp.* might be a better comparative model for the order Strongyloides. *C.elegans* was most closely related to the order Strongylida. Expressed sequence tags (EST) projects on a number of nematode species will allow further investigation into the molecular evolution of nematodes.

1.1.3 *Caenorhabditis elegans*

The free-living soil nematode *C.elegans* has been used as a model system in research for many years. This small nematode (1.5 mm long) can easily be maintained in the laboratory as thousands of animals can be grown on a single petri dish seeded with a lawn of *E.coli* and incubated at 20°C (Riddle *et al.*, 1997; Hope, 1999). The life cycle is rapid, approximately 3.5 days from egg to adult, and 300-350 progeny are produced by a single individual. The presence of male and hermaphrodite worms allows both inbreeding and cross-fertilisation of strains, offering workers an excellent tool for genetic studies. The life cycle is broadly similar to all nematodes including fertile eggs, four larval stages and adults.

Transformation, reverse-genetic and laser ablation technologies are well developed and have extended the usefulness of this model. The production of *C.elegans* mutant strains has introduced functionality into our knowledge of this nematode and the complete sequencing and physical mapping of the

C.elegans genome initiated projects to generate a mutant strain for each gene identified (Hope, 1999). As *C.elegans* can be viably stored for many years, a bank of mutants will be readily available for all workers. Analysis of gene function has recently progressed due to the discovery of RNA-mediated interference (RNAi) (Kuwabara and Coulson, 2000). This technique involves the disruption of a *C.elegans* gene by injecting sequence-specific double-stranded RNA into germline syncytium; soaking worms in dsRNA or feeding with *E.coli* expressing *C.elegans* dsRNA also results in RNAi. The injected animal and their offspring express the mutant phenotype, although this does not transfer to subsequent generations, allowing easy investigation of loss-of-function phenotypes and a novel tool for drug or vaccine target candidates.

1.1.4 Parasitic nematodes

Nematodes are serious pathogens of plants, humans and animals. Plant parasites cause damage to flowers, roots, stems and leaves and cause estimated losses of US$100 billion to agriculture worldwide (Lilley *et al.*, 1999). Human parasites cause a horrific number of diseases resulting in serious pathologies and contributing a great deal to the death toll of developing countries. Animal parasites are responsible for vast losses to the agricultural economy, through both production losses and control, and also infect companion animals. Zoonotic infections, whereby parasites are passed between vertebrate animals and man, can also result in pathology.

1.1.4.1 Animal parasites

The large intestinal roundworm *Ascaris suum* (15-40 cm long) is the causative agent of ascariasis in pigs and is closely related to the human nematode species *Ascaris lumbricoides*. The parasite has a direct life cycle with infection due to ingestion of fertilised eggs through contaminated food or drink (Whitfield, 1993; Smyth, 1994). The larvae hatch in the intestine and penetrate the intestinal wall before travelling to the liver, heart, lung, trachea, and larynx before returning to the small intestine where they develop into adults. The female can lay 200 to 200,000 eggs per day, which are released in the faeces and can survive up to 7 years. The main pathology is caused

by the adult worms and consists of diarrhoea, fever, malnutrition and intestinal obstruction. Migration of juveniles through the lung can cause allergic broncho-pneumonia in previously infected individuals. The large size and relative abundance of this parasite has allowed characterisation of its structure and physiology (Brownlee *et al.,* 2000). Much of the information regarding nematode neurobiology originated from *Ascaris* (Section 1.3).

The filarial worm *Dirofilaria immitis* occurs in carnivores in the chambers of the right side of the heart and adjacent blood vessels, including the pulmonary artery (Smyth, 1994). Microfilariae are carried from the heart, through the lungs, the left side of the heart and into the systemic circulation from where they are ingested by mosquitos during a blood meal. Juveniles moult and develop in the mosquito and infective L3-stage larvae migrate to the mouthparts of the host and infect their vertebrate host when the mosquito feeds. Juveniles spend about 80 days in the subcutaneous tissues and muscles before entering the heart as fourth-stage larvae. Pathogenicity is positively correlated with worm burden. Up to 60 worms cause circulatory problems and over 100 worms cause blockage of the right side of the heart and the pulmonary artery causing systemic degeneration. Zoonosis can occur if infected mosquitos feed on humans.

Members of the Family Tristrongylidae are parasites of the small intestine of vertebrates and a major agricultural problem. As several species have similar life cycles, a host can be infected with large numbers of multiple species, giving rise to severe pathologies and even death. In 1994, it was estimated that sheep roundworms cost the Australian grazing industry $222 million in production losses, including meat loss, wool loss and mortality (McLeod, 1995). This family includes the blood-feeding parasites of ruminants *Haemonchus contortus* and *Ostertagia spp. Ostertagia* are small reddish-brown worms found in the abomasum of ruminants in temperate climates. The life cycle is similar to *H. contortus* (section 1.1.5) but the L3 burrows into the gastric glands where it moults into immature adults before emerging and maturing to adult on the mucosal surface. A number of Tristrongylid nematodes exhibit "arrested development" whereby the life cycle is halted at

one or more stages if conditions are not optimal. The developmental cycle is completed when optimal conditions are perceived.

1.1.5 *Haemonchus contortus*

H.contortus is a haematophagous tristrongylid that lives in the abomasum of sheep and other ruminants (Smyth, 1994) (Figure 3). Sexual dimorphism is seen and the white ovaries of the large female wrap around her red intestine (due to blood-feeding) leading to a striped appearance and the common name of "barbers pole worm".

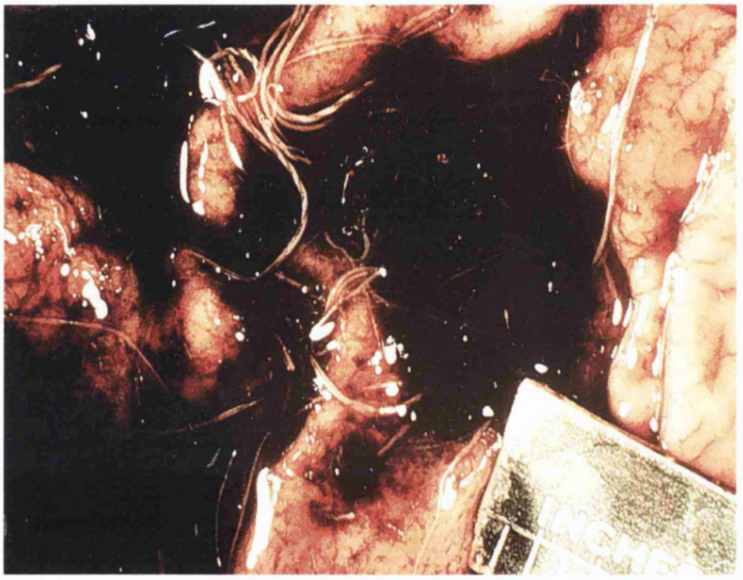

Figure 3 *H.contortus* attached to host abomasum. The female worm can be identified by her striped appearance.

This species infects sheep, goats, cattle and wild ruminants and costs the grazing industry millions of dollars per annum in production losses and treatment (McLeod, 1995). Adults live buried in the host abomasum and feed on blood; a single worm is thought to consume approximately 15 μl of blood per day. Each host may be infected with thousands of worms and medium infections cause anaemia and loss of condition whereas heavy infections can cause death. Lambs are particularly susceptible to infection, while animals over 6 months tend to develop an acquired immunity to *H.contortus*. A phenomenon known as "self cure" is often seen in endemic areas whereby

sheep develop an egg producing infection, but periodically expel adult worms.

Female *H.contortus* are prolific egg producers, with estimates of moderate infections resulting in ten million eggs released per day, and these fertile eggs are expelled in the host's faeces (figure 4).

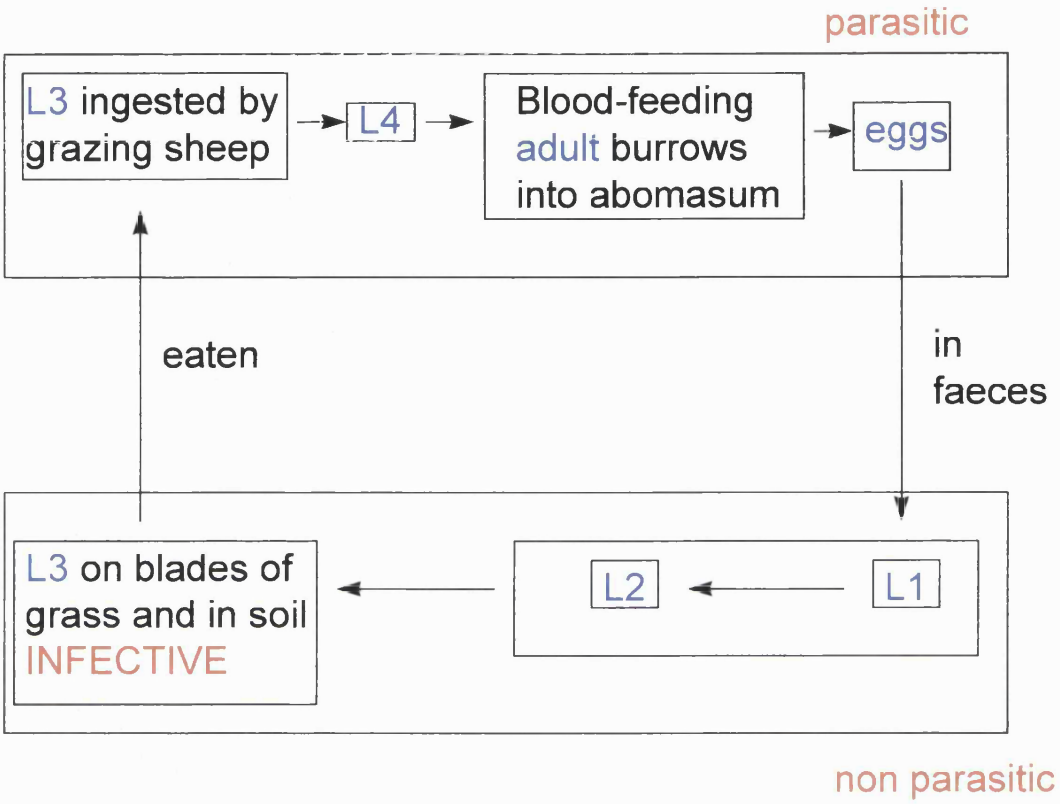

Figure 4 Life cycle of the sheep parasite *Haemonchus contortus*

The early larval stages are microbivorous and develop in the dung, in favourable climatic conditions. The third larval stage retains its sheath and is unable to feed, but survives by slow metabolism of stored food reserves. This stage is positively geotrophic and climbs up grass stems from where it is accidentally ingested by grazing animals. Exsheathment takes place in the forestomachs and on reaching the abomasum, it undergoes the third and fourth moults and becomes sexually mature.

Resistance to infection has been associated with an increase in serum antibodies, particularly IgA and IgG, and specific IgE responses to excretory-secretory antigens (Newton and Munn, 1999; Schallig, 2000). A type I immediate hypersensitivity response is suggested to play a leading role in worm expulsion (Schallig *et al.* 1997; Miller 1984; Miller, 1996) and eosinophils are thought to be involved in eliminating L3 in immune sheep (Meeusen, 1999). Young lambs are generally unresponsive to *H. contortus* challenge (Manton *et al.* 1962; Urquhart *et al*, 1966; Colditz *et al*, 1996) and this has been attributed, at least in part, to their lack of a Th2 immune response (Schallig *et al.* 1997; Gill *et al.* 1993), which may be due to their relatively low numbers of CD4+ T cells (Watson *et al*, 1994).

1.2 Control of parasitic nematodes

The World Health Organisation has instigated the control of many human parasitic nematode diseases in the last decade, through the development of integrated control strategies (W.H.O.,1998 , 1999, 2000). These commonly combine a number of control methods including education, to prevent transmission and infection and to alert people in endemic areas to signs of infection, vector targeting and drug therapy. Programs targeting the invertebrate host, thereby breaking the transmission cycle, have proved effective for many serious diseases including onchocerciasis, dracunculiasis and lymphatic filariasis. Drug treatment involves serial administration of one or more of the classes of anthelmintic (section 1.2.3). As this thesis will focus on the nematode parasites of ruminants, all further discussion of control methods will concentrate on these parasites.

1.2.1 Biological control

Increasing levels of resistance to the commercially available anthelmintics drugs (see section 1.2.4) has catalysed the development of additional control methods. Biological control methods are particularly attractive to organic farms as the preventative use of anthelmintics is banned (Larsen, 1999). It is improbable, however, that biological control (B.C.) would replace

chemotherapy as a control method; the levels of efficacy are not as high and not all life cycle stages are targeted. One element of the concept behind B.C. is that as some infective stage larvae are still viable, ruminants obtain a low level parasitic infection, which is enough to induce the development of acquired immunity but not to produce the morbidity and mortality associated with large worm burdens. B.C. is proposed as a component of an integrated control strategy, which may also involve pasture rotation, vaccines and dietary elements.

The most promising candidates for use in B.C. are the nematophagous trapping fungi (Thamsborg *et al*, 1999; Larsen, 1999). A number of species occur naturally in the dung and are able to survive the ruminant gastrointestinal tract (Hay *et al*, 1997). *Duddingtonia flagrans* has emerged as the most successful agent on numerous occasions (Thamsborg *et al*, 1999, Larsen, 1999; Gronvold *et al.*; 1993, Githigia *et al.*; 1997) and can control larval stages in the dung thereby reducing the number of infective-stage larvae on the pasture. A number of studies on the effect of *D.flagrans* on tristrongyle parasites of cattle (Gronvold *et al.*, 1993) and sheep (Githigia *et al.* 1997) show fewer larvae on pastures and lower worm burdens in fungal spore fed animals as compared to controls. There are still a number of issues to be resolved before commercial use of fungi as control agents is a viable option. These include the lack of suitable application system, lack of data from tropical and sub-tropical areas, dearth of knowledge regarding the long-term impact on the environment and non-target organisms and the acceptance by farmers of a non-chemical parasite control strategy.

1.2.2 Vaccines

A number of strategies for vaccine development have evolved during the past few years, particularly as DNA recombinant technology has advanced, however no new commercially available vaccines against nematodes have been developed for many years. There are presently two commercially available vaccines, which are based on attenuated larvae and target *Dictyocaulus viviparous* in cattle (Jarrett *et al.*, 1958) and *D.filaria* in sheep (Sharma *et al*, 1988). Irradiated *H.contortus* larvae protect mature sheep

from *H.contortus* infection but not young lambs, who are the major victims (Knox, 2000). Vaccines incorporating natural antigens, which are exposed to the host and evoke an immune response during an infection, are under investigation (Knox, 2000; Newton and Munn, 1999). For example, it is known that antibody-secreting cells are recruited to the site of a pathogenic infection. These can be harvested following infection and maintained *in vitro* for a few days. Secreted antibodies can be used to probe western blots of parasites allowing the detection and characterisation of antigens. This method has been used to identify protective antigens from *H.contortus* (Jacobs *et al.*, 1999) and *Teladorsagia circumcincta* (Meeusen, 1996). Another example of a potential vaccine based on *H.contortus* natural antigens is demonstrated by Schallig *et al.* (1997). Adult and L4 stage larvae express 15 and 24 kDa excretory/secretory antigens, identified by comparing serum antibody responses of partly immune sheep to primary and secondary infection. These antigens induce a protective immune response in sheep and as they have been fully cloned they are being tested in recombinant form.

Vaccines are also being developed which are based on "novel" antigens, which are not exposed to the host during infection and therefore do not result in an immune response. Within the numerous hidden antigens discussed in the literature (reviewed Knox, 2000; Newton and Munn, 1999) there are a number of protective vaccines based on *H.contortus* gut antigens. The most promising candidate for commercial development is the H11 antigen, which is an integral membrane glycoprotein (Munn *et al.*, 1997). This is expressed only in the microvilli of parasitic stage *H.contortus* and is an effective immunogen in young lambs (Andrews *et al.*, 1995; Munn *et al.*, 1997) across all breeds tested and is competent against anthelmintic resistant worms (Newton and Munn, 1999). All three isoforms of H11 have been cloned and expressed in the baculovirus-*sf9* insect cell system as full-length recombinant proteins and vaccine trials are ongoing for fragments of the extracellular domain expressed in *E.coli*. Homologous proteins have been identified in other gastrointestinal species and these have also shown promise as protective candidates.

A commercially viable vaccine would need to target multiple species of gastrointestinal nematode, be cost-effective and be accepted into farm management strategies (Knox, 2000). It is unlikely that a vaccine would be 100% efficacious, but vaccination effects persist for longer than drug treatment and long-term benefits may therefore be greater (Newton and Munn, 1999). Recent advances in recombinant DNA technology, in addition to increasing levels of resistance to all modern anthelmintics, have made the development of a successful vaccine a more likely scenario.

1.2.3 Chemical control

Chemotherapy is by far the most frequently used method of control of nematodes, because wide-spectrum anthelmintics with high potency are commercially available allowing up to 100% removal of worms. The target sites of all modern anthelmintics are pharmacologically distinct from the host, or unique to the parasite, resulting in low host toxicity. There are four major classes of anthelmintic drug used in the field: the benzamidazoles, the imidazothiazoles and tetrahydropyrimidines, piperazine and the avermectins and milbemycins, although piperazine is not as effective as the other classes and therefore does not comprise a significant part of the market. In 1996, parasiticides accounted for 13% and 39% of the world livestock and companion animal product sales respectively (Witty, 1999). The major part of the market was composed of the imidazothiazoles/tetrahydropyrimidines (US$260 million), benzimidazoles (US$365 million) and the avermectins and milbemycins, which commanded the greatest proportion by far at US$995 million. The most recent introduction of a new class of drugs into the market was in 1981 with the development of the broad-spectrum anthelmintic ivermectin. The high potency, broad-spectrum of activity and low host toxicity of these anthelmintics has led to their dominance of the market. In 1996, the cost of discovering and developing a new animal drug was estimated at US$57 million and the time-scale from idea to launch is likely to be about 10 years (Witty, 1999). It is therefore clear why very few pharmaceutical companies commit to the discovery of new classes of anthelmintic when the development of new analogues of an existing class is still a viable option.

However, the widespread development of anthelmintic resistance (see section 1.2.4) and the toxicity of the avermectins and milbemycins to non-target organisms in the environment (Wall and Strong, 1990) mean that new classes of drug and/or alternative control strategies are urgently required.

1.2.3.1 Benzamidazoles

The benzamidazoles, including thiabendazole, mebendazole, albendazole and fenbendazole, are broad-spectrum antheimintic agents of gastrointestinal parasites and are composed of a bicyclic ring system in which benzene has been fused to the 4- and 5- position of the heterocycle (figure 5) (De Silva *et al.*, 1997).

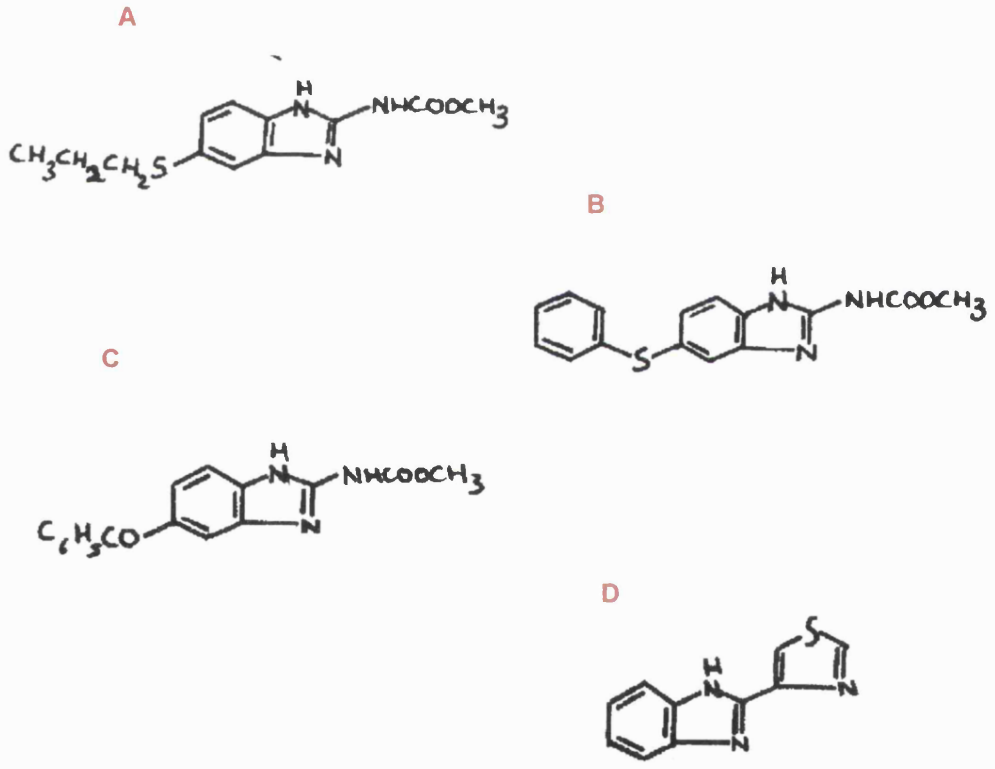

Figure 5 The chemical structures of commonly used benzamidazoles. A albendazole; B fenbendazole; C:mebendazole; D thiabendazole.

The potent anthelmintic thiabendazole was introduced in 1961 and the mode of action of this class of drugs has been extensively

investigated. The benzamidazoles selectively bind to nematode β-tubulin inhibiting its polymerisation with α-tubulin to form microtubules but without affecting host β-tubulin (Lacey, 1990; Lubega and Prichard, 1991a). Initial reports of the action of benzamidazoles indicated that nematode intestinal damage was observed following treatment with mebendazole (Martin *et al.*, 1997a; Van den Bossche *et al.* 1982). A loss of cytoplasmic tubules, loss of transport of secretory vesicles and inhibition of glucose uptake was associated suggesting the worms died of starvation (Beugnet *et al.*, 1996; Lacey, 1990). Many of the observed structural change to the intestine are likely to be a direct result of the inhibition of the microtubule polymerisation. (Beugnet *et al.,* 1996; Jasmer *et al.*, 2000; Lacey, 1990), however, the inhibition of secretory vesicle transport in the intestine may also play a role in intestinal damage by initiating the release of digestive enzymes that damage the intestinal cells. This damage could inhibit the digestion and absorption of food and cause starvation. Evidence from *C.elegans* suggests that benzamidazoles also interfere with the proper formation of oocytes (Enos and Coles, 1990; Bernt *et al.*, 1998). As an intact cytoskeleton is essential for successful meiosis this is consistent with their interaction with microtubules. Mitochondrial damage has also been observed (Beugnet *et al.*, 1996) and McCracken and Sillwell (1991) suggest an uncoupling of oxidative phosphorylation.

1.2.3.2 Piperazine

Piperazine is composed of a heterocyclic ring without a carboxyl group (figure 6), unlike GABA, and acts as a simple GABA antagonist, gating GABA receptors on nematode somatic muscle (Geary *et al*, 1992; Martin, 1982; Martin, 1985; Martin *et al.*, 1996). An increase in chloride conductance of the muscle membrane and a reduction in excitability are observed resulting in the relaxation of body muscle and flaccid paralysis.

Figure 6 The chemical structure of piperazine.

Piperazine is effective against large gastrointestinal nematodes and its activity is potentiated by high pCO_2. It is suggested that CO_2 may interact with the heterocyclic ring of piperazine and substitute for the carboxyl group of GABA (Geary *et al.*, 1992). This drug is 100 times less potent than GABA, with higher concentrations of piperazine required for the same channel opening rate in *Ascaris* muscle and a shorter mean duration of channel opening than GABA (Martin, 1985; Martin *et al.*, 1996). Piperazine is of relatively little importance in nematode control, as other anthelmintics are more broad spectrum and more potent (Geary *et al.*, 1992). This is illustrated by no mention of this drug in the major constituents of the livestock anthelmintic market (Witty, 1999).

1.2.3.3 Imidathiazoles and tetrahydropyrimidines

The structure of some of the imidathiazoles (levamisole) and the tetrahydropyrimidines (pyrantel, morantel) is shown in figure 7.

These compounds all act at the acetylcholine receptors of nematode muscle causing contraction and spastic paralysis at therapeutic concentrations. This has been demonstrated in many species including *A.suum* (Aubry *et al.*, 1970) *H.contortus* (Sangster *et al.*, 1991) and *C.elegans* (Lewis *et al.*, 1980). Application of levamisol, pyrantel or morantel to *A.suum* muscle cells resulted in depolarisation, increased spike frequency, contraction and an increase in input conductance of the membrane to sodium and potassium ions (Aubry *et al.*, 1970; Harrow and Gration, 1985). The same effect was seen when acetylcholine was applied, although the anthelmintics were more potent agonists.

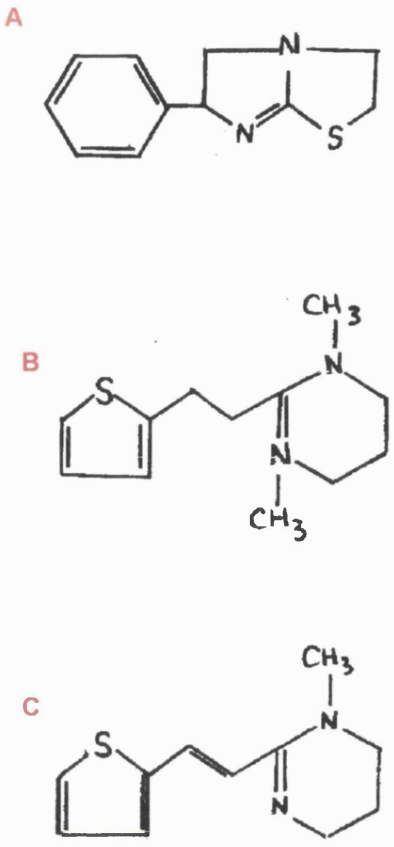

Figure 7 The chemical structures of some nicotinic anthelmintics. A levamisole; B morantel; C pyrantel.

Simultaneous application of acetylcholine and pyrantel indicated that both agonists act at the same nicotinic receptor. Patch clamp studies supported these findings as these anthelmintics were seen to open non-selective cation channels with similar properties to acetylcholine (Robertson and Martin, 1993; Robertson *et al*, 1994; Dale and Martin, 1995; Evans and Martin, 1996; reviewed Martin *et al.*, 1998). Lewis *et al.* (1980, 1987a, 1987b) show further evidence for the action of levamisole at nicotinic acetylcholine receptors as *C.elegans* mutants lacking this receptor were not paralysed by levamisole and showed a decrease in binding of [^{3}H] m-aminolevamisole. [^{3}H] m-aminolevamisole binding in wild-type *C.elegans* was inhibited by acetylcholine and a range of nicotinic agonists. Three of the eleven genes responsible for levamisole resistance in *C.elegans* have been shown to

encode subunits of the nicotinic acetylcholine receptor (Fleming *et al*, 1997). When expressed in *Xenopus* oocytes, these subunits encode channels gated by levamisole and currents are blocked by the nicotinic antagonists d-tubocurarine and mecamylamine. Levamisole and pyrantel have only low activity at vertebrate nicotinic receptors (Aubry *et al.*, 1970) and this selectivity allows nematodes to be killed with low host toxicity.

1.2.3.4 Avermectins and milbemycins (AM)

The avermectins and structurally related milbemycins are extremely potent anthelmintics and insecticides with a broad spectrum of activity in a wide range of hosts. The original compounds were natural fermentation products isolated from a novel *Streptomyces* species, termed *S.avermitilis* to indicate the creation of a "wormless" environment, from a Japanese soil sample. The name "avermectin" was developed to denote their potent activity against both worms and ectoparasites (Campbell, 1981). The compounds are composed of a 16 membered lactone ring (figure 8) and the avermectins have a dissacharide substituent at C-13. Ivermectin, a semi-synthetic analogue produced from the natural avermectin B1, was the first of these compounds to be released as a commercial anthelmintic, in 1981, and still commands a large percentage of the market (Chabala *et al.*, 1980; Campbell, 1981). The AM are used in both human and veterinary medicine and are active against most gastrointestinal nematodes and the larval stages of filarial worms. A number of the WHO control programs, including that for river blindness, include annual dosing with ivermectin. The lack of activity against adult filarial worms, although there is evidence of reduced fecundity, is not understood and has maintained a research effort for alternative chemotherapy (reviewed McKellar and Benchaoui, 1996; Campbell and Benz, 1984; Grant, 2000). The AM show 99% efficacy against GI parasites of cattle and sheep including *Haemonchus contortus* (Campbell and Benz, 1984) and *Ostertagia ostertagi* (Armour *et al*, 1980).

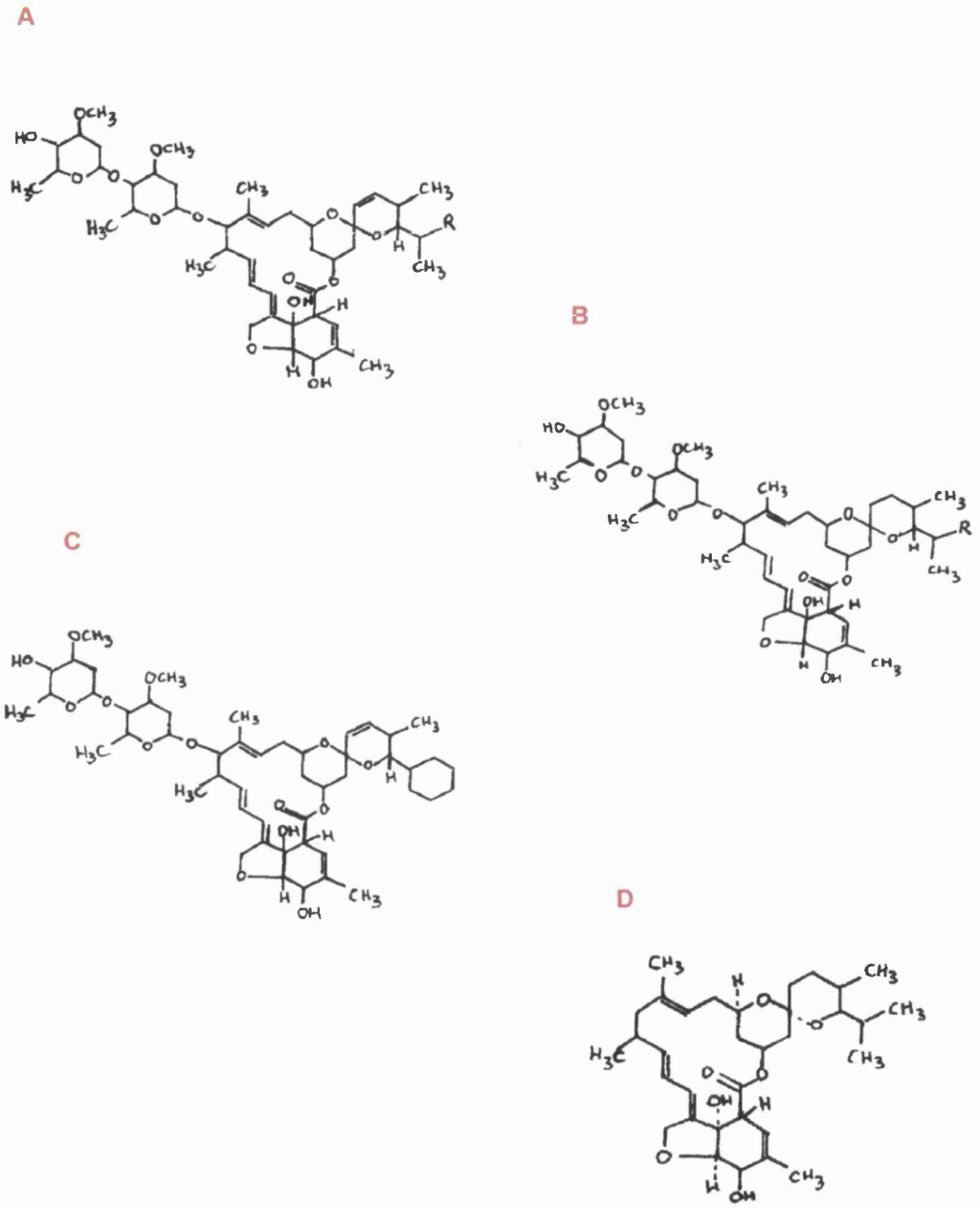

Figure 8 Structure of some of the avermectins and milbemycins. A abamectin; B doramectin; C ivermectin; D milbemycin D.

Numerous studies have demonstrated that the AM increase the chloride ion permeability of nematode muscle causing paralysis, which is recorded as neither flaccid nor tetonic (Martin, 1996; Martin and Pennington, 1989; Kass *et al.*, 1980; Geary *et al.*, 1992; Geary *et al.*, 1993; Gill *et al.*, 1995; Martin *et al.*, 1996). There has been some controversy over the site of action of the AM. Initial reports implicated activity at GABA-gated ion channels as application of avermectin B1a blocked transmission between an interneuron and an excitatory motorneuron in the ventral nerve cord in *Ascaris* (Kass *et al.*, 1980; Kass *et al.*, 1984). This block could be due to a number of factors including attenuation of an electrical signal down the excitatory interneuron before the motorneuron synapse is reached or inhibition at the excitatory interneuron and motorneuron synapse. Either way, the avermectins were shown to stimulate inhibitory neurones and their effect was reversed by the ligand-gated chloride channel blocker picrotoxin. At this time GABAergic neurons had been shown to be present in nematodes and therefore research concentrated on the effects of the AM on GABA receptors. They were observed to non-competitively block GABA receptors in *Ascaris* muscle at micromolar concentrations (Holden-Dye *et al.*, 1988; Holden-Dye and Walker, 1990), but had no effect on resting cells.

Martin and Pennington (1989) demonstrated essentially irreversible gating of GABA-independent chloride channels in *A.suum* muscle membrane at low nM concentrations of ivermectin as well as an antagonistic effect at GABA receptors at micromolar concentrations. The high concentrations of drug required to affect GABA receptors decree them unlikely candidates for the therapeutic mode of action of these anthelmintics. Concurrent work by Schaeffer and Haines (1989) identified a single high affinity ivermectin binding site in crude membrane preparations from *C.elegans* (K_d = 0.26 nM). The binding was a two-step mechanism with a fast reversible complex initially formed and following further incubation with ivermectin this converted to slowly reversible complex (Schaeffer and Haines, 1989; Cully and Paress, 1991). Competition studies with several avermectin derivatives showed comparable results with their nematocidal activity suggesting this as a physiologically relevant site of action. Ivermectin binding with these

therapeutically relevant concentrations demanded further investigation and injection of *Xenopus* oocytes with size fractionated poly $[A]^+$ yielded ivermectin-sensitive irreversible chloride currents which did not respond to GABA (Arena *et al.*, 1991). Glutamate was also shown to activate chloride currents when applied to oocytes expressing the same poly $[A]^+$ RNA fractions forming a reversible complex which desensitised in the continued presence of glutamate (Arena *et al.*, 1992). These currents were blocked by both picrotoxin and the non-selective chloride channel blocker flufenamate.
In addition to direct activation of glutamate-sensitive channels, ivermectin also potentiated the response to glutamate and slowed the desensitisation of the glutamate-sensitive current as well as showing the same pharmacology and current-voltage relationships as glutamate. This evidence indicated activation of the same chloride channel by glutamate and ivermectin and denoted a novel ion channel, the glutamate-gated chloride channel (GluCl) (section 1.3.3.2.3). The first GluCl subunit cDNAs, α and β, were discovered by library screening of *C.elegans* size fractionated RNA (Cully *et al.*, 1994). Expression of homomeric channels resulted in ivermectin- (alpha) or glutamate- (beta) sensitive chloride currents. Co-expression in *Xenopus* resulted in avermectin and glutamate sensitive chloride channels with similar properties to expressed *C.elegans* poly $[A]^+$ RNA and sequence analysis indicated homology to mammalian glycine receptors. A strong correlation was observed between the activation and potentiation of glutamate sensitive chloride currents and the nematocidal activity of a number of AM. This was also seen in oocytes expressing *C.elegans* poly $[A]^+$ substantiating the role of the GluCls as the primary site of action of the AM (Arena *et al.*, 1995). Inactivation of the *C.elegans* GluClα gene did not ablate ivermectin binding indicating the presence of additional GluCl subunits (Vassilatis *et al.*, 1997b). Further GluCl genes have been identified from *C.elegans* (Laughton *et al.*, 1997a; Horoszok *et al.*, in press; Dent *et al.*, 1997; Dent *et al.*, 2000; Cully *et al.*, 1996) and parasitic nematodes (Delany *et al.*, 1998; Jagannathan *et al.*, 1999; Forrester *et al.*, 1999).

A number of mechanisms appear to be involved in the nematocidal activity of the AM. Inhibition of motility and pharyngeal pumping have been reported in both *C.elegans* and parasitic nematodes, but the relative importance of the two sites of action remains unclear and may vary between species (Gill and Lacey, 1998). Pharyngeal pumping is inhibited by low concentrations (nM) of AM in *C.elegans* (Avery and Horvitz, 1990), *H.contortus* (Geary *et al.*, 1993; Paiement *et al.*, 1999) and *A.suum* (Martin, 1996; Brownlee *et al.*, 1997) and this would result in starvation and destruction of the hydrostatic pressure required for many of the nematode body functions. Martin (1996) demonstrated that this inhibition is caused by irreversible activation of chloride channels, which are also gated by glutamate. Differences in life-style at the different developmental stages may dictate altered effects of AM, but Gill *et al.* (1995) showed arrested development of *H.contortus* L1-stage larvae following AM treatment, which would result from starvation, and treatment of adults with biologically relevant (nM/pM) concentrations of AM (Geary *et al.*, 1993; Paiement *et al.*, 1999) also results in cessation of ingestion, as measured by [^{3}H] inulin uptake. AM effects on motility are only seen at higher concentrations (high nM, μM) and paralysis is restricted to the mid-body region, while the head and posterior regions retain normal motility (Geary *et al.*, 1993; Gill *et al.*, 1995). The structure/activity relationships of different AM on motility and pharyngeal activity were comparable in both *C.elegans* and *H.contortus*, suggesting a common site of action. Considering the high potency of the AM, and therefore the low concentrations which are required for nematode control, it appears feasible to deduce that the nematocidal activity of the AM is due to hyperpolarisation of pharyngeal muscle resulting in starvation rather than inhibition of motility.

Host drug metabolism and exposure of parasitic nematodes to AM *in vivo* may affect nematocidal activity and therefore investigation of the *in vivo* effects of the AM was required to substantiate this hypothesis (Gill and Lacey, 1998). Rapid expulsion of some tristrongylid gastrointestinal sheep nematode species following ivermectin treatment, at approximately the flow rate of the digesta, suggested that paralysis of somatic muscle, required to

maintain position in the digestive tract, was the crucial mode of action of ivermectin, at least in these adult gastrointestinal parasites. Mild inhibition of motility, as caused by nM concentrations of ivermectin, would probably be adequate to dislodge GI nematodes from the gut. Expulsion of one species, however, took longer suggesting different toxic modes of action of the AM in different species. Localisation of GluCl subunits in *C.elegans* (Laughton *et al.*, 1997b; Dent *et al.*, 1997) has shown expression of GluClβ promoter and GluClα2 in the M4 and M5 pharyngeal muscle cells that form synapses with the glutamatergic inhibitory M3 motorneuron. Weaker expression of GluClα2 (*avr-15*) and the *avr-14* gene products was observed in the dorsal and ventral nerve cords. This agrees with the observed effect of AM on free-living nematodes and free-living stages of parasitic nematodes.

Reduced fertility of female worms is also apparent following treatment with ivermectin (Le Jambre *et al.*, 1995; Duke *et al.*, 1991; Sasaki and Kitagawa, 1993; Grant, 2000). The release of eggs already *in utero* and the production of new eggs are inhibited and these effects are apparent in gastrointestinal and filarial nematodes. The recent reporting of inhibitory glutamate activity in the vagina vera of *Ascaris suum* allows supposition that ivermectin exerts its effects on reproduction through activation of GluCl (Fellowes *et al.*, 2000). This additional feature of the toxicity profile of AM has important implications as inhibition of reproduction may reduce infection levels. It is probable that the AM have different toxic effects on nematodes with different life-styles due to levels of exposure and possibly differences in the evolution of their major site of action, the GluCl.

The AM generally show extremely low host toxicity, but during treatment of *D.immitis* in Collies high concentrations of avermectin induced a toxic effect (reviewed Sutherland and Campbell, 1990). Studies on the activity of avermectins in vertebrate brain showed activity at $GABA_A$ (Adelsberger, 2000; Schaeffer and Haines, 1989; Sigel and Baur, 1987; Pong and Wang, 1980) and nicotinic α7 receptors (Krause *et al.*, 1998). The GABA and acetylcholine responses were potentiated by ivermectin, but the ivermectin binding affinity for these receptors was approximately 100 fold lower and

showed a different mechanism than for the nematode target receptor. The AM do not freely cross the blood/brain barrier and studies indicate that the lowest drug residue levels are found in the brain (reviewed Sutherland and Campbell, 1990; Burkhart, 2000). These facts, coupled with the low doses required for efficient removal of nematodes and no evidence for GluCls in vertebrates, probably account for the low host toxicity. The toxicity to Collies is thought to be due to a deficiency in the blood-brain barrier.

Following treatment of mammals with AM the majority of the drugs are excreted, largely unchanged, in the faeces (Ottesen and Campbell, 1993; McKellar and Benchaoui, 1996). This has resulted in concerns over detrimental environmental effects as the long-half life (91-217 days in winter) of the AM coupled with their potent insecticidal and acaricidal activity may cause toxicity of non-target invertebrates in the dung (Wall and Strong, 1987). Poor degradation of faeces from slow-release bolus ivermectin-treated cattle, as compared to untreated controls, suggested toxic effects on dung-degrading insects. The method of ivermectin administration appears to influence subsequent environmental impact, however, as dung from cattle treated with ivermectin by injection or pour-on formula degraded as control (McKeand *et al.*, 1988). The long-term environmental effects of the AM are not known.

1.2.4 Anthelmintic resistance

The widespread use of the major classes of anthelmintic has resulted in the evolution of resistant parasites. As yet, drug resistance has not been reported in human nematodes, but dosing regimes are such that treatment levels are far higher than is required to kill parasites and therefore resistant worms may be present without discovery for long periods of time. In addition, the mass chemotherapeutic parasite control schemes introduced by the WHO in the past decade will hasten the development of resistance. In contrast to the human situation, anthelmintic resistant nematodes have been reported in the majority of livestock, particularly in the tropics and subtropics (Waller, 1997; Chandrawathani, *et al.*, 1999; Van Wyk *et al.*, 1999; Waruiru,

et al., 1998; Jackson and Coop, 2000). Resistance was first reported to the benzamidazoles in S. Africa in 1975 in an *H.contortus* strain and over 90% of sheep farms in S. Africa are now reported to have resistance to at least one type of anthelmintic (Van Wyk *et al.*, 1997). Anthelmintic resistance is probably due to a pre-adaptive phenomenon, rather than to the appearance of a new mutation (Jackson and Coop, 2000). As such, individuals carrying alleles that are susceptible to the action of a drug are killed whereas those that possess alleles that reduce the toxic effect of a drug survive. The "resistance" allele is passed through generations and flourishes in the population and the "susceptible" allele diminishes. High genetic variability predisposes an organism to possess such a "resistance" allele. It is apparent that the tristrongylid nematodes are particularly susceptible to the development of resistance and reports of very high polymorphism in these species support this finding (Sangster, 1996). Selection of resistant alleles in a population has escalated at a far quicker rate than was predicted as a result of underdosing, use of poor quality anthelmintics and poor management.

The mechanism of resistance to the major classes of anthelmintic has been investigated at both the molecular and functional level. Benzamidazole resistance is fairly well understood and an alteration in the drug receptor is apparent (Lubega and Prichard, 1991b; Sangster *et al.*, 1985). Further studies indicated altered polymorphism in resistant nematode populations with progressive loss of β-tubulin alleles (Lubega *et al.*, 1994; Kwa *et al.*, 1993; Roos *et al.*, 1995). Two β-tubulin isotypes are present in nematodes and loss of isotype 1 alleles is associated with low level resistance followed by elimination of isotype 2 in very highly resistant individuals. Cloning studies have revealed the presence of a tyrosine residue at position 200 of β-tubulin isotype 1 in resistant individuals, whereas susceptible individuals have a phenylalanine at this position (Kwa *et al.*, 1993; Elard *et al.*, 1996; Geary *et al.*, 1999). The same mutation is seen in benzamidazole-resistant fungi (Fujimura *et al.*, 1992) and mammals naturally have a tyrosine at this position (Lewis *et al.*, 1985) suggesting that the parasites have learned to

mimic their host β-tubulin thus evading the drugs' toxic action. Kwa *et al.*, (1995) demonstrated rescue of the sensitive phenotype in *C.elegans* by transforming individuals expressing the benzamidazole-resistant allele with the *H.contortus* benzamidazole-sensitive allele thereby reinforcing the hypothesis that benzamidazole resistance is due to a loss of susceptible β-tubulin alleles from the population.

Alteration of the drug receptor has also been implicated in imidazothiazole/tetrahydropyrimidine resistance. Binding and egg-hatch studies have indicated reduced sensitivity to cholinergic agonists as well as levamisole in both *C.elegans* and parasitic species (Sangster *et al.*, 1991; Sangster, 1996; Lewis *et al.*, 1987b; Moreno-Guzman *et al.*, 1998) and, coupled with reduced binding affinity and an apparent increase in binding sites, this suggests changes in the drug receptor. Molecular studies implicated 11 genes in levamisole resistance in *C.elegans* (Fleming *et al.*, 1996, 1997), 3 of which encode acetylcholine receptor subunits. Comparison of cloned levamisole receptor subunits has yielded no mutations associated with levamisole resistance in *T.colubriformis*, *H.contortus* and *O.circumcincta* (Wiley *et al.*, 1996; Hoekstra *et al.*, 1997; Sangster and Gill, 1999). Electrophysiological investigation of levamisole-sensitive and -resistant *Oesophagostomum dentatum* muscle supports molecular studies as, at a therapeutic concentration of levamisole (30μM), there are less active channels in resistant than sensitive isolates (Martin and Robertson, 2000; Robertson *et al.*, 1999; Martin *et al.*, 1997b). Combined with the associated reduction in channel mean open time, this is proposed to result in a ten-fold decrease in levamisole current. The levamisole target-site shows varying conductances, which are suggested to be associated with altered combinations of subunits forming the receptor. One of these subtypes is missing from the levamisole-resistant isolate and this may contribute to the reduced levamisole efficacy.

The mechanism of AM resistance is not well understood. Resistance to this class developed very rapidly with ivermectin resistance being reported only 33 months after its introduction into the market (Shoop, 1993). At the

molecular level, a number of genes appear to have some involvement in AM resistance in *C.elegans* including amphid dysfunctional genes, GluCl receptor subunits and p-glycoproteins (Dent *et al.*, 1997; Dent *et al.*, 2000), but it is not known if these findings are applicable to parasitic nematodes. Binding studies do not implicate alteration of GluCl receptors in resistance in *H.contortus* and *Telodorsagia circumcincta* (Rohrer *et al.*, 1994; Hejmadi *et al.*, 2000) but investigation of the functional channel would be more conclusive. GluCl receptor subunits have been cloned from ivermectin-resistant *H.contortus* isolates and do not appear to be involved, at least in terms of sequence, in the development of resistance (Delany, 1998, Jagannathan, 1998).

P-glycoproteins (pgp) can transport compounds from the inside to the outside of cells and have been shown to mediate drug resistance in humans (Gottesman *et al.*, 1993; Higgins, 1995). There are 14 genes for pgp in *C.elegans* but none of the genes associated with avermectin, levamisole or benzamidazole resistance map to the pgp loci. However, a number of studies of avermectin resistance in *H.contortus* have demonstrated pgp involvement (Xu *et al.*, 1998; Blackhall *et al.*, 1998; Sangster and Gill., 1999; Molento and Prichard, 1999) and reports suggesting that ivermectin is a pgp substrate in mammalian cells support the hypothesis that pgps may play a role in avermectin resistance (Pouliot *et al.*, 1997). These findings are not universal however (Kotze, 1998; Kwa *et al.*, 1998), highlighting the need for more research in this area.

Functional studies of AM resistance indicate alterations at both sites of action (Gill *et al.*, 1995; Gill and Lacey, 1998; Sangster, 1996; Kotze, 1998; Paiement *et al.*, 1999) as inhibition of both motility and pharyngeal pumping require higher levels of drug in resistant isolates. It is evident that the resistant phenotype is dependent upon the selection procedure and therefore mechanisms of AM resistance may differ both between and within species (Gill *et al.*, 1998; Gill and Lacey, 1998).

1.3 Neurobiology

The rampant spread of resistance to all classes of broad-spectrum anthelmintics dictates an urgent requirement for the development of novel drugs and has highlighted our lack of knowledge of the mode of action of those drugs currently in use. It is known that three anthelmintic classes selectively act at the nematode nervous system; however much information regarding the exact mechanism by which they exert their effect, their pharmacodynamics and the molecular mechanisms involved in resistance is missing. Studies of basic nematode neurobiology will improve our understanding of the mode of action of these drugs and may also yield novel targets for mechanism-based screening, thereby re-igniting interest in anthelmintic discovery programs within pharmaceutical companies.

1.3.1 The anatomy of the nervous system

The majority of information regarding the nematode nervous system is derived from studies of the free-living species *C.elegans* and the parasite *Ascaris*. The neuroanatomy of these two species is comparable suggesting continuity throughout the phylum. All neurons and their synaptic connections have been mapped and indicate a simple system with approximately 300 neurons, the majority of which are found in the anterior nerve ring surrounding the pharynx (Rand and Nonet, 1997; Thomas and Lockery, 1999; Davis and Stretton, 1996) (figure 9). The nerve ring contains almost all the inter neurons and axons from most of the sensory neurons which project towards the anterior of the worm. Two main nerve cords extend in a posterior direction from the circumpharyngeal nerve ring almost to the tail in dorsal and ventral positions and contain inter neurons and the body muscle motor neurons. The ventral nerve cord contains the cell bodies of all the

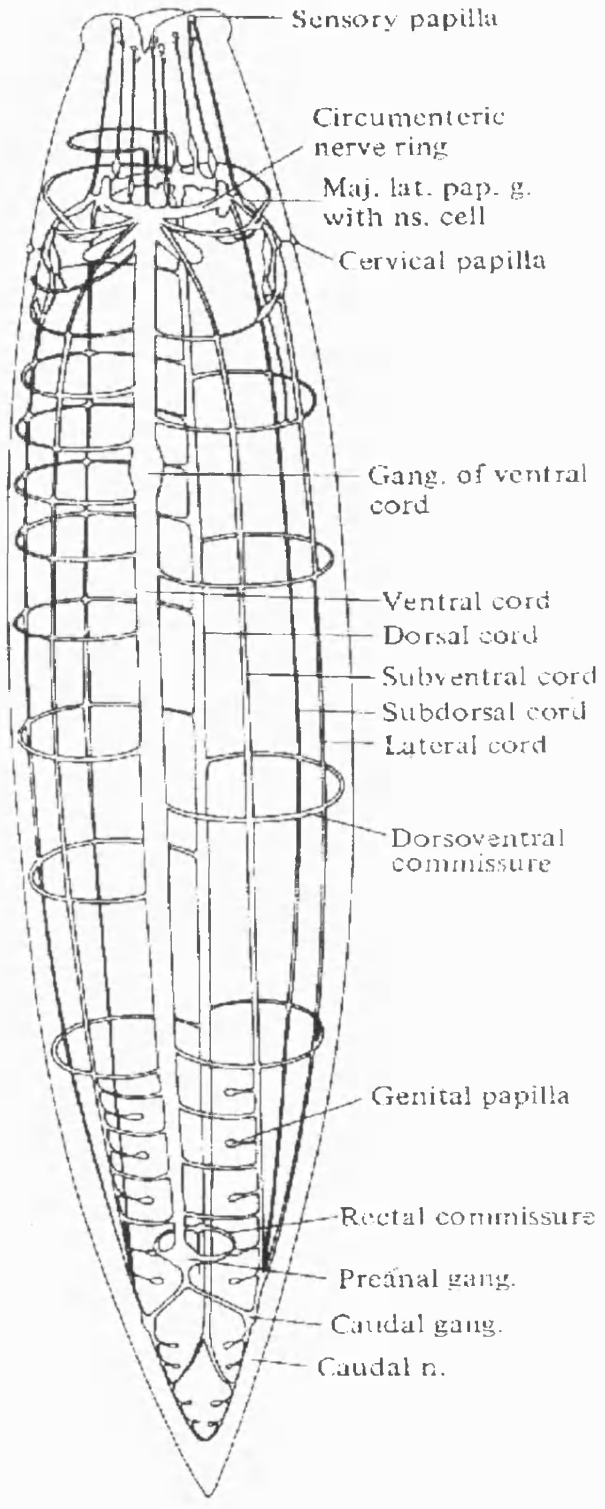

Figure 9 The *Ascaris* nervous system (Withers, 1992)

motor neurons and communication to the dorsal nerve cord is via frequent connections by lateral commissures.

1.3.2 Neurotransmission

The simplicity of the nematode nervous system in terms of anatomy is not reflected in its neurochemistry. Many of the classical mammalian neurotransmitters are also present in nematodes including γ-aminobutyric acid (GABA), acetylcholine, glutamate, serotonin, dopamine and octopamine (reviewed Brownlee *et al*, 2000; Bargmann, 1998). The distribution of nematode neurotransmitters has been investigated using direct techniques, such has immunohistochemistry, and by detection of synthetic enzymes and transporters. As with anatomical studies, the majority of information is derived from *A.suum* and *C.elegans*, with initial localisation and pharmacological observations being carried out on the former. The *C.elegans* genome project has yielded a wealth of genes with homology to mammalian neurotransmitters and their receptors and molecules involved in their synthesis, transport and reuptake (Bargmann, 1998). Functional studies are still in progress, but mutation analysis has already provided some information regarding the localisation and role of identified genes.

1.3.2.1 GABA

In 1964, GABA was shown to hyperpolarise *Ascaris* muscle cells (Del Castillo *et al.*, 1964). This has subsequently been observed by other workers (Martin, 1980; Holden-Dye *et al.*, 1988) and GABA's role as the major inhibitory neurotransmitter in nematodes confirmed. The observed hyperpolarisation of muscle membrane is associated with relaxation of muscle and is a pure chloride event. Therefore, it is unsurprising that inhibitory motor neurons in *A.suum* are GABAergic (Johnson and Stretton, 1987). In total, twenty-six GABA positive cells have been defined in both *A.suum* (Guastella *et al.*, 1991) and *C.elegans* (McIntire *et al.,* 1993a). The functional roles of these neurons have been investigated by laser ablation and all but one are motor neurons. Molecular analysis of *C.elegans* has

yielded genes for GABA expression (*unc-25*), GABA receptors (see section 1.3.3.2.1) and GABA release (*unc-46* and *unc-47*) (McIntyre *et al.*, 1993b; McIntyre *et al.*, 1997). UNC-25 and UNC-47 were localised to GABA positive cells. The UNC-25 protein shows 45% identity to mammalian glutamic acid decarboxylase, the enzyme that synthesises GABA from glutamic acid, and mutants in this gene have no apparent GABA. *Unc-47* is thought to be involved in vesicular GABA transport; vertebrate homologs can package GABA or glycine. Mutants in GABAergic transmission, although viable, have several motor defects including a tendency to simultaneously contract both the dorsal and ventral muscles instead of the usual sinusoidal wave of locomotion. Although GABA's main role is inhibitory, two excitatory motor neurons involved in muscle contraction during defecation also appear GABAergic (Reiner and Thomas, 1995).

1.3.2.2 Acetylcholine

It has been known for many years that acetylcholine is present in nematodes (Mellanby, 1955) and bath application causes contraction of *Ascaris* muscle strips (Baldwin and Moyle, 1949; Norton and De Beer, 1957). Supporting electrophysiological data shows depolarisation of muscle (Del Castillo *et al.*, 1963) and an increase in conductance that is mainly due to sodium ions (Colquhoun *et al.*, 1991) and acetylcholine (ACh) is now accepted as the major excitatory neurotransmitter in this phylum. Acetylcholine esterases and choline acetyl transferase (ChAt) were also found in the *Ascaris* nervous system (Lee, 1962; Johnson and Stretton, 1985) and it is unsurprising that studies with ventral cord indicated the highest ChAt activity in the excitatory motor neurons. Molecular studies have identified genes for choline acetyl transferase (*cha-1*), a synaptic vesicle ACh transporter (*unc-17*), receptors (section 1.3.3.2.2) and three classes of acetylcholine esterase (*ace-1X, ace-2I, ace-3II*) in *C.elegans* (Alfonso *et al.*, 1993; Alfonso *et al.*, 1994; Culotti *et al.*, 1981; Johnson *et al.*, 1981; Kolson and Russell, 1985 a, 1985b). The expression patterns of *unc-17* and *cha-1* are almost identical and are in agreement with results from *Ascaris* ventral cord, with motor neurons of the dorsal nerve cord, pharynx and sublateral motor neurons also showing

expression (Rand and Nonet, 1997). Completely acetylcholine deficient *C.elegans* mutants are not viable.

1.3.2.3 Glutamic acid

The distribution of this neurotransmitter in nematodes is not as well characterised as GABA and acetycholine. Analysis of glutamate receptors (section 1.3.3.2.3) and transporters and the pharmacology of nematode tissues have shed some light on the function of glutamate as a neurotransmitter and it appears to play both an excitatory and inhibitory role. Injection of glutamic or kainic acid into *A.suum* causes paralysis indicating a role for these amino acids in locomotion (Davis and Stretton, 1996). Further analysis shows that excitatory motor neurons are depolarised following application of glutamate, this is a sodium ion event, and a putative glutamate transporter has been identified in the same neurons (Davis, 1998). Cloning of several potential glutamate receptor genes from *C.elegans* further establishes the excitatory role of glutamate in nematodes. Mutants of one of these subunits, *glr-1* showing 40% identity to vertebrate AMPA receptor subunits, illustrate that several classes of sensory neuron use glutamate in this capacity (Hart *et al.,* 1995; Maricq *et al.*, 1995; Zheng *et al.*, 1999). In *Ascaris*, the inhibitory role of glutamate has been demonstrated both by hyperpolarisation of the DI motor neurons and by a chloride-dependent hyperpolarisation of the pharynx (Davis and Stretton, 1996; Martin, 1996; Adelsberger, 1997). This is supported by findings in *C.elegans* that the inhibitory M3 motor neuron which controls the timing of pharyngeal pumping is glutamatergic and the action of this neuron is mimicked when glutamate is applied to the pharyngeal muscle (Dent *et al.*, 1997; Li *et al.*, 1997). A number of cDNAs encoding subunits of a novel glutamate-gated chloride channel have been cloned (section 1.3.3.2.3) and localised to the pharynx and nerve cords.

1.3.3 Neurotransmitter receptors

The identification of neurotransmitters in nematodes and their effects on membrane potentials suggested the presence of fast-acting neurotransmitter receptors. Three of the anthelmintic classes currently in use act at these receptors highlighting their importance. Their pharmacology was often assessed in terms of known vertebrate receptor classes and much of the initial characterisation was carried out in *Ascaris* but, once again, *C.elegans* has been an excellent resource for molecular studies and has provided a plethora of putative neurotransmitter receptor genes.

1.3.3.1 Vertebrate ligand-gated ion channels

In vertebrates, fast neurotransmission is mediated by a superfamily of receptors known as ligand-gated ion channels (LGIC), including acetycholine, glutamate, 5-HT, GABA and glycine receptors. The vertebrate nicotinic ACh receptor is the most well characterised of all LGIC due to its relative abundance in the electric organ of the electric eel allowing early studies access to workable quantities of receptor. The receptor is composed of a pentameric structure of subunits surrounding a central cation pore, which is directly gated by binding of acetylcholine (figure 10A and B) (Changeux, 1993; Unwin, 1995). Molecular heterogeneity has been demonstrated and a number of classes of subunit have been identified ($\alpha\beta\gamma\delta$ in muscle and $\alpha\beta$ in neurons) (Corringer *et al.*, 2000). $GABA_A$ receptors are also heteromeric and multiple isotypes have been identified for many of the nACh and GABA subunit classes (MacDonald and Olsen, 1994; Stephenson, 1995). Each subunit possesses a long, glycosylated, hydrophilic extracellular amino terminal region, four hydrophobic membrane-spanning regions (TM1-4) and a long variable intracellular loop between the third and fourth transmembrane regions (figure 10C). The hydrophilic region contains a conserved pair of cysteines that form a disulphide bridge. LGIC with this general structure are grouped into a subfamily, the cys-loop LGIC (cLGIC), which includes nACh, $GABA_A$, glycine and $5\text{-}HT_3$ receptors in vertebrates and nACh, GABA and inhibitory glutamate receptors in invertebrates.

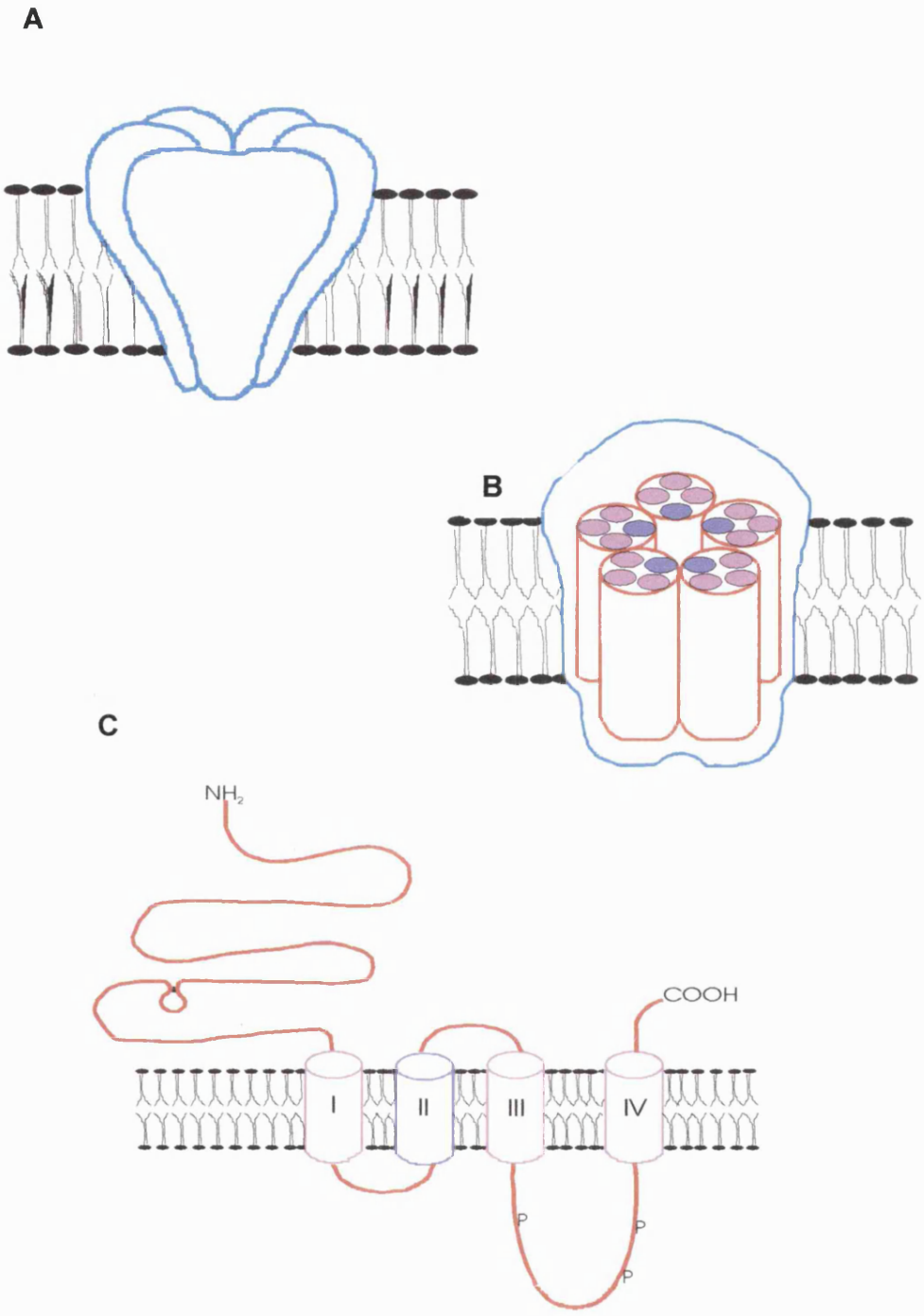

Figure 10 Model of a cys-loop ligand-gated ion channel. A illustrates the pentameric structure of the functional receptor. The five subunits cluster around a central ion pore composed of their TM2 regions (B). C shows the composition of an individual subunit with its large extracellular domain and four transmembrane regions, denoted I-IV. = denotes the cysteine loop. P indicates potential phosphorylation sites (adapted from Changeux, 1993).

The extracellular region, at least of the α-subunit, of cLGIC is thought to contain the neurotransmitter binding sites. Three putative binding domains have been identified in similar regions for each of ACh, GABA, and glycine in their respective receptor. (Smith and Olsen, 1995; Galzi and Changeux, 1994). Identification of neurotransmitter binding sites on non-α subunits led to the proposal that the neurotransmitters bind at the interface of alpha and non-alpha subunits in the functional receptor (Blount *et al.*, 1990; Gu *et al.*, 1991; Saedi *et al.*, 1991; Stephenson, 1995). The second transmembrane region of each subunit lines the ion channel and bestows ion charge selectivity upon the receptor (figure 10B) (Galzi *et al.*, 1991). Negatively charged amino acid rings are present at the top and bottom of the ACh receptor channel (Unwin, 1993), allowing entry only to cations, whereas in anion-selective inhibitory channels positive or neutral residues occupy these positions (Barnard, 1992). This selectivity process was confirmed by the conversion of the α7 nACh channel to anion selectivity by the substitution of three amino acids in the TM2 domain with three from glycine or GABA (Galzi *et al.*, 1992). An uncharged ring of leucines is observed at the centre of the ion channel and is thought to participate in closing the channel (Unwin, 1993). The large intracellular loop of many subunits contains putative phosphorylation sites, which may regulate the function and expression of the receptor (Miles and Huganir, 1988; Wallace *et al.*, 1991; Huganir and Grungard, 1990; Krishek *et al.*, 1994; McDonald *et al.*, 1998; McDonald and Moss, 1994; Brandon *et al.*, 1999).

1.3.3.2 Nematode ligand-gated ion channels

Over a hundred genes encoding LGIC have been uncovered by the *C.elegans* genome project (Bargmann, 1998) including excitatory receptors for acetylcholine and glutamate and inhibitory receptors for $GABA_A$ and glutamate, although the encoded protein function of many of the genes is not yet known. Glycine and its receptor have not been identified in nematodes as yet, but a novel class of inhibitory ionotropic glutamate receptors apparently not present in vertebrates has been found. Nematode LGIC show similarities to their vertebrate counterparts in terms of sequence and

proposed structure. Cloning of multiple subunits and detection of differential channel recordings suggests that nematode LGIC are also heteromeric and that neurotransmission is further complicated by the wide variety of receptor subunits available to these organisms. The *Xenopus laevis* oocyte expression system, whereby injected mRNA is translated in the oocyte into proteins that usually have similar properties to the donor tissue, has been an invaluable technique for physiological characterisation of subunits.

1.3.3.2.1 GABA Receptor

The observation of a fast chloride-dependent hyperpolarisation of nematode muscle following application of GABA indicated the presence of GABA-gated ion channels. Pharmacological analysis of *Ascaris* showed these receptors to be most similar, but not identical, to vertebrate $GABA_A$ receptors (Holden-Dye *et al.*, 1988) although $GABA_A$ antagonists had little or no activity and the chloride channel blocker picrotoxin had very low potency. Molecular investigation of *C.elegans* GABA receptors produced an unusual result in that, in contrast to the multiple genes encoding vertebrate $GABA_A$ receptors, a single gene, *unc-49* appears to encode all subunits for functional GABA receptors, at least in body wall muscle. Mutants in this gene have no muscle response to GABA or the GABA receptor agonist muscimol (McIntire *et al.*, 1993a; Richmond and Jorgensen, 1999) and show an uncoordinated "shrinker" phenotype, whereby simultaneous contraction of dorsal and ventral muscles is observed. Further research by Bamber and colleagues (1999) showed that *unc-49* is alternatively spliced to form three subunits with identical N-terminal domains but different C-terminal regions (figure 11). Alternative splicing also occurs in some $GABA_A$ subunits.

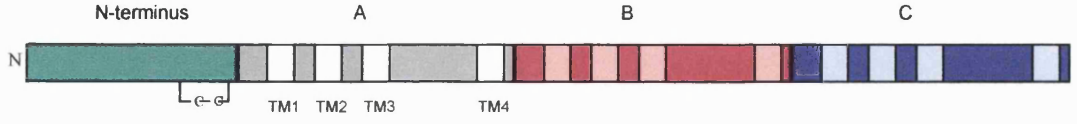

Figure 11 The *unc-49* gene arrangement. A single copy of the N-terminus is present followed by three tandem copies of the C-terminal region. The LGIC conserved cysteine loop and transmembrane regions are indicated. The mRNA is spliced such that three subunits are encoded containing common N-terminal domains.

The resulting GABA receptor subunits all contain conserved residues for GABA binding, anion selectivity and phosphorylation. Localisation studies demonstrated co-expression of UNC-49B and -C mainly at neuromuscular junctions, with the most intense staining in the head and body wall. They also co-assemble *in vitro* in *Xenopus* oocytes to form a functional receptor with GABA-induced chloride currents, which are lower in cells co-expressing these subunits than in those expressing only UNC-49B. Analysis of *unc-49* mutations indicated that only UNC-49B is essential for receptor function and this subunit is expressed without UNC-49C in the sphincter muscle. It is thought that the observed decrease in chloride conductance when subunits are co-expressed may indicate a method for regulation of channel properties *in vivo* in certain cells or developmental stages by combining different subunits. UNC-49A is expressed at very low levels and its localisation and role *in vivo* is unknown.

Approximately thirty genes have been identified in *C.elegans* with some level of homology to known GABA, glutamate and glycine receptors (Bargmann, 1998), but sequence analysis suggest that only two of these are likely to encode additional GABA receptor subunits (Bamber *et al.*, 1999). These may form a distinct receptor sub-type in a particular neuron or muscle other than those required for locomotion, or they may co-localise with UNC-49 but require UNC-49 for GABA activation.

1.3.3.2.2 Nicotinic acetylcholine receptor

More than forty nicotinic acetylcholine receptor genes are predicted by the *C.elegans* genome project (Bargmann, 1998). Once again, the pharmacology of these receptors, as assessed by studies on body muscle, is indicative of a class of receptors that are similar to their vertebrate counterparts, but some differences are seen (Colquhoun *et al.*, 1991; Colquhoun *et al.*, 1993; Avery and Horvitz, 1990; Lewis *et al.*, 1980). None of the vertebrate nicotinic acetylcholine receptor (nAChR) antagonists are very potent at the nematode receptor and the imidathiazole class of anthelmintics are potent agonists of the nematode, but not the vertebrate receptor.

A number of confirmed nAChR subunits have been cloned and characterised from *C.elegans* and all show the hallmarks of the LGIC superfamily. Investigation of levamisole-resistant mutants led to the discovery of three nAChR genes, one α and two non-α (Lewis *et al.*, 1980; Lewis *et al.*, 1987; Fleming *et al.*, 1996). Mutations in two of these, *unc-38* and *unc-29*, results in a very uncoordinated phenotype and, coupled with their localisation mainly to neuromuscular junctions, this suggests these subunits are part of the locomotory nAChR. The complete loss of levamisole sensitivity in these double mutants suggests that the two subunits co-exist in the same receptor and their co-expression in *Xenopus* oocytes results in the formation of a functional receptor that is gated by both levamisole and ACh. Homologues of *unc-38* and/or *unc-29* have been cloned from the parasitic nematodes *T.columbriformis*, *O.volvulus* and *H.contortus* (Donelson *et al.*, 1988; Fleming *et al.*, 1996; Wiley *et al.*, 1996; Hoekstra *et al.*, 1997).

The presence of residual locomotory function and a response to ACh in *unc-38/unc-29* mutants implies that other subunits also exist. Further alpha subunits have been identified and cloned (Mongan *et al.*, 1998) including *ce-21* and *deg-3*, which show the highest sequence similarity to vertebrate α7 subtype (Ballivet *et al.*, 1996; Treinin and Chalfie, 1995). Expression of *ce-21* in *Xenopus* oocytes results in a functional cation channel that is gated by both nicotine and ACh, but not levamisole. *Deg-3* is expressed by a small subset of sensory neurons suggesting differential expression of nAChR subunits depending on cell type and required function. Cloned non-α subunits include *acr-2*, which is expressed in multiple motor neurons and mutants of which have a shrinking uncoordinated phenotype (Squire *et al.*, 1995), acr-3 (Baylis *et al.*, 1997) and *ce-13* (Ballivet *et al.*, 1996) as well as the levamisole resistance subunits *unc-29* and *lev-1*. Homomeric expression of non-α subunits does not result in a functional receptor, but co-injection into *Xenopus* oocytes with *unc-38* results in levamisole-induced currents. Localisation of unc-38 to neurons as well as neuromuscular junctions suggests that this subunit may associate *in vivo* with subunits other than those implicated in levamisole sensitivity. Two AChR gene products, EAT-2,

a β subunit, and EAT-18, have been localised to the pharynx and mutant analysis indicates they may be involved in the control of pharyngeal pumping (Raizen *et al.*, 1995; McKay, Raizen and Avery, personal communication).

1.3.3.2.3 Glutamate-gated chloride channel receptors

Investigations into the mode of action of the avermectins and milbemycins (AM) led to the discovery of a novel class of inhibitory ionotropic receptor, the glutamate-gated chloride channel (GluCl). The AM were known to have an inhibitory action on motorneurons and muscle and fast activation of chloride channels was observed, but their site of action was elusive (section 1.2.3.4). Following the discovery of high affinity ivermectin-binding sites (K_d=0.2 nM) on *C.elegans* membrane (Schaeffer and Haines, 1989), poly $[A]^+$ RNA from this species was size-fractionated on a 10-30% sucrose gradient and injected into *Xenopus laevis* oocytes for pharmacological analysis (Arena *et al.*, 1991). A mRNA fragment of between 1 and 2.5 kb encoded a protein which responded to both ivermectin phosphate (EC_{50} = 90 nM) and L-glutamate (EC_{50} = 350 μM) by increasing the membrane permeability to chloride ions (Arena *et al.*, 1992). Glutamate activates fast, reversible, desensitising chloride current whereas the ivermectin response is slower and essentially irreversible. The application of maximal concentrations of ivermectin significantly decreases responses to glutamate and low concentrations of ivermectin (2 nM) potentiate the glutamate response (EC_{50} reduced from 350 μM to 80 μM) suggesting that the two ligands are acting at the same channel. A structural analogue of L-glutamate, ibotenate, also activates the same chloride channel and with higher potency than glutamate (EC_{50} = 87 μM), but the channel is GABA insensitive. The chloride channel blockers flufenamate (100 μM) and picrotoxin (500 μM) decrease the glutamate- or ivermectin-induced current, but no vertebrate glutamate-gated cation channel agonists or antagonists significantly altered the glutamate response.

The first GluCl subunits, GluClα and GluClβ were found by cloning cDNA from the mRNA fractions that elicited responses to glutamate and/or ivermectin (Cully *et al.*, 1994). These subunits showed all the features of a

typical cLGIC, but had an additional pair of cysteines in the extracellular domain, as do the vertebrate glycine receptor subunits. Molecular phylogenetic analysis indicated that these subunits share a common ancestral gene with the vertebrate $GABA_A$ and glycine receptors, but form a distinct sub-branch of the cLGIC superfamily which is orthologous to the glycine receptor alpha subunit (Cully *et al.*, 1996; Vassilatis *et al.*, 1997a). Both subunits form functional homomeric chloride channel receptors when expressed in *Xenopus* oocytes, although similarity to other LGIC predicts that the *in vivo* receptor is heteromeric. The α subunit is gated by ivermectin but not glutamate and the β subunit is gated only by glutamate, suggesting that different binding sites are present and giving further support to the idea that the functional receptor is heteromeric. The presence of a glutamate-binding site in the N-terminal region of the alpha subunit that is not coupled to channel gating suggests that all subunits may have the constituents for ligand binding, but that combinations of subunits are required for a functional channel (Etter *et al.*, 1996).

Co-expression of GluClα, 1.4 kb, and GluClβ, 1.3 kb, resulted in a chloride channel gated by both glutamate and ivermectin with broadly similar responses to those seen with *C.elegans* poly $[A]^+$ RNA. Closer inspection of channel properties highlighted some differences including an increase in the glutamate EC_{50} (350 μM to 1,360 μM) and a reversed order of potency for glutamate and ibotenate, suggesting that they do not associate *in vivo* and that further GluCl subunits are present. This was confirmed by studies on a *C.elegans* strain with an inactive GluClα gene as these mutants were still ivermectin sensitive, although a decrease in the number of ivermectin binding sites in their membrane and a reduction in the glutamate and ivermectin-induced amplitude when their mRNA was expressed in *Xenopus* were noted (Vassilatis *et al.*, 1997b). This led to the cloning of another alpha subunit, GluClα2 (*avr-15*), with 75% amino acid identity to α1. The GluClα2 gene is alternatively spliced producing a long form, 2.2 kb, with an extended N-terminal region and a shorter form, 1.7 kb, with a N-terminal region of a similar length to other GluCl (Dent *et al.*, 1997). Both subunits show typical

features of the cLGIC and have the additional cysteine pair in the N-terminus. The function of the longer N-terminus is not known. Homomeric expression led to a channel irreversibly activated by ivermectin (EC_{50} = 107 nM) and reversibly by glutamate (EC_{50} = 208 μM). Co-assembly with GluClβ produced a receptor with similar properties to those initially seen with injection of *C.elegans* mRNA proffering this as a naturally occurring combination.

One of the effects of ivermectin is the inhibition of pharyngeal pumping. The presence of GluClα2 in the pharynx was implicated by a cessation of the fast inhibitory glutamatergic response to the M3 motorneuron in the pharynx of *avr-15* mutants (Dent *et al.*, 1997). This was followed by its localisation, by GFP-fusion, to the pharyngeal muscle and this pattern of expression overlapped with that of GluClβ, as recorded by lac-Z reporter gene constructs (Laughton *et al.*, 1997b). This suggests that these subunits probably co-assemble in the functional receptor and that GluClα2 is an essential component of the pharyngeal receptor. Other subunits must also exist which are responsible for the organisms reduced motility in response to the AM.

Additional subunits cloned from *C.elegans* include another α-subunit *glc-3* that forms functional homomeric channels gated by both ivermectin and glutamate (Horoszok *et al*, in press) and another alternatively spliced gene, *gbr-2* (*avr-14*) (Laughton *et al.*, 1997a). The subunits encoded by *gbr-2* share N-terminal regions, but splicing just prior to the TM1 results in polypeptides with different transmembrane domains (figure 12). This suggests that the ligand-binding domains will be similar, but that the two isotypes will have differing channel properties. The gbr-2a cDNA is unusual in that it contains the transmembrane regions of the gbr-2b subunit as an open reading frame in its untranslated region.

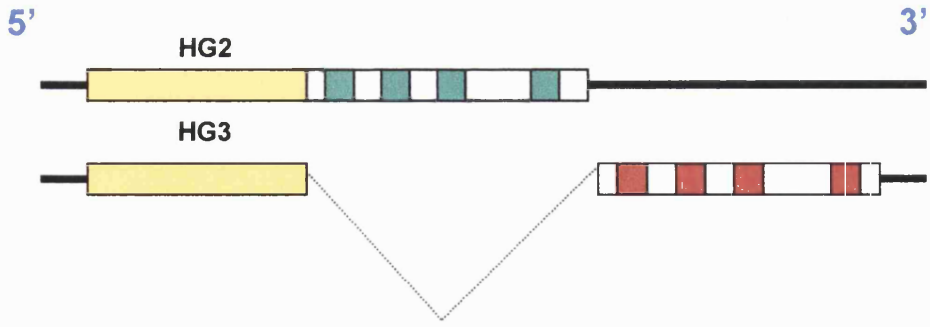

Figure 12 Alternative splicing of *gbr-2*. The encoded subunits have identical N-terminal domains (in yellow) but different transmembrane regions (red/green). Sequences for the transmembrane regions of HG3 are present within the untranslated region of HG2.

Sequence identity to other alpha subunits is only 45-55%, which is too low to assign them additional members of the alpha subtype, but neither are they similar to the GluClβ subunit. Expression of *gbr-2* has been demonstrated in the extrapharyngeal neurons in the ring ganglia of the head, motorneurons in the ventral nerve cord and mechanosensory neurons suggesting differential expression of GluCl subunits in nematodes.

Glutamate-gated chloride channel receptor subunits have also been identified in parasitic nematodes (appendix 1). In molecular terms, the species in which the GluCl have been studied in most detail is *Haemonchus contortus*. Three genes encoding four GluCl subunits are known in this species and these show a high level of sequence identity with the *C.elegans* GluCl (appendix 1). Orthologues of two *C.elegans* GluCl genes were identified in *H.contortus*, including a β-subunit, HG4, which shares 82% amino acid identity with its *C.elegans* counterpart, ce-gluclβ (Delany *et al.*, 1998). In contrast to ce-gluclβ, antibodies to HG4 localised its expression to motor neuron commissures in the mid-body portion of the worm and to the nerve cords, suggesting a role in locomotion. The expression pattern of HG4 is identical to the non-pharyngeal regions inhibited by the AM implying that this subunit, probably in combination with one or more different subunits, may be responsible for the effects of AM on motility. This is in agreement with the findings of Kass *et al.* (1980) as the activation of GluCl on

motorneurons may modulate their transmission of excitatory signals. Evidence for the involvement of GluCl, rather than GABA, receptors includes the picrotoxin sensitivity of these neurons, as nematode GABA receptors appear to be insensitive to this toxin (Holden-Dye *et al.*, 1988). Gbr-2 orthologues have also been cloned from both *H.contortus* and *A.suum*, but the pattern of alternative splicing is only conserved in *H.contortus* and the expression pattern of these subunits has yet to be investigated (Jagannathan *et al.*, 1999). An additional subunit, HG5, with no clear *C.elegans* orthologue is also present in *H.contortus* (Delany, 1998). This subunit shows highest similarity to the *C.elegans* alpha subunits (appendix 5).

The AM also target the nematode pharynx resulting in inhibition of pharyngeal pumping in *H.contortus* and coupled with an observed increase in chloride ion conductance of *A.suum* pharyngeal muscle following application of ivermectin or glutamate this implies the presence of GluCl receptors in the pharynx of at least these parasitic nematodes (Martin, 1996; Adelsberger *et al.*, 1997). It is probable that further GluCl subunits are still to be identified from *H.contortus*.

As yet, there have been no published tests of the ability of the AM to interact with recombinant GluCl from parasitic nematodes. High affinity binding has been recorded to *H.contortus* whole membrane preparations and ivermectin is known to gate channels formed by some *C.elegans* GluCl subunits. Knowledge of the interaction of the AM with their target site would be interesting from both a scientific and a commercial perspective. Characterisation of GluCl from parasites may also shed some light on the development of resistance to the AM.

1.4 Aims of this research

The major goal of this research is to assess the pharmacology of the *H.contortus* GluCl receptor subunits. Although the full-length sequences of four *H.contortus* GluCl are deposited in the EMBL database, two of these remain to be cloned. The full-lengths of these two GluCl receptor subunits

are to be amplified and cloned. All four GluCl subunits will be characterised by radioligand binding studies, following their expression in mammalian cell lines, to determine which, if any, form part of the ivermectin-binding site. Further analysis of their pharmacology will then be undertaken by competing against the [^{3}H] ivermectin binding with other ligands, such as avermectin derivatives. The rapidly increasing spread of resistance to the four major classes of anthelmintic will have catastrophic consequences if it is allowed to continue and no alternative therapies are introduced. Alterations in the major target of the avermectin/milbemycin (AM) class of anthelmintics, the GluCl, may be involved in resistance to these drugs and comparison of receptors from ivermectin-sensitive and –resistant nematodes could improve understanding of the mechanism of AM resistance. All but one of the GluCl subunits have already been cloned from *H.contortus* field isolates that are resistant to ivermectin and no coding alterations that could be attributed to the development of resistance were identified. The remaining subunit, HG5, will be cloned from ivermectin-resistant *H.contortus* to uncover any sequence alterations. If differences are present, expression studies will be carried out and the pharmacology compared with HG5 from ivermectin-sensitive worms.

2. Materials and Methods

2.1 General materials

2.1.1 Molecular biology reagents

Molecular biology grade chemicals were purchased from BDH chemicals (Poole, UK) Sigma Chemical Company Ltd (Poole, UK) or Fisons Scientific Equipment (Leicestershire, UK) Agarose was supplied by Biogene Ltd. (Kimbolton, UK) and ethidium bromide and diethyl pyrocarbonate (DEPC) by Sigma.

2.1.1.1 Enzymes

Restriction endonucleases and their buffers (10 x) were supplied by NEB (Hitchin, UK). T4 DNA ligase was from Gibco BRL (Renfrewshire, Scotland)

Enzyme	**Buffer Components**
T4 DNA Ligase	50 mM Tris-Cl (pH 7.5), 10 mM $MgCl_2$, 10 mM dithiothreitol, 1 mM ATP, 25 μg/ml BSA
BamHI	Buffer 2: 150 mM NaCl, 10 mM Tris-Cl, 10 mM $MgCl_2$, 1 mM dithiothreitol (pH 7.9 @ 25°C). Supplemented with 100 μg/ml BSA
ClaI	Buffer 4: 50 mM potassium acetate, 20 mM Tris-acetate, 10 mM magnesium acetate, 1 mM dithiothreitol ((pH 7.9 @ 25°C). supplemented with 100 μg/ml BSA
EcoRI	Unique Buffer: 50 mM NaCl, 100 mM Tris-HCl, 10 mM $MgCl_2$, 0.025% Triton X-100 (pH 7.5 @ 25°C)
HindIII	Buffer 2
KpnI	Buffer 1: 10 mM Bis Tris Propane HCl, 10 mM $MgCl_2$, 1 mM dithiothreitol (pH 7 @

	25°C) supplemented with 100 μg/ml BSA
NdeI	Buffer 4
NruI	Unique buffer: 100 mM KCl, 50 mM Tris-Cl, 10 mM $MgCl_2$ (pH 7.7 @ 25°C)
XbaI	Buffer 2 supplemented with 100 μg/ml BSA
XhoI	Buffer 2 supplemented with 100 μg/ml BSA

2.1.2 General Buffer Compositions

Buffer	**Components**
50 x TAE	2 M Tris Acetate, 50 mM EDTA; pH 8
10 x TBE	0.89 M Tris-Cl, 0.89 M boric acid, 20 mM EDTA; pH 8.0
TE	10 mM Tris-Cl, 1 mM EDTA; pH 7.6
PBS	140 mM NaCl, 2.7 mM KCL, 10 mM Na_2HPO_4, 1.76 mM KH_2PO_4; pH 7.4

2.1.3 Microbiological reagents

Media reagents were suppied by Difco laboratories (East Molesey, UK) and Sigma (Poole, UK) while glycerol was purchased from BDH (Poole, UK). Both IPTG and X-Gal were supplied by Alexis Corporation (Bingham, UK) and ampicillin, tetracycline and dimethylformamide were obtained from Sigma.

2.1.3.1 Bacterial culture media

Medium	**Components /L**
LB broth	10 g tryptone, 5 g yeast extract, 5 g NaCl
LB agar	As above with the addition of 15 g agar
SOC medium	20 g bacto-tryptone, 5 g yeast extract, 10 mM NaCl, 2.5 mM KCl, 10 mM $MgCl_2$, 10 mM $MgSO_4$, 20 mM glucose
DYT broth	16 g tryptone, 10 g yeast extract, 5 g NaCl

2.1.3.2 Bacterial strains and plasmids

Strain/Plasmid	Genotype	Supplier
E.coli XL1-Blue	SupE44, hsdR17, recA1, endA1, gyrA46, thi, relA1 lac-, F [ProAB+, LacIq, LacZ, delM15, Tn10(tetR)]	Invitrogen,
pBluescript	Amp^r ,lacZ, 2.96 kb	Stratagene
pCR®-Blunt II-TOPO	Kan^r, lacZα, Zeo^r, ccdB 3.6 kb	Invitrogen,
pFLAG-CMV-5c	CMV, hGH, amp^r, Flag, 4.7 kb	Sigma
pcDNA3	CMV, BGH, Amp^r, Neo^r 5.4kb	Stratagene

2.1.4 Cell culture reagents

L929 cells and COS 7 cells were supplied by European Collection of Cell Cultures (ECACC) (Salisbury, UK). These were maintained in Dulbecco's Modified Eagles Medium supplemented with 10% (v/v) Foetal Bovine Serum, 2 mM L-glutamine, 100,000 units penicillin and 100mg streptomycin (all Sigma). Trypsin EDTA was also supplied by Sigma. FuGENE™ 6 transfection reagent was purchased from Roche Molecular Biochemicals (Lewes, E.Sussex, UK) and G418 sterile-filtered solution was purchased from Calbiochem (Nottingham, UK).

2.1.5 Immunocytochemistry reagents

Mouse anti-flag monoclonal antibodies were supplied by Chemicon International (Harrow, UK). FITC-conjugated goat anti-mouse antibody was

purchased from Jackson Scientific, PA, USA. Vectashield® antifade mounting media was purchased from Vector Laboratories, CA. USA.

2.1.6 Radioligand binding

Coomassie® Plus Protein Assay Reagent Kit was supplied by Pierce (Rockford, USA). [^{3}H] ivermectin (specific activity 1.74TBq/mmol) custom synthesised by Amersham International (Bucks., UK) was a gift from Pfizer (Sandwich, UK). Unlabelled ivermectin (avermectin B1), HEPES, Triton X-100, polyethyleneimine (PEI), PMSF, leupeptin and pepstatin were from Sigma. UK compounds were a gift from Pfizer, (Sandwich, UK).

2.1.7 Western blotting and immunodetection

Chemicals were purchased from Sigma (Poole, UK). Electrode Paper Novablot filter paper, the Multiphor II Novablot electrophoretic transfer unit, the chemiluminescence ECL detection kit, nitrocellulose membrane and the rainbow molecular weight marker (10-250 kda) were from Amersham Pharmacia International (Aylesbury, UK). Anti-HG2 and -HG3 antibodies were purified from rabbits by Virginia Portillo.

2.2 Methods

2.2.1 General molecular biology methods

2.2.1.1 Agarose gel electrophoresis

Agarose gels were made by the addition of 1-1.5% (w/v) agarose to 1 x TAE or TBE buffer. The agarose was dissolved by heating in a microwave oven. Visualisation of DNA was achieved by the addition of 5 μg/ml ethidium bromide to this solution. Gels were poured in perspex gel rigs and allowed to set before running in 1 x TAE or TBE in horizontal gel apparatus. DNA samples were loaded with 0.25 vol. loading dye (15% (w/v) Ficoll, 0.25% (w/v) bromophenol blue, 0.25% (w/v) xylene cyanol) into the gel. Molecular weight markers were also run (100 bp, 1 kb or PstI cut lambda DNA).

2.2.1.2 Purification of DNA from agarose gels

The "Geneclean II®" method was used for purification (Bio101, La Jolla, USA). The DNA band was excised from a TBE agarose gel and weighed in a microcentrifuge tube. The gel slice was incubated at 55°C with 4.5 volumes 6M NaI and 0.5 volumes "TBE modifier" until the agarose slice had completely dissolved (5-6min). "Glassmilk" silica matrix (5 μl) was added and the tube was incubated on ice for 5 min with occasional resuspension of resin. This was followed by a 5 second pulse in a microcentrifuge, removal of supernatant and resuspension of resin in 700 μl of "New Wash" (NaCl/Tris/EDTA in 95% (v/v) ethanol). This was centrifuged for 5 seconds and the wash procedure repeated twice more. DNA was then eluted by the addition of 5μl TE buffer followed by incubation of the tube for 3 min at 55°C. The suspension was centrifuged for 30 sec to make a solid pellet and the supernatant containing the DNA was removed.

2.2.1.3 Restriction endonuclease digestion of DNA

DNA samples of 1-5μg were digested with one or two restriction enzymes (10-20 units) in the reaction buffer (4 μl) recommended by the manufacturer. Sterile water was added to a volume of 40 μl and the reaction incubated at 37°C for 1-4 hours.

2.2.1.4 Phenol/Choroform extraction and ethanol precipitation of DNA

Phenol (Tris-equilibrated, pH 8), chlorofom and isoamyl alcohol were added to restriction digested DNA in the ratio 25:24:1 in a sterile microfuge tube. This was shaken to form a milky suspension and spun at 12,000 x g for 1 min. The top aqueous layer was then transferred to a clean microfuge tube and an equal volume of chloroform added before centrifugation at 12,000 x g for 1 min. The top aqueous layer was again transferred to a new tube and 1/10 vol. sodium acetate (3 M pH 5.3) and 2 x vol. ethanol were added. This was left at 4°C overnight to allow precipitation of DNA. The solution was then spun at 12,000 x g for 1 hour at 4°C before washing the pellet in 75% (v/v) ethanol for 1 hour at 12,000 x g at 4°C. The DNA pellet was dried and resuspended in ddH_2O.

2.2.1.5 Ligation of DNA

Approximately 200 ng of linerised plasmid DNA were mixed with the fragment to be subcloned in a 1:1 vector:fragment molar ratio. T4 DNA ligase (1 unit) and 10x ligase buffer (2 μl) (250 mM Tris-Cl, pH 7.5, 100 mM $MgCl_2$, 100 mM DTT, 4 mM ATP, 50 μg/ml BSA) were added and the contents mixed. Ligations were carried out at 16°C overnight.

2.2.1.6 Preparation of *E.coli* competent cells

XL-1 Blue cells were made competent using calcium chloride. DYT (50 ml) was inoculated with 0.5 ml fresh overnight cultured XL-1 Blue cells in a 250 ml conical flask. This was incubated at 37°C with shaking until the $O.D._{550}$ reached 0.3. The culture was then rapidly chilled and centrifuged at 4,500 x g for 15 min at 4°C. Cells were resuspended in 20 ml of ice-cold 100 mM $CaCl_2$. Following 20 min on ice, cells were centrifuged at 4,500 x g for 15 min and resuspended in 2 ml ice-cold $CaCl_2$. The cells were transformed immediately.

2.2.1.7 Transformation of competent cells

Competent cells (300 μl) were mixed with 5 μl of the ligated DNA mixture in pre-chilled microfuge tubes and left on ice for 45 min. Cells were heat-shocked for 2 min at 42°C and then chilled on ice for 2 min. DYT (1ml) was added and the cells incubated for 1 hour at 37°C before plating onto LB agar containing 50 μg/ml ampicillin. After overnight incubation at 37°C individual colonies were transferred to 5 ml LB broth containing 50 μg/ml ampicillin. This was incubated overnight with at 37°C with shaking.

2.2.1.8 Small-scale preparation of plasmid DNA

The CONCERT™ Rapid Plasmid Purification System (Gibco BRI, Refrewenshire, UK) was used to isolate plasmid DNA from bacterial cultures.

Solution	Components
Cell suspension buffer	50 mM Tris-HCl (pH 8), 10 mM EDTA
Rnase A	20 mg/ml in water
Cell lysis solution	200 mM NaOH, 1% SDS (w/v)
Neutralization buffer	contains acetate and guanidine hydrochloride
Wash buffer	contains NaCl, EDTA and Tris-HCl (pH 8)

An overnight culture (3-5 ml) was centrifuged at 12,000 x g for 2 min. and all medium removed. The resulting pellet was resuspended in 210 μl cell suspension buffer (containing Rnase A) to form a homogenous solution. Cell lysis solution (210 μl) was added and mixed by inversion before incubation at room temperature for 5 min to produce a clear solution. Neutralisation buffer (280 μl) was added and the solution mixed by inversion before centrifugation of samples at 12,000 x g for 10 min. The resulting supernatant was placed into a spin cartridge, containing silica-based membranes where the plasmid DNA is selectively absorbed, which was contained in a 2 ml wash tube. Following removal of the flow-through the column was washed with 700 μl wash buffer at 12,000 x g for 1 min. DNA was eluted by the addition of 75 μl warm TE buffer, incubation for 1 min at room temperature and then final centrifugation at 12,000 x g for 2 min.

2.2.1.9 Large-scale plasmid preparations using the Qiagen Plasmid Maxikit (Qiagen, Surrey, UK)

Bacterial cells were cultured overnight in 100 ml LB broth. These were harvested by centrifugation at 6,000 x g for 15 min at 4°C.

Buffer	Composition
Resuspension Buffer	50 mM Tris-HCl, pH 8.0, 10 mM EDTA, 100 μg/ml RNaseA
Lysis Buffer	200 mM NaOH, 1% (w/v) SDS
Neutralisation Buffer	3.0 M potassium acetate, pH 5.5
Equilibration Buffer	750 mM NaCl, 50 mM MOPS, pH 7.0,

	15% (v/v) isopropanol, 0.15% (v/v) Triton®X-100
Wash Buffer	1.0 M NaCl, 50 mM MOPS, pH 7.0, 15% (v/v) isopropanol
Elution Buffer	1.25 M NaCl, 50 mM Tris-HCl, pH 8.5, 15% (v/v) isopropanol

The pelleted cells were completely resuspended in 10 ml resuspension buffer and then lysed in 10 ml lysis buffer for 5 min. Chilled neutralisation buffer (10 ml) was added and after mixing the sample was incubated on ice for 20 min. The sample was mixed again and centrifuged at 20,000 x g for 30 min at 4°C. The supernatant was re-centrifuged at 20,000 x g for 15 min at 4°C and the resulting clear supernatant was applied to an equilibrated Qiagen-tip 500 and allowed to move through by gravity flow. The tip was washed twice with 30 ml wash buffer to remove contaminants. Elution buffer was applied to the tip and eluted plasmid DNA was precipitated by the addition of 10.5 ml room temperature isopropanol followed by centrifugation at 15,000 x g for 30 min at 4°C. Precipitated salts were removed from the resulting pellet by two 70% (v/v) ethanol washes. Plasmid DNA was dissolved in TE, pH 8.0.

2.2.2 Production of mRNA from *Haemonchus contortus*

2.2.2.1 Isolation and purification of *H.contortus* eggs

Worm-free lambs were experimentally infected (G .Coles, University of Bristol, Bristol UK) with 5000 *H.contortus* larvae of either the wild type isolate, susceptible to anthelmintics, or the South African White River isolate, resistant to anthelmintics (van Wyk and Malan, 1988). The lambs were maintained in an indoor helminth-free environment. Faeces were collected overnight in polythene nappies approximately 3 weeks post-infection. Faeces were homogenised in a blender with an equal volume of water to a thin paste. The mixture was washed through a 158 μm pore sized sieve removing the majority of the debris and allowing eggs and liquid to be

collected in a jug. The filtrate was centrifuged at 1,500 rpm for 2 min. The supernatant was discarded and another 50 ml filtrate was added and spun down as before. This was repeated until approximately a 5 ml pellet was observed. The pellet was then resuspended in a saturated NaCl solution until a meniscus formed over the top of the tube. A large glass cover slip was placed over the top, ensuring no air bubbles were present and the tubes were spun at 1,000 rpm for 2 min. A film of eggs was then observed on the cover slips and this was quickly washed with distilled water into a new Falcon™ tube and spun at 1,500 rpm for 2 min. The supernatant was removed and the eggs weighed into cryotubes and frozen under liquid nitrogen.

2.2.2.2 Isolation of adult *H.contortus*

An *H.contortus* infected sheep was slaughtered and had its abomasum removed. The stomach lining was cut through and contents washed out with water (G.Coles, University of Bristol, Bristol, UK). It was then placed into an isolation apparatus (figure 13) containing DMEM and kept at 37°C using a heat-emitting lamp. Adult worms detached themselves from the gut lining and were collected live in a Falcon tube. Worms were washed in clean DMEM (37°C) to removed debris before transferring them to cryotubes. These were centrifuged at 1,500 rpm for 2 min and all liquid removed before freezing them in liquid nitrogen.

2.2.2.3 Isolation of total RNA from *H. contortus* adults and eggs

Total RNA was isolated using TRIzol® Total RNA Isolation Reagent, a monophasic solution of phenol and guanidine isothiocyanate (Life Technologies. Paisley, UK) developed from the single-step RNA isolation method described by Chomczynski and Sacchi (1987). Frozen tissue was ground to a powder under liquid nitrogen. The powder was rapidly dispersed in 10 ml TRIzol® Reagent per 1 g tissue and homogenised in a glass Teflon homogeniser before transfer to a 30 ml Corex tube. This was incubated at

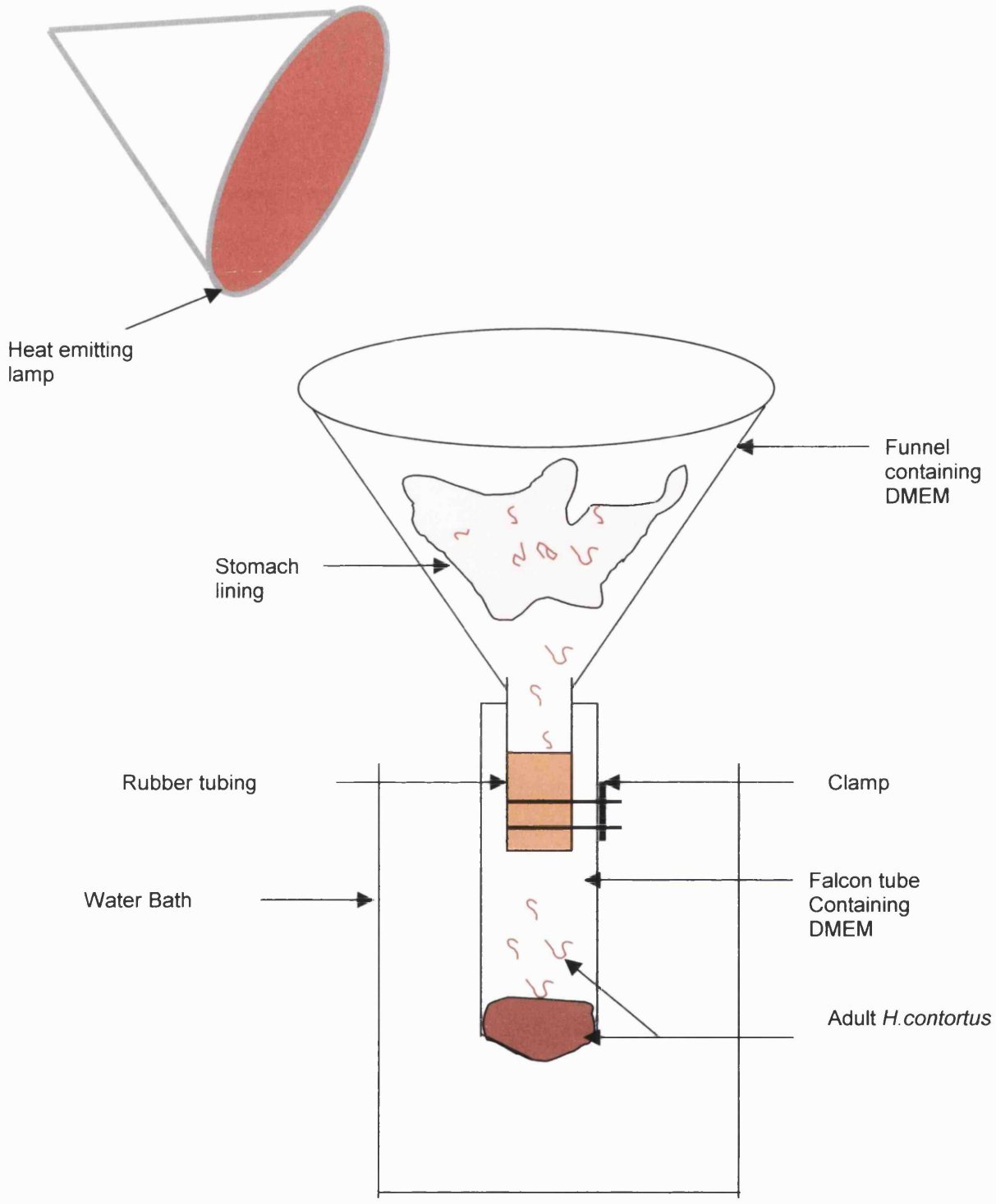

Figure 13 Isolation apparatus for *H.contortus* adults. Designed by G.Coles, University of Bristol.

room temperature for 5 min to permit the complete dissociation of nucleoprotein complexes. 2 ml chloroform was added per 10 ml TRIzol® and the tubes vigorously shaken for 15 seconds. The samples were incubated for a further 3 min at room temperature before centrifugation at 12,000 x *g* for 15 min at 4°C. The upper aqueous phase, containing the RNA, was transferred to another Corex tube and the RNA was precipitated by the addition of 5 ml isopropanol per 10 ml TRIzol® used for the initial homogenisation. Samples were incubated at room temperature for 10 min and centrifuged at 12,000 x *g* for 10 min at 4°C. The supernatant was removed and the RNA pellet resuspended in 10 ml 75% (v/v) ethanol per 10 ml TRIzol® initially used. Samples were then centrifuged at 7,500 x *g* for 5 min at 4°C. The RNA pellet was vacuum dried for 5 min and dissolved in 0.5% (w/v) SDS by passing a few times through a pipette tip and incubating for 10 min at 55-60°C.

2.2.2.4 Quantitation of RNA solutions

The amount of total RNA isolated was estimated by determining the $O.D._{260}$ of a 1:100 dilution of the sample in DEPC-treated sterile ddH_2O using a spectrophotometer. A 1:100 dilution of 0.5% (w/v) SDS in sterile ddH_2O was used as a blank. The concentration was calculated using the equation:

RNA $\quad Absorbance_{260} \times 40 \times$ dilution factor

Standards: 1 O.D. unit for RNA corresponds to a concentration of 40 μg/ml

The ratio of $O.D_{260}/O.D_{280}$ was also determined as an indication of purity.

2.2.2.5 Purification of mRNA

Poly-$[A]^+$ RNA was isolated using Dynabeads®oligo $(dT)_{25}$ magnetic beads (Dynal, Wirral, UK), 2.8 μm in diameter, with a 25 nucleotide long chain of deoxythymidylate attached covalently to the bead surface via a 5' linker group.

Buffer	Components
Binding buffer	20 mM Tris-Cl; pH 7.5, 1 M LiCl, 2 mM EDTA
Washing buffer	10 mM Tris-Cl; pH 7.5, 0.15 M LiCl, 1 mM EDTA
Tris-HCl	10 mM Tris-Cl; pH 7.5

Beads were stored in PBS containing 0.02% (w/v) NaN_3. A sample (0.2 ml, 1 mg) of bead suspension was transferred to a 1.5 ml microfuge tube and this was placed into a Dynal MPC®-E magnetic particle concentrator and the supernatant removed. The beads were washed by the addition and removal of 100 µl 2x binding buffer followed by resuspension in 100 µl 2x binding buffer. 200 µg total RNA was dissolved in 100 µl DEPC-treated water, heated for 2 min at 65°C to disrupt secondary structure and added to the washed beads. The mRNA was allowed to anneal for 5 min on a rotating platform at room temperature and then placed on the concentrator to allow removal of the supernatant. The beads were washed twice with 200 µl washing buffer and re-suspended in 30 µl elution buffer before heating at 65°C for 2 min. Eluted poly $[A]^+$ RNA was extracted immediately after separation from the beads and used directly for northern blot or RT-PCR.

2.2.3 Northern Blot Analysis

Solution	Components
10 x MESA*	200 mM MOPS, 50 mM Sodium Acetate, 10 mM EDTA; pH 7.0
Electrophoresis buffer*	1 x MESA
Formaldehyde gel loading buffer*	7.2 ml deionised formamide, 1.6 ml 10 x MESA, 2.6 ml deionised formaldehyde, 2.6 ml water, 1 ml 80% glycerol, 0.01% (v/v)

	bromophenol blue
Formaldehyde	Commercially available as a 37% (w/v) solution (12.3 M) in water
DIG Easy-hyb buffer*	Commercially available hybridization buffer granules reconstituted in water (Roche Molecular Biochemicals, E. Sussex, UK))
20 x SSC*	3 M NaCl, 300 mM sodium citrate; pH 7
Maleic acid buffer*	100 mM maleic acid, 150 mM NaCl; pH 7.5
Blocking solution*	Commercially available solution diluted 1:10 in maleic acid buffer (Roche Molecular Biochemicals, E. Sussex, UK)
Detection Buffer*	100 mM Tris-Cl, 100 mM NaCl; pH 9.5

*RNase-free solutions were prepared in 0.1% DEPC treated water

2.2.3.1 Labelling RNA with Digoxigenin (DIG) labeled UTP mix

A 200-500 bp fragment of the gene of interest was sub-cloned into pBluescript SK^+ vector. The recombinant plasmid was linearised downstream of the cloned sequence by restriction digestion allowing the creation of run-off transcripts of uniform length. This was followed by purification of the DNA by phenol/chloroform extraction and ethanol precipitation. The labelling reaction was then set up as follows: 1 μg purified DNA template, 2 μl NTP labeling mix (10 mM ATP, 10 mM CTP, 10 mM GTP, 6.5 mM UTP, 3.5 mM DIG UTP; in Tris-Cl, pH 7.5), 2 μl 10 x transcription buffer (400 mM Tris-Cl, pH 8; 60 mM $MgCl_2$, 100 mM dithioerythritol, 20 mM spermidine, 100 mM NaCl), 0.5 μl RNase inhibitor (20 units/μl), DEPC-treated (Roche Molecular Biochemicals, E. Sussex, UK). Following mixing and brief centrifugation, this reaction was allowed to proceed at 37°C for 2 hr before the addition of 2 μl RNase free, DNase I (10 units/μl) for a further 15 min at 37°C. 200 mM EDTA, pH8 (2μl) was added to terminate the reaction.

2.2.3.1.1 Estimation of yield of DIG-labelled RNA

The yield of DIG-labelled RNA was estimated by comparison against labelled control RNA in a spot test. Labelled control RNA (5 µl) was mixed with 20 µl DEPC-treated water (final concentration 20 ng/µl). This was then diluted using the following scheme:

DIG-labelled control RNA starting concentration	Stepwise dilution	Final concentration
20 ng/µl	1:20	1 ng/µl
1 ng/µl	1:10	100 pg/µl
100 pg/µl	1:10	10 pg/µl
10 pg/µl	1:10	1 pg/µl
1 pg/µl	1:10	0.1 pg/µl
0.1 pg/µl	1:10	0.01 pg/µl

The experimental probe was diluted in the same way. Each control dilution (1 µl) was then spotted on a piece of dry positively charged nylon membrane (Roche Boehringer Mannheim). The experimental RNA dilutions were spotted on a second row and the nucleic acids were fixed to the membrane by UV cross-linking for 5 min. The membrane was briefly washed in washing buffer (maleic acid buffer with 0.3% (v/v) Tween®20) before incubation in blocking buffer for 30 min. Anti-DIG antibody was diluted 1:10,000 in blocking buffer and the membrane was incubated for 30 min in the diluted antibody solution at room temperature. The membrane was washed twice, 15 min per wash, in washing buffer at room temperature before equilibration of membrane in detection buffer for 2 min. A 1:100 dilution of CSPD® (25 mM Disodium 3-(4-methoxyspiro {1,2-dioxetane-3,2'-(5'-chloro)tricyclo[3.3.1.1^{3,7}]decan}-4-yl) phenyl phosphate) in detection buffer was carried out before applying 0.5 ml of this chemiluminescent substrate dropwise to the membrane between two sheets of acetate. The acetate was sealed at all sides using a heat sealer and the filter was incubated at 37°C

for 15 min to shorten exposure time. The membrane was then exposed to X-ray film for 2 hours.

2.2.3.2 Denaturing formaldehyde gel electrophoresis

Agarose (1 g) was added to 124 ml DEPC treated water in a conical flask and heated in a microwave to melt the agarose. 10 x MESA (15 ml) and 11 ml 37% (w/v) formaldehyde were added and following swirling to mix the gel was poured immediately in a perspex gel rig, and left to set. All apparatus was pre-treated with 1% (v/v) hydrogen peroxide to denature RNAses. The gel rig was placed in a horizontal electrophoresis tank and 1 x MESA was added until the gel was submerged. Samples were prepared by mixing poly $[A]^+$, or total, RNA with 10-20 μl freshly prepared formaldehyde gel loading buffer and the DIG-labelled RNA molecular weight marker was prepared by the addition of 16 μl loading buffer to 4 μl marker. All samples were incubated at 65°C for 15 min and then chilled on ice. Samples were loaded onto the gel and the gel was run at 80V for 4 hours. The cast and gel were then transferred to a tupperware box and washed with 20 x SSC to remove formaldehyde.

2.2.3.3 Northern transfer

The RNA was blotted from the gel onto Boehringer positively charged nylon membrane by capillary transfer overnight at room temperature. RNA was then UV cross-linked to the membrane for 5 min.

2.2.3.4 Hybridisation and detection of Northern blot

Following removal of the marker lane, the blot was placed in a hybridisation bottle and incubated with 20 ml prehybridisation solution (DIG Easy Hyb, Roche Boehringer Mannheim) at 68°C for 1 hour. The DIG-labelled probe was meanwhile heat-denatured in a boiling water bath for 10 min and diluted in 5 ml prehybridisation solution to a concentration of 100 ng/ml (hybridisation buffer). Prehybridisation buffer was discarded and the blot was incubated with hybridisation buffer at 68°C overnight. Following hybridisation the blot was washed twice, 15 min per wash, in 2 x wash solution (2 x SSC,

containing 0.1% (w/v) SDS) at room temperature followed by 2 washes in 0.5 x wash solution (0.5 x SSC, containing 0.1% (w/v) SDS at 68°C. All further steps were carried out at room temperature unless stated. The marker lane was included in all further steps. The membrane was then equilibrated in washing buffer for 1 min (maleic acid buffer containing 0.3% (v/v) Tween®20). This was discarded and the membrane was blocked by gentle agitation in blocking solution for 1 hour. Anti-Digoxigenin antibody was meanwhile diluted 1:10 000 in blocking solution and the blot was then incubated in this solution, with gentle agitation for 30 min. The antibody solution was discarded and the membrane gently washed twice in washing buffer. The membrane was then equilibrated in detection buffer for 2 min. meanwhile CSPD® was diluted 1:100 in detection buffer. The membrane was placed between 2 sheets of acetate and 0.5 ml chemiluminescent substrate was scattered dropwise on the surface. The top sheet was then lowered and wiped with a damp tissue to remove air bubbles and the bag was sealed and incubated at room temperature for 5 min. To decrease time taken for the chemiluminescent substrate to reach equilibrium, the membrane was incubated at 37°C for 15 min before exposure to X-ray film overnight. Films were developed using a X-Ograph Compact X2 processor.

2.2.4 Amplification of cDNA

2.2.4.1 Oligonucleotide production

As full-length sequences of all genes investigated were available, gene specific primers were designed with the following common parameters: 1) The length of the primer was a minimum of 18 nucleotides. Each additional nucleotide made the primer four times more specific. 2) The terminal nucleotide in the primer had a G or C residue. 3) Primer pairs, particularly at 3' ends, were not complementary to each other to avoid primer-dimers. 4) Primers were best designed with ~50% GC content. Primer pairs were designed such that their GC content and Tm (melting temperature, defined as the dissociation of the primer/template duplex) were similar. 5)
The Tm was calculated using the equation (Lowe *et al.*, 1990)

$$Tm = 81.5+16.6(\log10(Na^+)) + \frac{41(G+C)-675}{A+G+C+T}$$

where Na^+ is assumed to be 0.1 M.

Oligonucleotides were custom synthesised by Life Technologies, Paisley, UK. They were supplied lyophilised and were reconstituted in sterile ddH_2O on receipt to give a stock concentration of 20 μM.

2.2.4.2 Reverse transcription-polymerase chain reaction (RT-PCR)

The Titan™ RT-PCR system (Roche Molecular Biochemicals) or Access RT-PCR (Promega, Madison, USA) were used to amplify cDNAs of interest. The Titan™ system uses the AMV reverse transcriptase for first strand synthesis and the Expand™High Fidelity enzyme blend, which consists of Taq DNA polymerase and Pwo DNA polymerase, for the PCR. The combination of thermostable Taq DNA polymerase and Pwo DNA polymerase allows 3'-5' proofreading to occur increasing the fidelity of the reaction. The Access System uses AMV reverse transcriptase for first strand synthesis and *Tfl* DNA polymerase for the PCR. Tfl DNA polymerase does not have 3' exonuclease activity. Poly $[A]^+$ RNA from wild-type *H.contortus* eggs was used for all full-length amplifications of subunits. Poly $[A]^+$ RNA from ivermectin resistant *H.contortus* adults was used for full length amplifications of subunits Total RNA was used for amplification from cell lines. All reactions were carried out on a PTC-150 hot-bonnet minicycler (GRI, Braintree, UK).

2.2.4.2.1 Titan™ RT-PCR system

A typical Titan™ reaction contained 4 μl dNTP mix (10 mM each triphosphate), 2.5 μl DTT (100 mM), 1 μl Rnase inhibitor (5 units/μl), 0.4 μM of both sense and anti-sense primers, 100 ng Poly $[A]^+$ RNA, 10 μl 5 x RT-PCR buffer, 1 μl RT-PCR enzyme mix (1 unit/μl) and nuclease-free water to give a final volume of 50 μl. Thermocycling conditions included an initial reverse transcription of 30 min at 55°C followed by denaturation of cDNA for 2 min at 94°C. This was followed by 30 sec at 94°C, primers were made to hybridise to the template at previously calculated annealing temperature for

30sec-1min and then strands were elongated at 72°C for 2 min and this was repeated for 40 cycles. Finally a 7 min step at 72°C was included to ensure the PCR fragments were fully elongated. The exact parameters of the temperature cycling, however, were determined by the primers used. Following thermocycling 20 μl of the reaction was run on an agarose electrophoretic gel for analysis. If cloning of the gene was required, a TAE gel was used and the DNA was purified from the gel using the Geneclean II® method.

2.2.4.2.2 Access RT-PCR system

A typical Access RT-PCR system reaction contained 10 μl AMV/*Tfl* reaction buffer (5 x), 1 μl dNTP mix (10mM), 2.5 μl of both sense and anti-sense primers (20 μM), 2 μl $MgSO_4$ (25 mM), 1 μl AMV reverse transcriptase (5 u/μl), 1 μl *Tfl* DNA polymerase (5 u/μl), 100ng poly $[A]^+$ RNA or 1 μg total RNA and nuclease-free water to give a final volume of 50μl. Thermocycling conditions were as the Titan™ RT-PCR system except for the initial reverse transcription which was carried out at 48°C for 45 min.

2.2.4.3 Blunt-ending PCR products

As *Tfl* DNA Polymerase does not have proofreading activity, it was necessary to remove any non-template dependent nucleotides that may have been added to the 3' end of the PCR product to allow cloning into the pCR®-Blunt II-TOPO vector. T4 DNA Polymerase has 3' exonuclease activity and will therefore convert a 3'-protruding end to a blunt end. Gel-purified DNA was resuspended in T4 DNA polymerase buffer (33 mM Tris-acetate, pH 7.9, 66 mM potassium acetate, 10 mM magnesium acetate, 0.5 mM DTT) containing 100 μM of each dNTP and 0.1 mg/ml BSA. Five units of T4 DNA Polymerase were added per microgram of DNA in a final volume of 20 μl. The reaction was incubated at 37°C for 5 min., before termination by heating at 75°C for 10 min.

2.2.5 Cloning of PCR products

PCR products were cloned into the vector pCR®-Blunt II-TOPO using the Zero Blunt™ TOPO™ PCR cloning kit (Invitrogen, Holland). The vector was supplied linearised and has vaccinia virus topoisomerase 1 covalently bound to the 3' end allowing spontaneous ligation of the vector with a blunt-ended PCR product. Approximately 50 ng purified PCR product and 1 μl pCR®-Blunt II TOPO vector were added to sterile water, in a final volume of 5μl. The reaction was mixed gently and incubated for 5 min at room temperature. Following the incubation, 1 μl 6 x TOPO™ Cloning Stop Solution was added and the reaction was mixed and placed on ice. A vial of TOP10™ One Shot™ cells was thawed on ice and 20 μl of the ligation mix was added to the cells. This was gently mixed and incubated on ice for 30 min. Cells were then heat shocked for 30 sec in a 42°C water bath followed by immediate transfer to ice for 2 min. Room temperature SOC medium (250 μl) was added to the cells before horizontal shaking of tubes for 1 hour at 37°C to induce expression of antibiotic resistance genes. The transformed cells (50-100μl) were spread on pre-warmed LB agar plates containing 50 μg/ml kanamycin and these were incubated at 37°C overnight. Colonies were picked and grown for 12-16 hours in LB medium containing 50 μg/ml kanamycin and plasmid DNA was purified from the bacteria using the CONCERT™ Rapid Plasmid Purification System (Life Technologies, Paisley, UK). The DNA was analysed initially by restriction digest and then sequenced using the M13 forward and reverse primers.

2.2.5.1 Sequencing of clones

Approximately 1 μg of CONCERT™ DNA preparation was sent to DNAShef, Edinburgh, UK for sequencing. Sequence analysis was carried out on the GCG (Genetic Computer group, Wisconsin, USA) suite of programs, accessible via the gnome workstation, for analysis and comparison with existing sequences in the database.

2.2.6 Cell culture methods

2.2.6.1 Maintenance of L929 mouse fibroblast cells and COS 7 primate kidney fibroblast cells

Cells were grown in 75 cm^2 vented flasks containing 12 ml supplemented DMEM medium. These were incubated at 37°C with 5% CO_2. At 80-85% confluence cells were washed with pre-warmed PBS before harvesting with 2 ml trypsin/EDTA. Cells were split 1:8 for 85% confluence after 3-4 days.

2.2.6.1.1 Preparation of cells for storage in liquid nitrogen

Approximately 80% confluent cells were harvested into 10 ml media and centrifuged in sterile Sterilin 20 ml tubes at 1,500 rpm for 5 min. The resulting pellet was resuspended in 1 ml FBS containing 10% (v/v) DMSO (dimethylsulphoxide). The cell solution was then transferred to cryotubes and cooled slowly for 24 hours in liquid nitrogen fumes before transfer to liquid nitrogen.

2.2.6.1.2 Re-establishment of frozen cells

Frozen aliquots of cells were rapidly thawed in a 37°C water bath. They were then added to 10 ml fresh medium before centrifugation at 1,500 rpm for 5 min. The resulting cell pellet was resuspended in 15 ml fresh medium, transferred to a 75 cm^2 vented flask and incubated as before.

2.2.6.2 Establishment of stable cell lines

2.2.6.2.1 Optimisation of G418 selection

Cells were seeded in 6 well plates for 70-80% confluence the following day. After 24 hours incubation, cells were treated with 300, 350, 400, 450, 500 or 700 μg/ml G418 and incubated for a further 24 hours. Cells were observed for a further 48 hours and percentage confluence recorded.

2.2.6.2.2 Transfection of L929 mouse fibroblast cells

Cells were seeded overnight at $5x10^3$ in 4.5 mm cell culture dishes to reach 50-60% confluence the following day. FuGENE™ 6 transfection reagent (6

μl) was added directly to 94 μl serum-free medium and incubated at room temperature for 5 min. This mixture was then added dropwise to 3 μg DNA, mixed and incubated at room temperature for 15 min. This was then added dropwise to the cells, whilst swirling the flask for even distribution. The cells were incubated for 48 hours before resistance selection to the antibiotic G418 was begun by the addition of 450 μg/ml G418. This concentration of G418 will kill cells unless they contain the G418 (neomycin) resistance gene, which is present in the pcDNA3 genome. During the initial selection procedure, minimal essential medium (MEM) replaced DMEM to allow slower growth of cells. Colonies were apparent after 7 days and picked after 12 days for individual growth. Trypsin/EDTA/PBS (15 μl) was added directly to an individual colony and the colony was sucked into a pipette tip. Each colony was transferred to a well in a 24 well plate and selection pressure was maintained by the presence of 400μg/ml G418 in the medium. Cells were transferred to 6 well plates a week after initial transfer to 24 well plates. Four days later each colony was split into two and grown to 80% confluence. One set of the clones was then frozen and the other set had their RNA extracted.

2.2.6.2.3 Isolation of total RNA from cultured cells

TriPure® RNA isolation reagent (Roche Molecular Biochemicals, E.Sussex, UK) was used to extract total RNA from L929 cells. TriPure® Isolation Reagent (0.5 ml) was added directly to each well of a 6 well plate containing monolayers of transfected and untransfected (control) L929 cells. The cell lysate was passed through the pipette tip several times and transferred to 1.5 ml microfuge tubes. Each sample was incubated at room temperature for 5 min to ensure the complete dissociation of nucleoprotein complexes. 0.1 ml chloroform was then added and each tube shaken vigorously for 15 sec before incubation at room temperature for 15 min. Separation of phases was achieved by centrifugation of the samples at 12,000 *x g* for 15 min at 4°C. The RNA containing upper layer was transferred to a new microfuge tube and 0.25 ml isopropanol added to each sample Following mixing the samples were incubated at room temperature for 10 min to allow the RNA

precipitate to form. The samples were again centrifuged at 12,000 *x g* for at 4°C for 10 min. The resulting RNA pellet was then washed in 1 ml 75% ethanol by vortexing and centrifugation at 7 500 *x g* for 5 min at 4°C. The pellet was dried and the samples resuspended in 100 μl DEPC-treated water.

2.2.6.2.4 Transcription of cRNA

RNA from each gene to be investigated was required as a positive control during RT-PCR analysis of transfected cells. cDNA was available in a plasmid for each subunit to be investigated and therefore cRNA could be transcribed. The plasmid was linearised at the 5' end of the *H.contortus* cDNA of interest by restriction digestion and the resulting DNA purified by phenol/chloroform extraction. cRNA was transcribed using T7 RNA polymerase, as the plasmid contained the T7 promoter just downstream of the GluCl subunit sequences. A typical transcription reaction was composed of 10 μg linearised DNA, 10 μl 10 x transcription buffer, 10 μl DTT(100 mM), 4 μl RNAguard (38 units/μl), 5 μl rNTPs (5 mM), 2 μl T7 RNA polymerase (20 units/μl) and sterile, RNase-free water to 100 μl. This was incubated at 37°c for 1 hour before the addition of 5μl RNase-free DNase 1 (10 units/μl) for an additional 15 min at 37°C to remove residual DNA. A phenol (water-saturated)/chloroform extraction was then carried out and the purified DNA was resuspended in 25 μl Rnase-free water.

2.2.6.3 Transient expression in COS 7 cells

2.2.6.3.1 Transfection of COS 7 cells

Cells were seeded overnight in 75 cm^2 tissue culture flasks to reach approximately 40% confluence the following day. For transfection of cells, 15 μl FuGENE™ 6 transfection reagent was added directly to 85 μl serum-free media and incubated at room temperature for 5 min. This mixture was then added dropwise to 10 μg DNA, mixed and incubated at room temperature for 15 min. This was then added dropwise to the cells, whilst swirling the flask

for even distribution. The cells were incubated for 48 hours before harvesting.

2.2.7 Immunofluorescence

COS 7 cells were seeded overnight on glass cover slips, contained in 6 well plates, to give a confluence of approximately 40% the following day. Cells were added only to the cover slips and incubated for 1 hr to allow attachment before flooding the plate with 2 ml medium. The cells were transfected as previously described, using a ratio of 3 μl FuGENE™ 6:1 μg DNA and incubated for 48 hours. The medium was removed and the cover slips washed 3 times (5 min each) with PBS before fixing cells with 4% (w/v) paraformaldehyde in PBS at room temperature for 20 min. Cells were washed with PBS (3 x 5 min) and permeabilised with 0.1% (v/v) Triton X-100 in PBS for 5 min to allow antibody to bind within the cells. Following washing with PBS (5 min) cells were blocked with 0.2% (w/v) BSA in PBS for 30 min at room temperature. Cover slips were inverted onto 70 μl primary antibody diluted in 0.2% (w/v) BSA in PBS and incubated for an hour at room temperature. Cover slips were returned to their well and washed 2 x 5 min in 0.2% (w/v) BSA and 2 x 5 min washes in PBS to remove any unbound primary antibody. Coverslips were inverted onto 70 μl mouse anti-flag antibody diluted in 0.2% (w/v) BSA in PBS and incubated for an hour at room temperature. Cover slips were returned to their well and washed 2 x 5 min in 0.2% (w/v) BSA and 2 x 5 min washes in PBS to remove any unbound primary antibody. Cover slips were inverted onto 70 μl goat anti-mouse (FITC-conjugated) secondary antibody diluted in 0.2% (w/v) BSA for 20 min in the dark, to prevent bleaching of fluorescence. They were returned to their well and washed as after primary antibody to prevent background fluorescence. Cover slips were mounted onto a drop of Vectashield® mounting media on a microscope slide and left overnight in the dark. Cells were viewed on a Zeiss LSM 510 inverted Axiovert 100M confocal microscope using a fluorescein filter set.

2.2.8 Membrane preparation

2.2.8.1 Preparation of membranes from cultured cells

Transiently transfected COS 7 cells were harvested 48 hours post-transfection by which time they were approximately 85% confluent. Control cells and stably transfected L929 cells were harvested at approximately 85% confluence. Medium was removed from the flask by aspiration and the cells were washed three times with ice-cold 50 mM HEPES (pH 7.4) containing 0.01% (w/v) sodium azide. The cells were harvested using a cell scraper and resuspended in 10 ml 50 mM HEPES (pH 7.4), 0.01% (w/v) sodium azide. Cells were disrupted further by sonication (3 x 15 sec pulses). They were then transferred to 10 ml ultracentrifuge tubes and centrifuged at 28,000 rpm for 30 min at 4°C. The resulting pellet was resuspended in 1 ml ice-cold 50 mM HEPES (pH 7.4) containing 0.01% (w/v) sodium azide and 0.2 mM PMSF. The protein was quantified using the Coomassie® plus Protein Assay Reagent Kit (Pierce, Rockford, USA).

2.2.8.2 Membrane preparations from *H.contortus* L3-stage larvae

L3-stage larvae were supplied by Gerald Coles (University of Bristol, Bristol, UK). Approximately 1-4g larvae were used per preparation. These were suspended in 7ml membrane buffer (50 mM HEPES (pH 7.4), 0.2 mM PMSF, leupeptin (0.5 μg/ml), pepstatin (0.7 μg/ml)) and the nematode cuticle was disrupted by the addition of 15-20 crushed glass cover slips followed by approximately 5 cycles of 1 min vortexing and 2 min cooling on ice. This procedure was continued until all worms appeared broken upon microscopic inspection. The volume of homogenate was adjusted to 40 ml with 50 mM HEPES (pH 7.4) and this was centrifuged at 1,000 x g for 10 min. The pellet was discarded and the supernatant centrifuged at 28,000 x g for 30 min at 4°C. Membranes were resuspended in 50 mM HEPES buffer (pH 7.4) to a final concentration of 1 mg/ml (quantified by Coomassie® plus Protein Assay Reagent Kit) and stored at -20°C.

2.2.8.3 Quantitation of protein in membrane preparations

The protein content of each membrane preparation was analysed by comparison with a series of standard bovine serum albumin (BSA) solutions in 50 mM HEPES (pH 7.4) ranging from 0.1 to 1 mg/ml using the Coomassie® protein assay kit. This is a variation on the Bradford, Coomassie®, colorimetric method (Bradford, 1976) whereby the binding of Coomassie® Brilliant Blue G-250 to protein causes a shift in the maximum absorbance of the dye from 465 to 595 nm under acidic conditions. The assay can be monitored by the simultaneous colour change of the reagent from green/brown to blue. The assay was carried out in a 96 well plate using only 10 μl of each sample with 300 μl of Coomassie® Protein Assay Reagent (contains Coomassie® G-250, methanol, phosphoric acid and solubilizing agents in water). Standards were measured in quadruplicate and cell samples were diluted 1/10 before analysis. All samples were measured against a blank of 10 μl buffer with 300 μl protein reagent. The optical density was measured at 595 nm.

2.2.9 Radioligand binding

2.2.9.1 Binding of [^{3}H] ivermectin to membrane preparations

[^{3}H] ivermectin binding experiments were carried out in 5 ml polypropylene test tubes. Membranes were incubated with [^{3}H] ivermectin in 50 mM HEPES (pH 7.4) with 5-40 μg protein. Non-specific binding was determined by binding in the presence of 10 μM unlabelled ivermectin. Final assay volumes were 1ml and reactions were incubated at room temperature for 2 hours. The binding reaction was terminated by dilution with 3 ml cold wash buffer (50 mM HEPES (pH 7.4) containing 0.25% (v/v) Triton X-100) followed by filtration through type A/B glass fibre filters (Whatman, Kent, UK)) which were pre-soaked in 0.15% (v/v) Polyethyleneimine (PEI) in wash buffer. Filters were washed twice more with 3 ml wash buffer (Hejmadi *et al.*, 2000, Rohrer *et al.*, 1994, Smith *et al.*, 2000). Bound radioactivity was determined by liquid scintillant spectrometry in mini-vials containing 5 ml Optiphase Safe (Wallac, Bucks., UK). For the competition studies, membranes were

incubated with 140 pM (HG3) or 150 pM (HG5) [^{3}H]ivermectin at room temperature for 2 hours with various concentrations of competing ligands. Non-specific binding was determined in the presence of 10μM unlabelled ivermectin. All reactions were carried out in duplicate and experiments were repeated between 3 and 6 times.

2.2.9.2 Radioligand binding data analysis

Non-linear regression analysis (Sigma plot v 4.0, Jandel Scientific) was used to determine the dissociation constant for the equilibrium binding of the radiolabel (K_d) fitted to a single-site binding model. Data were fitted to the equation

$$y = (B_{max}[[^3H]ligand])/K_d + [[^3H]ligand].$$

The parameters, IC_{50} (the concentration of competing drug that inhibits 50% of the specific binding) and K_i (the affinity of the inhibitor for the receptor) were determined from competition assays. Data were fitted to the Hill equation to determine IC_{50} values for each competitor.

$$B = 100\%/1+([ligand]/IC_{50})^{nH}$$

(where B = % bound radiolabel, [ligand] = concentration of displacing ligand and nH = Hill number)

These were converted to K_i using the equation

$$K_i = IC_{50}/1 + ([radioligand]/K_d).$$

2.2.10 Protein analysis

2.2.10.1 SDS-Polyacrylamide gel electrophoresis

Reagents	Component
Protogel® solution (National diagnostics, Hull, UK)	30% (w/v) acrylamide, 0.8% (w/v) bis acrylamide
Resolving gel buffer (4x)	1.5 M Tris-Cl, 0.4% (w/v) SDS (pH 8.8)*
Stacking gel buffer (4x)	0.5 M Tris-Cl, 0.4% (w/v) SDS (pH 6.8)*
APS	10% (w/v) ammonium persulphate in

	$ddH_2O^{\blacklozenge}$
6x SDS loading buffer	0.35 M Tris-Cl, pH 6.8, 10.28% (w/v) SDS, 36% (v/v) glycerol, 5% (v/v) β-mercaptoethanol, 0.012% (w/v) bromophenol blue[#]
5x running buffer	3 g Tris-base, 14.4 g glycine, 0.5 g SDS in 100 ml ddH_2O

*Adjusted to pH 8.8 with 1 N HCl, filtered through a 0.45μm filter and stored at 4°C. ♦Stored at 4°C for 5 days only. #Stored at -20°C.

To prepare two 12% (v/v) separating gels, 6 ml Protogel® solution was mixed with 3.75 ml 4 x resolving gel buffer and 5.25 ml ddH_2O. The mixture was de-gassed under vacuum for 10 min and 100 μl APS and 10 μl TEMED were added immediately before pouring into Atto™ mini-gel rigs. The gel was overlaid with isopropanol and allowed to polymerise. Once set, the isopropanol was removed from the gel and the gel interface washed with ddH_2O. A 4% (v/v) stacking gel (0.65 ml Protogel® solution, 1.25 ml stacking buffer, 3.05 ml ddH_2O, 25 μl APS, 5 μl TEMED) was pipetted over the separating gel and a comb inserted. Once set, gels were placed into an electrophoretic chamber and 1 x running buffer was added. Combs were removed and wells rinsed with ddH_2O. Membrane preparations were prepared for loading (10-20 μg) by the addition of 6 x SDS loading buffer and denaturation by incubation in a boiling water bath for 5 min. A rainbow molecular weight marker (10-250 kda) (Amersham Life Sciences, Bucks., UK) was also run. Samples were spun down at 12,000 rpm for 1 min immediately prior to loading. Gels were run at 100 V until the bromophenol blue tracking dye had just run off the bottom.

2.2.10.1.1 Western Blotting and Immunodetection

2.2.10.1.1.1 Electrophoretic transfer to nitrocellulose

Gels were placed in a tray containing SDS transfer buffer. A sheet of nitrocellulose blotting membrane and 18 sheets of filter paper were cut to the size of the gel and pre-wet in SDS transfer buffer. Nine sheets of pre-wet

filter paper were placed on the anode of the Multiphor II Novablot electrophoretic transfer unit and air bubbles removed by rolling with a 5 ml pipette tip. The nitrocellulose was placed on the filter paper, followed by a gel and the other nine sheets of pre-wet filter paper. The cathode surface of the transfer unit was wet before placing on top of the anode. The transfer was run at 0.8 mA/cm^2 of gel for 1 hr 50 min.

2.2.10.1.1.2 Immunoprobing and detection

Buffer	Components
Transfer buffer	25 mM Tris-Cl, pH 8.3, 150 mM glycine, 0.037% (w/v) SDS, 20% (v/v) ethanol*
TBST	10 mM Tris-Cl pH 8, 150 mM NaCl, 0.1% (v/v) Tween 20
Blocking solution	5% (w/v) Marvel™ non-fat milk powder in TBST

* ethanol was added immediately before use

A nitrocellulose membrane containing transferred protein was washed briefly in washing buffer before incubating overnight at 4°C in blocking solution. The blot was rinsed in washing buffer to remove any unbound milk proteins before incubation with primary antibody diluted in blocking solution for 1 hour at room temperature. The membrane was rinsed in washing buffer for 5 min, 10 min and 15 min on a rotating platform to remove unbound primary antibody before incubating with secondary antibody (horseradish peroxidase-conjugated), diluted in blocking buffer, for 1.5 hrs. The blot was washed as after primary antibody incubation. The chemiluminescence ECL detection kit was used to detect immunoreactivity in the blot. An equal volume of detection solution 1 and detection solution 2 were mixed and incubated on the membrane for 1 min at room temperature. Excess fluid was removed and the blot placed between acetate before exposing to X-ray film (Roche Molecular Biochemicals, E. Sussex, UK) for 2-5 min. Films were developed using a X-Ograph Compact X2 processor.

3. Molecular analysis of *Haemonchus contortus* Glutamate-gated Chloride Channels

Previous workers in the laboratory identified five partial cDNAs from *H.contortus* by Reverse Transcription-Polymerase Chain Reaction (RT-PCR), using degenerate oligonucleotides primers corresponding to conserved regions of ligand-gated chloride channels (Laughton, 1993). Four of the cDNAs showed characteristic features of the cys-loop ligand-gated ion channels and had highest sequence identity to the *C.elegans* glutamate-gated chloride channel subunits. A full-length *C.elegans* β-subunit homologue, HG4 (Hc-gluclβ), which shared 82% amino acid identity with its *C.elegans* counterpart (Cully *et al.*, 1994), was cloned from *H.contortus* eggs (Delany *et al.*, 1998). Jagannathan (1998) demonstrated by Rapid Amplification of cDNA ends (RACE) PCR that the *gbr-2* (*avr-14*) gene was present in *H.contortus* eggs and that the pattern of alternative splicing which had been observed in *C.elegans* (Laughton *et al.*, 1997) appeared to be conserved. Two subunits, with identical N-terminal regions but different C-terminal domains, are thereby produced from a single gene. Although one of these subunits, HG3 (gbr-2b), had been amplified and cloned, problems were encountered detecting sufficient quantities of HG2 (gbr-2a) mRNA to allow cloning. Semi-quantitative PCR analysis suggested that very low levels of the HG2 variant were present in *H.contortus* eggs and it was assumed that there was insufficient mRNA for successful cloning.

An additional subunit, HG5, with no clear *C.elegans* homologue was also amplified, but although sufficient partial cDNAs were amplified and cloned to publish the full sequence of this subunit, attempts to amplify the entire subunit were ineffective (Delany, 1998). Forrester *et al.*, (1999) suggest that this gene may also be alternatively spliced resulting in two products, one of which is truncated at the 5' end. They also indicated, by semi-quantitative PCR, that expression of HG5 varies through the *H.contortus* life cycle and is maximal in adults. HG5 shows high sequence identity to *C.elegans* GluClα2 (60%) and gbr-2a (62%).

As discussed (section 1.2.4), anthelmintic resistance is a major problem in the livestock industry. The mechanism of nematode resistance to the avermectins and milbemycins (AM) is not known, but in benzamidazole and imidathiazole resistance an altered site of action is involved. It is possible that altered GluCl subunits may contribute to the observed AM resistance. No consistent coding changes were observed in HG2, HG3 or HG4 cDNA from ivermectin-resistant field-isolated *H.contortus* (Delany, 1998, Jagannathan, 1998), but allelic changes in the remaining subunit, HG5, have been discovered in laboratory isolates (Blackhall *et al.*, 1998).

Full-length clones of all four *H.contortus* GluCl subunits were required for expression studies (chapters 4 and 5). Alternative methods to assess the quantity of HG2 mRNA and to amplify and clone this subunit and HG5 are discussed in this chapter. Knowledge of the full-length sequence of these two cDNAs allowed gene-specific oligonucleotides to be produced and used in the sensitive technique of RT-PCR to amplify the complete HG2 and HG5 cDNAs from *H.contortus* eggs. Amplification of the full-length HG5 subunit cDNA was also attempted from ivermectin-resistant *H.contortus* for sequence comparison with HG5 from ivermectin-sensitive *H.contortus.*

3.1 Results

3.1.1 Expression of HG2 and HG3 mRNA in *H.contortus* eggs

Semi-quantitative PCR is not always a reliable method of quantifying the expression levels of DNA as there are so many variables in a PCR reaction, nor can it always be used as conclusive proof of alternative splicing of a gene transcript. Northern hybridisation, however, is carried out on RNA and does not have the huge number of variables that are found in semi-quantitative PCR. The relative abundance of HG2 and HG3 in *H.contortus* mRNA was investigated by northern blot analysis using a cRNA probe and the Digoxygenin method. The Digoxigenin (DIG) method of hybridisation is non-isotopic, but instead allows detection of RNA by binding of an anti-DIG antibody-alkaline phosphatase conjugate to a DIG-labelled probe hybridised to the RNA of interest. The signal is then detected using chemiluminescent alkaline phosphatase substrates (DIG System User Guide, Boehringer Mannheim). *H.contortus* eggs, rather than adults or larvae, were used to

maintain continuity with previous work. Eggs are easy to obtain and purify in large quantities and yield high quality mRNA without necessitating the sacrifice of the infected animal.

3.1.1.1 Northern Blot probe design and production

A probe was designed to incorporate the HG3 intracellular loop region, as this is also present in the untranslated region of HG2 and the probe would consequently detect both mRNAs (figure 14). The intracellular loop is the most variable part of the GluCl subunits and the probe would therefore not detect subunits other than HG2 and HG3 in the mRNA.

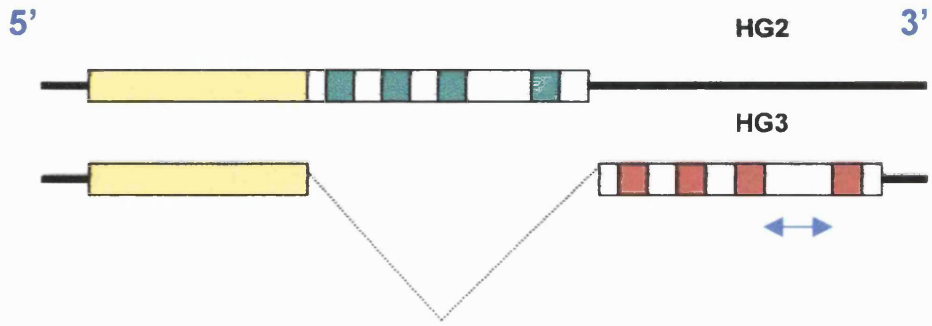

Figure 14 *gbr-2* probe design. The 180bp northern blot probe was designed to the HG3 intracellular loop.

Extracellular domain Transmembrane domains

Probe Untranslated region

RNA probes are recommended for use with northern blots as an RNA:RNA bond is stronger than RNA:DNA. cDNA encoding the intracellular loop of HG3 was amplified by PCR and cloned into the vector pCRBlunt (appendix 2) by Virginia Portillo. The HG3 cDNA was digested from its original vector (figure 15) and subcloned into the multiple cloning site of pBluescript II (appendix 3) to allow the T7 promoter to be used for RNA transcription. The approximately 180 bp DNA band was cut from the gel and purified before ligation with EcoRI/BamHI digested pBluescript II DNA. Competent XL-1 Blue bacterial cells were transformed with the ligated DNA (5 μl). The resulting recombinant plasmid was linearised with XbaI (10 units)(2 hours at 37°C) and 1 μg was used as a template for RNA transcription. RNA was Digoxigenin-

11-UTP (DIG) labelled during transcription, with one DIG molecule incorporated every 20-25 nucleotides. The DIG protocol predicted 2-10 μg of labelled RNA to be transcribed from 1 μg DNA template.

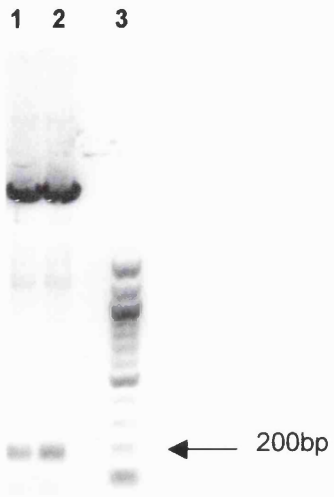

Figure 15 Restriction endonuclease digestion of HG3 intracellular loop from pCRBlunt. The restriction enzymes EcoRI and BamHI (10 units each) (in buffer 2) were used to cut 10 μg DNA for three hours at 37°C. The DNA was electrophoresed through a 1.5% (w/v) agarose gel in TAE buffer. Lanes 1 and 2: digested recombinant plasmid. Lane 3: 100 bp molecular weight marker.

A more accurate assessment of the quantity of RNA present after the transcription reaction was required to ensure the correct amount of RNA was used as a probe. The yield of DIG-labelled RNA was estimated by comparison against a DIG-labelled control (figure 16).

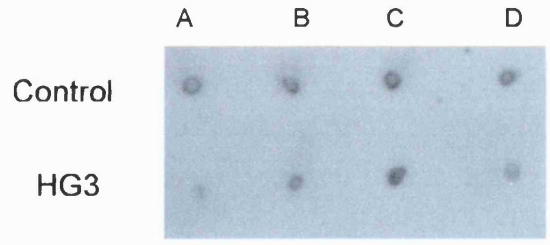

Figure 16 Spot test to estimate the concentration of the HG3 RNA probe. Control DIG-labelled RNA of known concentration was serially diluted and compared against the HG3 RNA probe by spotting on positively charged nylon membrane and detection using chemiluminescence. A = 1 ng/μl, B = 100 pg/μl, C = 10 pg/μl, D = 1 pg/μl.

The HG3 RNA probe was labelled at a slightly lower concentration than control and 6.825 μg labelled RNA was estimated to be present in the final 20 μl volume.

3.1.1.2 *H.contortus* Northern Blot

Total RNA was extracted from 1.9 g *H.contortus* eggs and final resuspension was in 500 μl 0.5% SDS. The purity and quantity of the RNA was assessed initially by agarose gel electrophoresis (figure 17) followed by spectrophotometric analysis ($O.D._{260}$), which estimated a final concentration of 5.5 μg/μl and a purity ratio ($O.D._{260}/O.D._{280}$) of 1.8. In general, a reduction in non-specific hybridisation can be obtained by using mRNA, rather than total RNA, in a northern hybridisation. This additional step also concentrates the target message and therefore, poly $[A]^+$ RNA was extracted from 1 mg *H.contortus* total RNA using magnetic beads coated with $Oligo(dT)_{25}$ (Dynabeads®, Dynal). The poly A residues at the 3' end of the mRNA base pair with the oligo dT residues on the beads, whereas RNA species lacking a poly A tail do not and can be washed off. The expected mRNA yield was approximately 10 μg, which was resuspended in 50 μl Rnase-free water.

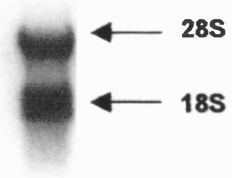

Figure 17 *H.contortus* egg RNA. 5μl total RNA (5.5 μg/μl) was electrophoresed through a 1% (w/v) agarose gel in TBE buffer. The 18S and 28S bands are indicated.

Following denaturation, the mRNA was electrophoresed through a 0.7% (w/v) agarose denaturing formaldehyde (2.2 M) gel alongside a DIG-labelled RNA marker for 4 hours at 80V. A total RNA (100μg) sample was also included as

a control. This lane was removed and stained with ethidium bromide (figure 18).

Figure 18 Ethidium bromide stained total RNA following denaturing 0.7% (w/v) agarose formaldehyde gel electrophoresis. The gel lane containing the total RNA (100μg) was removed and stained for 5 minutes with ethidium bromide (5 μg/ml) in the dark. Excess ethidium bromide was removed by washing for 2 hours in RNase-free water.

The probe detected two mRNAs, which correspond to the predicted size of HG2 (2 kb) and HG3 (1.3 kb) (figure 19) and confirmed that the *gbr-2* gene is alternatively spliced. It is evident that the two spliced variants are equally prevalent in the mRNA as the detected bands were of similar intensity.

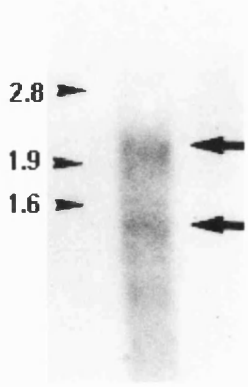

Figure 19 Northern blot analysis of *H.contortus* gbr-2 mRNAs. 10 μg poly $[A]^+$ RNA from *H.contortus* eggs was electrophoresed through a 0.7% (w/v) agarose formaldehyde denaturing gel and hybridised to a DIG-labelled RNA probe (100 ng/ml) representing the intracellular loop of the *H.contortus* HG3 sequence. Arrows on the right hand side of the figure indicate the two bands identified by the probe. The position of DIG labelled RNA markers (in kb) are indicated by arrowheads on the left-hand side of the figure.

3.1.2 Amplification and cloning of HG2 cDNA

3.1.2.1 HG2 cDNA amplification

The similar levels of expression of the *gbr-2* spliced variants, HG2 and HG3, suggested that the problems experienced in amplifying full-length HG2 were not due to a lower mRNA concentration than HG3. Amplification of HG2 was attempted using sequence-specific primers and the sensitive detection technique reverse-transcription PCR (RT-PCR) technique. The full length HG2 sequence was available and gene-specific primers were designed to the regions just preceding the start codon and just succeeding the stop codon (figure 20). The untranslated region of HG2, which contains the sequence for the HG3 C-terminal domain, was not required for subsequent work and primers were not designed to include this region in transcription and amplification.

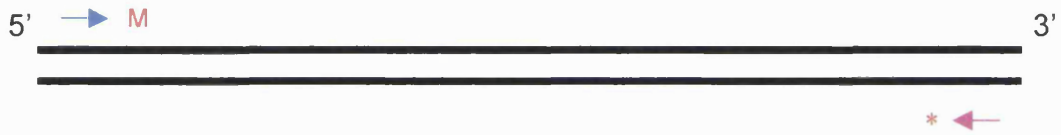

Figure 20 Schematic of primer design strategy for amplification of full length HG2 cDNA. Primers were designed to the available sequence on the EMBL database. M corresponds to the start codon. * represents the stop codon. → corresponds to 5HG2full. ← represents 3HG2full. Primer sequences are shown in appendix 4.

The Titan™ RT-PCR system was used for amplification of HG2 cDNA. Initial attempts to amplify HG2 cDNA from total RNA were unsuccessful, resulting in non-specific or no product. Poly $[A]^+$ RNA was used as template for subsequent reactions, both to ensure contaminating genomic DNA was not present and to enrich the targeted message.

A RT-PCR reaction including the sequence specific oligonucleotides 3HG2full and 5HG2full successfully amplified a PCR product of approximately 1.4 kb as predicted (figure 21).

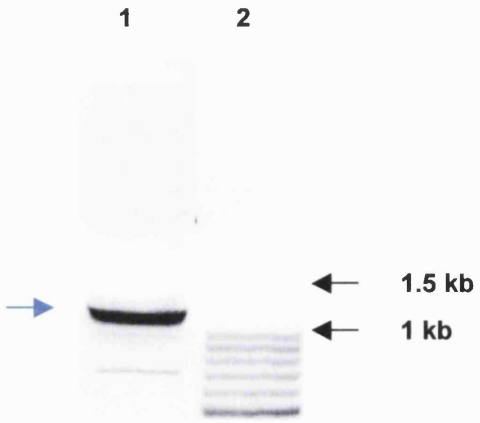

Figure 21 Amplification of full length HG2 cDNA from *H.contortus* eggs' mRNA. The gene-specific oligonucleotides 5HG2full and 3HG2full were used. RT-PCR conditions were as follows: 30 min incubation at 55°C, 2 min at 94°C and then 40 cycles of 94°C for 30 sec, 55°C for 1 min, 52°C for 1 min and 72°C for 2 min followed by 72°C for 7 min. Amplification products were identified by electrophoresis through a 1% (w/v) agarose gel and staining with ethidium bromide. Lane 1; RT-PCR amplification products. Lane 2; 100 bp molecular weight markers. → indicates the PCR product of approximately 1.4 kb.

3.1.2.2 Cloning and sequence analysis of HG2 cDNA

The approximately 1.4 kb PCR amplification product (figure 20) was cut from the gel and cloned into the bacterial expression vector pCRBlunt. Before seqencing, clones were digested to ensure the correct size of insert was present (figure 22).

Restriction endonuclease digestion of recombinant pCRBlunt indicated that cloning of the PCR product had been successful and two clones were sequenced. The pCRBlunt vector sequence includes the M13 forward and reverse priming sites and sequencing of the full-length cDNA was achieved using the M13 primers and the primer HG2seq (appendix 4). Sequence analysis confirmed that the clones were HG2 cDNA. Figure 23 illustrates the amino acid sequence for the two clones. As shown, HG2 cDNA was successfully amplified from the initial methionine to the stop codon. The cDNA contains 1360 nucleotides.

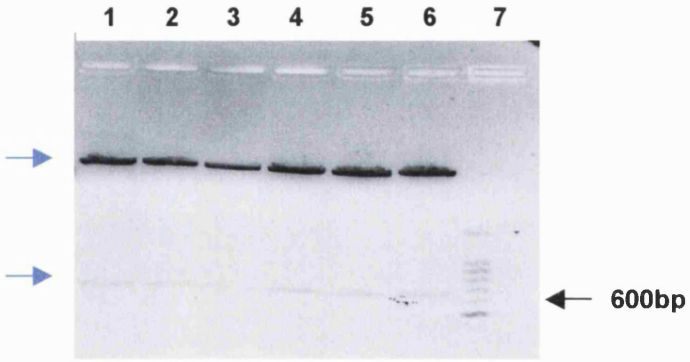

Figure 22 Restriction endonuclease digestion of recombinant pCRBlunt. DNA (5μg) was cut with Nde I and Xba I (10 units each) (in buffer 2) for 2 hours at 37°C. The digests were run on a 1.3% (w/v) agarose gel in TAE buffer. Successful HG2 cloning resulted in digestion products of approximately 670 bp and 4.22 kb in all clones. Lanes 1-6: digested recombinant pCRBlunt. Lane 7: 1 kb molecular weight marker.

```
HG2cl1 MRNSVPLATR IGPMLALICT VSTIMSAVEA KRKLKEQEII QRILNNYDWR
HG2cl2 MRNSVPLATR IGPMLALICT VSTIMSAVEA KRKLKEQEII QRILNNYDWR
                                                        100
HG2cl1 VRPRGLNASW PDTGGPVLVT VNIYLRSISK IDDVNMEYSA QFTFREEWVD
HG2cl2 VRPRGLNAS* PDTGGPVLVT VNIYLRSISK IDDVNMEYSA QFTFREEWVD

HG2cl1 ARLAYGRFED ESTEVPPFVV LATSENADQS QQIWMPDTFF QNEKQARRHL
HG2cl2 ARLAYGRFED ESTEVPPFVV LATSENADQS QQIWMPDTFF QNEKQARRHL
                                                        200
HG2cl1 IDKPNVLIRI HKDGSILYSV RLSLVLSCPM SLEFYPLDRQ NCLIDLASYG
HG2cl2 IDKPNVLIRI HKDGSILYSV RLSLVLSCPM SLEFYPLDRQ NCLIDLASYG

HG2cl1 YTTQDIKYEW KEQNPVQQKD GLRQSLPSFE LQDVVTKYCT SKTNTGEYSC
HG2cl2 YTTQDIKYEW KEQNPVQQKD GLRQSLPSFE LQDVVTKYCT SKTNTGEYSC
                                                        300
HG2cl1 LRTQMVLRRE FSYYLLQLYI PSFMLVIVSW VSFWLDKDSV PARVTLGVTT
HG2cl2 LRTQMVLRRE FSYYLLQLYI PSFMLVIVSW VSFWLDKDSV PARVTLGVTT

HG2cl1 LLTMTTQSSG INANVPPVSY TKAIDVWIGV CLAFIFGALL EFALVNYAAR
HG2cl2 LLTMTTQSSG INANVPPVSY TKAIGVWIGV CLAFIFGALL EFALVNYAAR
                                                        400
HG2cl1 KDMSCGQRMM KQLPQDGYRP LAGSQPRTSF CCRIFVRRYK ERSKRIDVVS
HG2cl2 KDMSCGQRIM KQLPQDGYRP LAGSQPRTSF CCRIFVRRYK ERSKRIDVVS
                                 422
HG2cl1 RLVFPIGYAC FNVLYWAVYL M*
HG2cl2 RLVFPIGYAC FNVLYWAVYL M*
```

Figure 23 Alignment of RT-PCR amplified HG2 clones. Blue indicates transmembrane regions. Conserved cysteine pairs are shown in green. Amino acids shown in red indicate differences between clones. Stop codons are represented by *.

Three amino acid differences were found between the clones including the conversion of a tryptophan to a stop codon in clone 2. Subsequent experiments were carried out with clone 1.

```
Y14233  MRNSVPLATR IGPMLALICT VSTIMSAVEA KRKLKEQEII QRILNNYDWR
HG2cl1  MRNSVPLATR IGPMLALICT VSTIMSAVEA KRKLKEQEII QRILNNYDWR

        51                                                  100
Y14233  VRPRGLNASW PDTGGPVLVT VNIYLRSISK IDDVNMEYSA QFTFREEWVD
HG2cl1  VRPRGLNASW PDTGGPVLVT VNIYLRSISK IDDVNMEYSA QFTFREEWVD

        101                                                 150
Y14233  ARLAYGRFED ESTEVPPFVV LATSENADQS QQIWMPDTFF QNEKEARRHL
HG2cl1  ARLAYGRFED ESTEVPPFVV LATSENADQS QQIWMPDTFF QNEKEARRHL

        151                                                 200
Y14233  IDKPNVLIRI HKDGSILYSV RLSLVLSCPM SLEFYPLDRQ NCLIDLASYG
HG2cl1  IDKPNVLIRI HKDGSILYSV RLSLVLSCPM SLEFYPLDRQ NCLIDLASYG

        201                                                 250
Y14233  YTTQDIKYEW KEQNPVQQKD GLRQSLPSFE LQDVVTKYCT SKTNTGEYSC
HG2cl1  YTTQDIKYEW KEQNPVQQKD GLRQSLPSFE LQDVVTKYCT SKTNTGEYSC

        251                                                 300
Y14233  LRTQMVLRRE FSYYLLQLYI PSFMLVIVSW VSFWLDKDSV PARVTLGVTT
HG2cl1  LRTQMVLRRE FSYYLLQLYI PSFMLVIVSW VSFWLDKDSV PARVTLGVTT

        301                                                 350
Y14233  LLTMTTQSSG INANVPPVSY TKAIDVWIGV CLAFIFGALL EFAWVNYAAR
HG2cl1  LLTMTTQSSG INANVPPVSY TKAIDVWIGV CLAFIFGALL EFALVNYAAR

        351                                                 400
Y14233  KDMSCGQRMM KQLPQDGYRP LAGSQPRTSF CCRIFVRRYK ERSKRIDVVS
HG2cl1  KDMSCGQRMM KQLPQDGYRP LAGSQPRTSF CCRIFVRRYK ERSKRIDVVS

        401                 422
Y14233  RLVFPIGYAC FNVLYWAVYL M*
HG2cl1  RLVFPIGYAC FNVLYWAVYL M*
```

Figure 24 Alignment of the HG2 amino acid sequence available on the EMBL database (accession number Y14233) and RT-PCR amplified HG2. Transmembrane regions are shown in blue. Conserved cysteine residues are shown in green. Differences between the sequences are highlighted in red. * represents the stop codon.

Comparison of clone 1 with the HG2 sequence available on the EMBL database (accession number Y14233) identified one amino change at the 3' end of the TM3 region (position 344 shown in red) (figure 24). A trypotophan

residue has been replaced by a leucine. The *C.elegans* homologue CE-GBR2A has a leucine in this position (Laughton *et al.*, 1997).

3.1.3 Amplification and cloning of HG5 cDNA

3.1.3.1 HG5 cDNA amplification

Previous workers had cloned HG5 as two partial cDNAs, but experienced difficulties in amplifying the entire sequence as a single clone (Delany, 1998). The partial HG5 cDNAs had been amplified from eggs and so RT-PCR was attempted using poly $[A]^+$ RNA from this life-cycle stage. Subunit-specific oligonucleotides were designed to the regions just prior to the start codon (5HG5full) and after the stop codon (3HG5full) (see appendix 4).

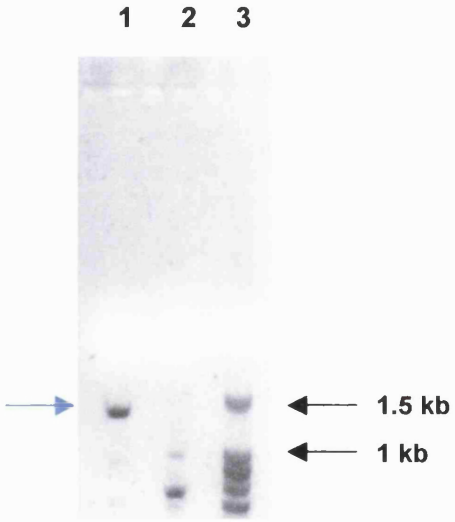

Figure 25 Amplification of HG5 full length cDNA from *H.contortus* eggs' mRNA. The gene-specific oligonucleotides 5HG5full and 3HG5full were used for amplification. RT-PCR conditions were as follows: 30 min at 55°C, 2 min at 94°C and then 40 cycles of 94°C for 45 sec, 54°C for 1 min, 50°C for 1 min, 72°C for 2 min followed by 72°C for 7 min. Amplification products were identified by electrophoresis through a 1% agarose gel and staining with ethidium bromide. Lane 1; amplification products. Lane 2; control amplification. Lane 3; DNA molecular weight marker. indicates the PCR product of approximately the expected molecular weight of HG5.

RT-PCR amplification of HG5 cDNA using the Titan™ RT-PCR system appeared successful as a band of approximately 1.4 kb was detected following gel electrophoresis as predicted (figure 25).

3.1.3.2 Cloning and sequence analysis of HG5 cDNA

The approximately 1.4 kb band was cut from the gel and cloned into the bacterial expression vector pCRBlunt. Purified recombinant plasmid DNA was digested with enzymes with unique restriction sites to ensure HG5 cloning had been successful before sequencing was undertaken (figure 26).

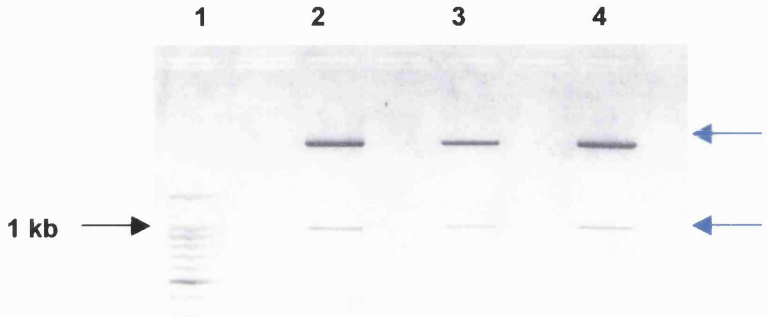

Figure 26 Analysis of recombinant pCRBlunt by restriction endonuclease digestion. DNA (3μg) was cut with Nde I and Pst I (10 units each) (in buffer 4) for 2 hours at 37°C. The digests were run on a 1% (w/v) agarose gel in TAE buffer. Successful cloning of HG5 was evident as digestion resulted in DNA bands of approximately 990 bp and 3.96 kb. Lane 1: 100 bp molecular weight marker. Lanes 2-4: digested recombinant pCRBlunt.

Restriction endonuclease digestion of recombinant pCRBlunt (figure 26) implied that cloning had been successful so two clones were sequenced. The M13 forward and reverse primers were used in conjunction with the primers 5hg5seq and 3hg5seq (appendix 4) to sequence the amplified cDNA. Sequence analysis confirmed that the clones were HG5 cDNA. As shown, this subunit had been successfully amplified from the initial methiothine to the stop codon (figure 27). A quite high degree of nucleotide variation was found between the clones but few coding differences were seen.

```
HG5cl1 MFALILPFLL HFTRSEGFGY EKLLDEQKII KHLLESPYSD YDWRVRPRGR
HG5cl2 MFALILPFLL HFTRSEGFGY EKLLDEQKIT KHLLESPYSD YDWRVRPRGR
                                                          100
HG5cl1 LGPADDDDYD SEPVFITVNM YLRSISKVDD VNMEYSLHFT FREEWIDERL
HG5cl2 LGPADDDDYD SEPVFITVNM YLRSISKVDD VNMEYSLHFT FREEWIDERL

HG5cl1 YFNSPTLKHI VLSPGQRIWV PDTFFQNEKD GKKHDIDTPN ILIRIHNGTG
HG5cl2 YFNSPTLKHI VLSPGQRIWV PDTFFQNEKD GKKHDIDTPN ILIRIHNGTG

                                                          200
HG5cl1 KILYSCRLTL TLSCPMRLAD YPLDVQTCVV DFASYAYTTK DIEYGWKEEK
HG5cl2 KILYSCRLTL TLSCPMRLAD CPLDVQTCVV DFASYAYTTK DIEYGWKEEK

HG5cl1 PIQIKDGLRQ SLPSFLLSNV KTGNCTSVTN TGAYSCLRTI IELKREFSYY
HG5cl2 PIQIKDGLRQ SLPSFLLSNV KTGNCTSVTN TGAYSCLRTI IELKREFSYY
                                                          300
HG5cl1 LLQLYIPSFM LVAVSWVSFW LDKDSVPARV TLGVTTLLTM TTQASGVNAN
HG5cl2 LLQLYIPSFM LVAVSWVSFW LDKDSVPARV TLGVTTLLTM TTQASGVNAN

HG5cl1 LPPVSYTKAI DIWIGVCLAF IFGALLEFAL VNWAARQDLV AHSRARYRQS
HG5cl2 LPPVSYTKAI DIWIGVCLAF IFGALLEFAL VNWAARQDLV AHSRARYRQS
                                                          400
HG5cl1 PLFFRNPDSR QENSHHFYAP IQQEVTLEDL PFSWWDKIWK IRYKERSRRI
HG5cl2 PLFFRNPDSR QENSHHFYAP IQQEVTLEDL PFSWWDKIWK IRYRERSRRI
                                                436
HG5cl1 DLISRVMFPL CFIIFNIMYW WRYLIPYMAV QAQLE*
HG5cl2 DLISRVMFPL CFIIFNIMYW WRYLIPYMAV QAQLE*
```

Figure 27 Alignment of HG5 cDNA amplified by RT-PCR. Blue indicates transmembrane regions. Conserved cysteine pairs are shown in green. Amino acids shown in red indicate differences between clones. Stop codons are represented by *.

There are two almost identical sequences deposited in the EMBL database corresponding to HG5. In addition to that identified by our laboratory (accession number AJ131347) a sequence deposited by Forrester *et al.*, (1999) (accession number AF076682) shows only two amino acid differences to HG5, but is identified as an alpha subunit. All available full-length HG5 sequences were compared to find a consensus (figure 28). Very few coding differences are seen between HG5 sequences. The RT-PCR amplified clone 2 has three nucleic acid mutations resulting in variations in the encoded amino acid (positions 30,171, 394). The mutation at position 171 results in an additional cysteine within the first cysteine loop. The RT-PCR amplified clone 1 is identical to the consensus sequence.

```
   HG5cl1 MFALILPFLL HFTRSEGFGY EKLLDEQKII KHLLESPYSD YDWRVRPRGR
   HG5cl2 MFALILPFLL HFTRSEGFGY EKLLDEQKIT KHLLESPYSD YDWRVRPRGR
 AF076682 MFALILPFLL HFTRSEGFGY EKLLDEQKII KHLLESPYSD YDWRVRPRGR
   NSDcl1 MFALILPFLL HFTRSEGFGY EKLLDEQKII KHLLESPYSD YDWRVRPRGR
   NSDcl2 MFALILPFLL HFTRSEGFGY EKLLDEQKII KHLLESPYSD YDWRVRPRGR
 AJ131347 MFALILPFLL HFTRSEGFGY EKLLDEQKII KHLLESPYSD YDWRVRPRGR
Consensus MFALILPFLL HFTRSEGFGY EKLLDEQKII KHLLESPYSD YDWRVRPRGR
                                                              100
   HG5cl1 LGPADDDDYD SEPVFITVNM YLRSISKVDD VNMEYSLHFT FREEWIDERL
   HG5cl2 LGPADDDDYD SEPVFITVNM YLRSISKVDD VNMEYSLHFT FREEWIDERL
 AF076682 LGPADDDDYD SEPVFITVNM YLRSISKVDD VNMEYSLHFT FREEWIDERL
   NSDcl1 LGPADDDDYD SEPVFITVNM YLRSISKVDD VNMEYSLHFT FREEWIDERL
   NDScl2 LGPADDDDYD SEPVFITVNM YLRSISKVDD VNMEYSLHFT FREEWIDERL
 AJ131347 LGPADDDDYD SEPVFITVNM YLRSISKVDD VNMEYSLHFT FREEWIDERL
Consensus LGPADDDDYD SEPVFITVNM YLRSISKVDD VNMEYSLHFT FREEWIDERL

   HG5cl1 YFNSPTLKHI VLSPGQRIWV PDTFFQNEKD GKKHDIDTPN ILIRIHNGTG
   HG5cl2 YFNSPTLKHI VLSPGQRIWV PDTFFQNEKD GKKHDIDTPN ILIRIHNGTG
 AF076682 YFNSPTLKHI VLSPGQRIWV PDTFFQNEKD GKKHDIDTPN ILIRIHNGTG
   NSDcl1 YFNSPTLKHI VLSPGQRIWV PDTFFQNEKD GKKHDIDTPN ILIRIHNGTG
   NSDcl2 YFNSPTLKHI VLSPGQRIWV PDTFFQNEKD GKKHDIDTPN ILIRIHNGTG
 AJ131347 YFNSPTLKHI VLSPGQRIWV PDTFFQNEKD GKKHDIDTPN ILIRIHNGTG
Consensus YFNSPTLKHI VLSPGQRIWV PDTFFQNEKD GKKHDIDTPN ILIRIHNGTG

                                                              200
   HG5cl1 KILYSCRLTL TLSCPMRLAD YPLDVQTCVV DFASYAYTTK DIEYGWKEEK
   HG5cl2 KILYSCRLTL TLSCPMRLAD CPLDVQTCVV DFASYAYTTK DIEYGWKEEK
 AF076682 KILYSCRLTL TLSCPMRLAD YPLDVQTCVV DFASYAYTTK DIEYGWKEEK
   NSDcl1 KILYSCRLTL TLSCPMRLAD YPLDVQTCVV DFASYAYTTK DIEYGWKEEK
   NSDcl2 KILYSCRLTL TLSCPMRLAD YPLDVQTCVV DFASYAYTTK DIEYGWKEEK
 AJ131347 KILYSCRLTL TLSCPMRLAD YPLDVQTCVV DFASYAYTTK DIEYGWKEEK
Consensus KILYSCRLTL TLSCPMRLAD YPLDVQTCVV DFASYAYTTK DIEYGWKEEK

   HG5cl1 PIQIKDGLRQ SLPSFLLSNV KTGNCTSVTN TGAYSCLRTI IELKREFSYY
   HG5cl2 PIQIKDGLRQ SLPSFLLSNV KTGNCTSVTN TGAYSCLRTI IELKREFSYY
 AF076682 PIQIKDGLRQ SLPSFLLSNV KTSNCTSVTN TGAYSCLRTI IELKREFSYY
   NSDcl1 PIQIKDGLRQ SLPSFLLSNV KTGNCTSVTN TGAYSCLRTI IELKREFSYY
   NSDcl2 PIQIKDGLRQ SLPSFLLSNV KTGNCTSVTN TGAYSCLRTI IELKREFSYY
 AJ131347 PIQIKDGLRQ SLPSFLLSNV KTGNCTSVTN TGAYSCLRTI IELKREFSYY
Consensus PIQIKDGLRQ SLPSFLLSNV KTGNCTSVTN TGAYSCLRTI IELKREFSYY
                                                              300
   HG5cl1 LLQLYIPSFM LVAVSWVSFW LDKDSVPARV TLGVTTLLTM TTQASGVNAN
   HG5cl2 LLQLYIPSFM LVAVSWVSFW LDKDSVPARV TLGVTTLLTM TTQASGVNAN
 AF076682 LLQLYIPSFM LVAVSWVSFW LDKDSVPARV TLGVTTLLTM TTQASGVNAN
   NSDcl1 LLQLYIPSFM LVAVSWVSFW LDKDSVPARV TLGVTTLLTM TTQASGVNAN
   NSDcl2 LLQLYIPSFM LVAVSWVSFW LDKDSVPARV TLGVTTLLTM TTQASGVNAN
 AJ131347 LLQLYIPSFM LVAVSWVSFW LDKDSVPARV TLGVTTLLTM TTQASGVNAN
Consensus LLQLYIPSFM LVAVSWVSFW LDKDSVPARV TLGVTTLLTM TTQASGVNAN

   HG5cl1 LPPVSYTKAI DIWIGVCLAF IFGALLEFAL VNWAARQDLV AHSRARYRQS
   HG5cl2 LPPVSYTKAI DIWIGVCLAF IFGALLEFAL VNWAARQDLV AHSRARYRQS
 AF076682 LPPVSYTKAI DIWIGVCLAF IFGALLEFAL VNWAARQDLV AHSRARYRQS
   NSDcl1 LPPVSYTKAI DIWIGVCLAF IFGALLEFAL VNWAARQDLV AHSRARYRQS
   NSDcl2 LPPVSYTKAI DIWIGVCLAF IFGALLEFAL VNWAARQDLV AHSRARYRQS
 AJ131347 LPPVSYTKAI DIWIGVCLAF IFGALLEFAL VNWAARQDLV AHSRARYRQL
Consensus LPPVSYTKAI DIWIGVCLAF IFGALLEFAL VNWAARQDLV AHSRARYRQS
                                                              400
```

```
   HG5cl1 PLFFRNPDSR QENSHHFYAP IQQEVTLEDL PFSWWDKIWK IRYKERSRRI
   HG5cl2 PLFFRNPDSR QENSHHFYAP IQQEVTLEDL PFSWWDKIWK IRYRERSRRI
 AF076682 PLFFRNPDSR QENSHHFYAP IQQEVTLEDL PFSWWDKIWK IRYKERSRRI
   NSDcl1 PLFFRNPDSR QENSHHFYAP IQQEVTLEDL PFSWWDKIWK IRYKERSRRI
   NSDcl2 PLFFRNPDSR QENSHHFYAP IQQEVTLEDL PFSWWDKIWK IRYKERSRRI
 AJ131347 PLFFRNPDSR QGNSHHFYAP IQQEVTLEDL PFSWWDKIWK IRYKERSRRI
Consensus PLFFRNPDSR QENSHHFYAP IQQEVTLEDL PFSWWDKIWK IRYKERSRRI
                                                  436
   HG5cl1 DLISRVMFPL CFIIFNIMYW WRYLIPYMAV QAQLE*
   HG5cl2 DLISRVMFPL CFIIFNIMYW WRYLIPYMAV QAQLE*
 AF076682 DLISRVMFPL CFIIFNIMYW WRYLIPYMAV QAQLE*
   NSDcl1 DLISRVMFPL CFIIFNIMYW WRYLIPYMAV QAQLE*
   NSDcl2 DLISRVMFPL CFIIFNIMYW WRYLIPYMAV QAQLE*
 AJ131347 DLISRVMFPL CFIIFNIMYW WRYLIPYMAV QAQLE*
Consensus DLISRVMFPL CFIIFNIMYW WRYLIPYMAV QAQLE*
```

Figure 28 Alignment of available HG5 (Hcgluclα) amino acid sequences. Blue indicates transmembrane regions. Conserved cysteine pairs are shown in green. Amino acids shown in red indicate differences between clones. Stop codons are represented by *. AF076682 and AJ131347 are deposited in the EMBL database. NSDcl1 and NSDcl2 were available from previous workers in the laboratory (Delany, 1998).

3.1.4 Amplification and cloning of HG5 cDNA from ivermectin resistant *H.contortus*.

3.1.4.1 Amplification of HG5 cDNA from ivermectin-resistant *H.contortus*

Initially attempts to amplify HG5 cDNA from the ivermectin-resistant (IVR) South African White River II *H.contortus* isolate (Van Wyk and Malan, 1988) incorporated poly $[A]^+$ RNA isolated from eggs and the same sequence specific oligonucleotides (5HG5full and 3HG5full) and reaction condition that had previously proved successful in amplifying HG5 from ivermectin-sensitive *H.contortus* (IVS) (30 min at 55°C, 2 min at 94°C and then 40 cycles of 95°C for 2 min, 54°C for 1 min, 50°C for 1 min, 72°C for 2 min followed by 72°C for 2 min).

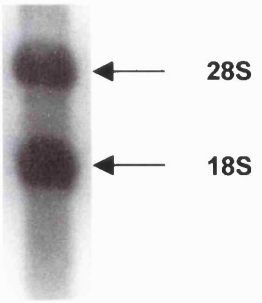

Figure 29 Total RNA extracted from IVR *H.contortus* eggs (720 mg). RNA (5 μl at [1.6 μg/μl]) was electrophoresed through a 1% agarose gel in TBE buffer. Ribosomal RNA bands are indicated.

No product was amplified under these conditions. Analysis of total RNA did not implicate degradation as the cause of this problem (figure 29). Differential expression of HG5 has been observed through the life cycle of *H.contortus*, with the maximum level in the adult stage (Forrester *et al.*, 1999). Poly [A]+ RNA was extracted from IVR adults and RT-PCR amplification was attempted.

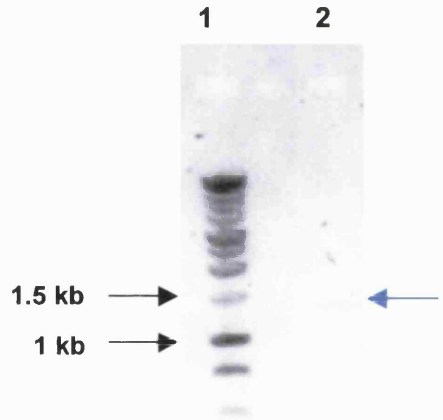

Figure 30 Amplification of HG5 from IVR *H.contortus* adults. The gene-specific oligonucleotides 5HG5full and 3HG5full were used with the Titan™ RT-PCR system for amplification. RT-PCR conditions were as follows: 30 min at 55°C, 2 min at 94°C and then 40 cycles of 94°C for 45 sec, 54°C for 1 min, 50°C for 1 min, 72°C for 2 min followed by 72°C for 7 min. Amplification products were identified by electrophoresis through a 1% agarose gel and staining with ethidium bromide. Lane 1; 1 kb molecular weight marker. Lane 2; PCR amplification product. A very faint band could be seen at approximately 1.35 kb.

Attempts to amplify HG5 cDNA from IVR adults maintaining IVS HG5 reaction conditions resulted in a very low yield of a product of approximately the correct molecular weight for HG5 (figure 30). The quantity of cDNA was too low to allow cloning.

The Titan™ RT-PCR system employs AMV reverse transcriptase and *Taq* and *Pwo* DNA polymerases for RNA detection. Many other DNA polymerase enzymes are available with differing levels of fidelity. The Access RT-PCR kit includes AMV for first strand synthesis, but *Tfl* DNA polymerase for cDNA amplification. HG5 amplification from IVR *H.contortus* adults was undertaken using the Access RT-PCR kit in combination with the gene specific primers 5HG5full and 3HG5full.

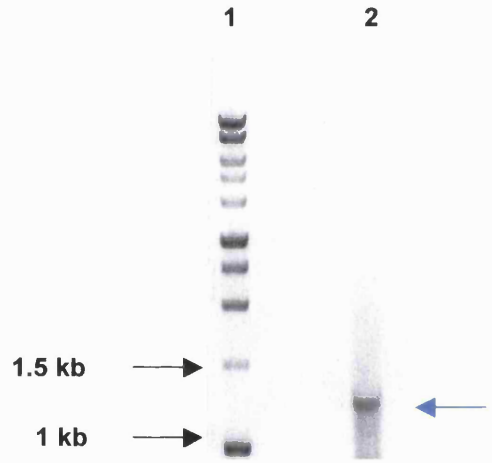

Figure 31 Amplification of HG5 from IVR *H.contortus* adults. The gene-specific oligonucleotides 5HG5full and 3HG5full were used with the Access RT-PCR kit for amplification. Reaction conditions were as follows: 45 min at 48°C, 2 min at 94°C and then 40 cycles of 94°C for 45 sec, 54°C for 1 min, 50°C for 1 min, 72°C for 2 min followed by 72°C for 7 min. Amplification products were identified by electrophoresis through a 1% agarose gel in TAE buffer and staining with ethidium bromide. Lane 1: 1 kb molecular weight marker. Lane 2: RT-PCR amplification products. cDNA of approximately 1.35 kb was detected.

A RT-PCR reaction including the enzymes AMV reverse transcriptase and *Tfl* DNA polymerase appeared to amplify HG5 from IVR adults as cDNA of

approximately 1.35 kb was evident following gel electrophoresis of PCR products (figure 31). HG5 cDNA from IVS eggs contains 1331 bp.

3.1.4.2 Cloning and sequence analysis of HG5 from ivermectin-resistant *H.contortus* adults

The PCR product of approximately 1.35 kb was removed from the gel and blunt-ended before cloning into the bacterial expression vector pCRBlunt. Recombinant plasmid DNA was digested to ensure that HG5 cDNA was present (figure 32).

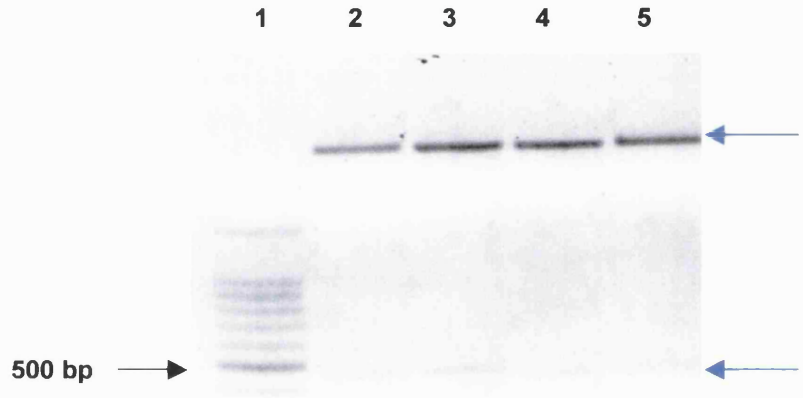

Figure 32 Restriction endonuclease digestion of recombinant pCRBlunt. The enzymes NdeI and PstI (10 units each) (in buffer 4) were used to analyse purified plasmid DNA (5 μg) for the presence of HG5. Digested DNA was electrophoresed through a 1.3% agarose gel in TBE buffer. Successful cloning is apparent, with cDNA of approximately 450 bp and 4.5 kb detected. Lane 1: 100 bp DNA molecular weight marker. Lanes 2-5: Digested recombinant pCRBlunt.

Digestion of recombinant pCRBlunt suggested that IVR HG5 cloning was successful and three clones were sequenced. Sequencing of the amplified cDNA was achieved with the oligonucleotides ivrseq and revivr (appendix 4) and the M13 forward and reverse primers. Sequence analysis confirmed that the clones were HG5 cDNA. The three clones were compared to obtain a consensus (figure 33). Although a fairly high level of nucleotide variation was seen between clones, there were very few coding changes.

```
   ivrcl1 MFALILPFLL HFTRSEGFGY EKLLDEQKII KHLLESPYSD YDWRVRPRGR
   ivrcl2 MFALILPFLL HFTRSEGFGY EKLLDEQKII KHLLESPYSD YDWRVRPRGR
   ivrcl3 MFALILPFLL HFTRSEGFGY EKLLDEQKII KHLLESPYSD YDWRVRPRGR
consensus MFALILPFLL HFTRSEGFGY EKLLDEQKII KHLLESPYSD YDWRVRPRGR
                                                             100
   ivrcl1 LGPADDDDYD SEPVFITVNM YLRSISKVDD VNMEYSLHFT FREEWIDERL
   ivrcl2 LGPADDDDYD SEPVFITVNM YLRSISKVDD VNMEYSLHFT FREEWIDERL
   ivrcl3 LGPADDDDYD SEPVFITVNM YLRSISKADD VNMEYSLHFT FREEWIDERL
consensus LGPADDDDYD SEPVFITVNM YLRSISKVDD VNMEYSLHFT FREEWIDERL
                                                             150
   ivrcl1 YFNSPTLKHI VLSPGQRIWV PDTFFQNEKD GKKHDIDTPN ILIRIHNGTG
   ivrcl2 YFNSPTLKHI VLSPGQRIWV PDTFFQNEKD GKKHDIDTPN ILIRIHNGTG
   ivrcl3 YFNSPTLKHI VLSPGQRIWV PDTFFQNEKD GKKHDIDTPN ILIRIHNGTG
consensus YFNSPTLKHI VLSPGQRIWV PDTFFQNEKD GKKHDIDTPN ILIRIHNGTG
                                                             200
   ivrcl1 KILYSCRLTL TLSCPMRLAD YPLDVQTCVV DFASYAYTTK DIEYGWKEEK
   ivrcl2 KILYSCRLTL TLSCPMRLAD YPLDVQTCVV DFASYAYTTK DIEYGWKEEK
   ivrcl3 KILYSCRLTL TLSCPMRLAD YPLDVQTCVV DFASYAYTTK DIEYGWKEEK
consensus KILYSCRLTL TLSCPMRLAD YPLDVQTCVV DFASYAYTTK DIEYGWKEEK
                                                             250
   ivrcl1 PIQIKDGLRQ SLPSFLLSNV KTGNCTSVTN TGAYSCLRTI IELKREFSYY
   ivrcl2 PIQIKDGLRQ SLPSFLLSNV KTGNCTSVTN TGAYSCLRTI IELKREFSYY
   ivrcl3 PIQIKDGLRQ SLPSFLLSNV KTGNCTSVTN TGAYSCLRTI IELKREFSYY
consensus PIQIKDGLRQ SLPSFLLSNV KTGNCTSVTN TGAYSCLRTI IELKREFSYY
                                                             300
   ivrcl1 LLQLYIPSFM LVAVSWVSFW LDKDSVPARV TLGVTTLLTM TTQASGVNAN
   ivrcl2 LLQLYIPSFM LVAVSWVSFW LDKDSVPARV TLGVTTLLTM TAQASGVNAN
   ivrcl3 LLQLYIPSFM LVAVSWVSFW LDKDSVPARV TLGVTTLLTM TTQASGVNAN
consensus LLQLYIPSFM LVAVSWVSFW LDKDSVPARV TLGVTTLLTM TTQASGVNAN
                                                             350
   ivrcl1 LPPVSYTKAI DIWIGVCLAF IFGALLEFAL VNWAARQDLV AHSRARYRQS
   ivrcl2 LPPVSYTKAI DIWIGVCLAF IFGALLEFAL VNWAARQDLV AHSRARYRQS
   ivrcl3 LPPVSYTKAI DIWIGVCLAF IFGALLEFAL VNWAARQDLV AHSRARYRQS
consensus LPPVSYTKAI DIWIGVCLAF IFGALLEFAL VNWAARQDLV AHSRARYRQS
                                                             400
   ivrcl1 PLFFRNPDSR QENSHHFYAP IQQEVTLEDL PFSWWDKIWK IRYKERSRRI
   ivrcl2 PLFFRNPDSR QENSHHFYAP IQQEVTLEDL PFSWWDKIWK IRYKERSRRI
   ivrcl3 PLFFRNPDSR QGNSHHFYAP IQQEVTLEDL PFSWWDKIWK IRYKERSRRI
consensus PLFFRNPDSR QENSHHFYAP IQQEVTLEDL PFSWWDKIWK IRYKERSRRI
                                                          436
   ivrcl1 DLISRVMFPL CFIIFNIMYW WRYLIPYMAV QAQLE*
   ivrcl2 DLISRVMFPL CFIIFNIMYW WRYLIPYMAV QAQLE*
   ivrcl3 DLISRVMFPL CFIIFNIMYW WRYLIPYMAV QAQLE*
consensus DLISRVMFPL CFIIFNIMYW WRYLIPYMAV QAQLE*
```

Figure 33 Alignment of HG5 clones amplified from IVR adult *H.contortus*. Blue indicates transmembrane regions. Conserved cysteine pairs are shown in green. Amino acids shown in red indicate differences between clones. Stop codons are represented by *.

HG5 consensus sequences from IVR and IVS *H.contortus* were compared to detect changes associated with the development of resistance. No coding differences were found in the sequences from ivermectin-resistant and -sensitive isolates (figure 34).

```
ivscon   MFALILPFLL HFTRSEGFGY EKLLDEQKII KHLLESPYSD YDWRVRPRGR
ivrcon   MFALILPFLL HFTRSEGFGY EKLLDEQKII KHLLESPYSD YDWRVRPRGR
                                                          100
ivscon   LGPADDDDYD SEPVFITVNM YLRSISKVDD VNMEYSLHFT FREEWIDERL
ivrcon   LGPADDDDYD SEPVFITVNM YLRSISKVDD VNMEYSLHFT FREEWIDERL

ivscon   YFNSPTLKHI VLSPGQRIWV PDTFFQNEKD GKKHDIDTPN ILIRIHNGTG
ivrcon   YFNSPTLKHI VLSPGQRIWV PDTFFQNEKD GKKHDIDTPN ILIRIHNGTG
                                                        200
ivscon   KILYSCRLTL TLSCPMRLAD YPLDVQTCVV DFASYAYTTK DIEYGWKEEK
ivrcon   KILYSCRLTL TLSCPMRLAD YPLDVQTCVV DFASYAYTTK DIEYGWKEEK

ivscon   PIQIKDGLRQ SLPSFLLSNV KTGNCTSVTN TGAYSCLRTI IELKREFSYY
ivrcon   PIQIKDGLRQ SLPSFLLSNV KTGNCTSVTN TGAYSCLRTI IELKREFSYY
                                                        300
ivscon   LLQLYIPSFM LVAVSWVSFW LDKDSVPARV TLGVTTLLTM TTQASGVNAN
ivrcon   LLQLYIPSFM LVAVSWVSFW LDKDSVPARV TLGVTTLLTM TTQASGVNAN

ivscon   LPPVSYTKAI DIWIGVCLAF IFGALLEFAL VNWAARQDLV AHSRARYRQS
ivrcon   LPPVSYTKAI DIWIGVCLAF IFGALLEFAL VNWAARQDLV AHSRARYRQS
                                                      ♦400
ivscon   PLFFRNPDSR QENSHHFYAP IQQEVTLEDL PFSWWDKIWK IRYKERSRRI
ivrcon   PLFFRNPDSR QENSHHFYAP IQQEVTLEDL PFSWWDKIWK IRYKERSRRI
                                            436
ivscon   DLISRVMFPL CFIIFNIMYW WRYLIPYMAV QAQLE*
ivrcon   DLISRVMFPL CFIIFNIMYW WRYLIPYMAV QAQLE*
```

Figure 34 Alignment of consensus HG5 sequences from IVS and IVR *H.contortus*. Blue indicates transmembrane regions. Conserved cysteine pairs are shown in green. Stop codons are represented by *. The conserved protein kinase C phosphorylation recognition sequence is shown (♦).

3.2 Discussion

Northern blot analysis of *H.contortus* mRNA confirmed that the pattern of alternative splicing of *gbr-2* observed in *C.elegans* is conserved. Expression of this gene and its products in a variety of nematodes suggests they play an important role in the nervous system, the partial GluCl subunit cDNA identified from *Onchocerca volvulus* shows 80% similarity to the *gbr-2* products (appendix 1). Alternative splicing of *gbr-2* has only been confirmed in *C.elegans* and *H.contortus*; only one gbr-2 product was detected in *Ascaris suum* (Jagannathan *et al.*, 1999) by RACE-PCR. It is possible that the partial gene duplication resulting in the two mRNAs occurred quite late in the evolution of nematodes as molecular phylogeny predicts *H.contortus* and

C.elegans to be closely related, whereas *Ascaris spp.* are found in a different clade (Blaxter, 1998). However, Northern blot analysis of *A.suum* may reveal conservation of gene duplication.

Attempts to compare the expression levels of the putative GluCl subunits HG2 and HG3 by semi-quantitative PCR indicated that HG2 was expressed at very low levels. HG2 and HG3 mRNAs were detected at very similar levels by Northern hybridisation, demonstrating that semi-quantitative PCR was not a reliable method of mRNA quantitation. Northern blot analysis was a more reliable method of detection, in this instance, as the two mRNAs could be directly compared in the same sample. The problems encountered by previous workers in the laboratory in amplifying HG2 were not due to very low mRNA levels

Full-length HG2 cDNA was amplified from *H.contortus* eggs and two clones were sequenced. Although a quite high level of nucleotide variation was apparent there were only three amino acid differences between the clones. One of these resulted in a coding change from a tryptophan to a termination signal (position 60) implying a PCR induced change. The sequence of the other HG2 clone was almost identical to that deposited in the EMBL database (accession number Y14233). One amino acid difference was found between the two sequences (position 344); a tryptophan residue was replaced with a leucine residue. Comparison with the *C.elegans* homologue CE-GBR2A revealed a leucine in this position suggesting that this alteration would not be detrimental to the expression of this subunit (Laughton *et al.*, 1997). It is possible that the amino acid residue at this position in the sequence deposited in the EMBL database is not representative of HG2 in the population.

Full-length cDNA of the putative GluCl subunit HG5 was amplified from *H.contortus* eggs and two clones were sequenced. A relatively high degree of non-coding nucleotide sequence variation has been observed between individual clones for all *H.contortus* receptor subunits reported as yet and this trend was continued in HG5. Three amino acid coding differences were seen between clones (positions 30, 171, 394), and the clones were compared with all available HG5 sequences. These include two sequences deposited in the EMBL database and sequences resulting from the amplification of partial

HG5 cDNAs in our laboratory. Very few coding differences were present between clones, even though one of the cDNAs had been amplified from adult *H.contortus* (AF076682) and the others originated from eggs. Comparison of all sequences produced a consensus and this was identical to RT-PCR amplified clone 1. Forrester *et al.*, (1999) indicated alternative splicing of the HG5 transcript by semi-quantitative PCR. This resulted in two cDNAs, one of which lacks 81 nucleotides at the 5' end (Forrester *et al.*, 1999). This phenomenon was not seen in any HG5 amplification in our laboratory.

A neighbour-joining tree was constructed to compare the *C.elegans* and *H.contortus* GluCl sequences, using the HG2 and HG5 sequences presented here (appendix 6). As shown previously, HG2 has a direct orthologue in *C.elegans*, gbr-2a, whereas, although HG5 is closely related to the gbr-2 gene products of both species, no clear *C.elegans* orthologue is identified for HG5. Orthologues of *C.elegans* GluClα1 and GluClα2 have not been identified in *H.contortus*. The upregulation of expression of HG5 in adult *H.contortus* as compared to larvae and eggs (Forrester *et al.*, 1999) coupled with the apparent lack of orthologues of this gene in the free-living species *C.elegans*, allows supposition that this gene may be the product of a novel gene that diverged as part of the adaptation to a parasitic life-style. Dent *et al.*, (2000) recently suggested that the *C.elegans* gbr-2 gene products are additional members of the alpha class of GluCl receptors (gluclα3). Inclusion of their *H.contortus* counterparts, HG2 and HG3, within this class appears plausible and the high level of identity of HG5 to the *gbr-2* products and GluClα2 suggests that this subunit is also a member of this class.

Resistance to the avermectin/milbemycin (AM) class of anthelmintics in livestock nematode populations is a serious problem worldwide. Although a great deal of research on this resistance has been undertaken the mechanism remains elusive. Resistance to the other classes of anthelmintic is apparently achieved by alteration of the drug target (section 1.2.4) and this is also a possibility in AM resistance. No coding differences were identified between the putative *H.contortus* GluCl subunits HG2, HG3 and HG4 from ivermectin-sensitive and ivermectin-resistant field isolates but population

genetic studies have identified alleles of the HG5 gene that may be selected during the evolution of ivermectin and moxidectin resistance (Blackhall *et al.*, 1998). HG5 cDNA sequences from ivermectin-sensitive and -resistant *H.contortus* strains were compared to determine if this subunit was involved in the development of drug resistance.

Amplification of HG5 cDNA from ivermectin-resistant *H.contortus* (IVR) eggs was unsuccessful when conditions that had achieved detection of this subunit from ivermectin-sensitive *H.contortus* (IVS) eggs were maintained. Downregulation of HG5 expression in *H.contortus* eggs as compared to adults has been reported (Forrester *et al.*, 1999). If resistance to ivermectin is achieved, at least in part, by reduced expression of HG5 it is possible that the mRNA message in eggs is reduced below detectable levels. Amplification was therefore attempted from adult worms and a very faint cDNA band of approximately the expected molecular weight for HG5 was observed. Alternative DNA polymerase enzymes were included in the RT-PCR reaction and the full-length cDNA was amplified and sequenced.

A quite high degree of nucleotide sequence variation was found between individual HG5 clones (<5%). As with subunits amplified from IVS isolates, few coding differences were seen implying that nucleotide variation is due to polymorphic parasite populations rather than PCR-induced error. Comparison of HG5 consensus sequences from IVR and IVS isolates revealed no coding alterations. This suggests that if selection at the HG5 gene occurs during the development of ivermectin resistance, as predicted by Blackhall and co- workers (1998), it results in altered expression of this subunit rather than modification of the amino acid sequence. The problems encountered in amplifying HG5 cDNA from IVR isolates substantiate this hypothesis. Northern blot or quantitative PCR analysis of HG5 expression in IVR and IVS *H.contortus* could be used to reveal altered regulation of HG5 message.

The results shown here cannot be directly compared with those of Blackhall and co-workers as different ivermectin-resistant isolates were used in the two studies. The White River II field isolate (Van Wyk *et al.*, 1988) was used in this study, whereas those used in the work of Blackhall *et al.* were laboratory isolates in which ivermectin resistance was induced by repeated exposure of

worms to increasing levels of drug. Gill *et al.* (1998; Gill and Lacey, 1998) present evidence that different selection protocols induce different resistant phenotypes in tristrongylids. The gradual selection of resistant *H.contortus* isolates using slowly increasing doses of ivermectin results in individuals that show no reduction in their sensitivity to the AM in terms of larval motility or development (e.g. IVC and TcR-1). In contrast, single-step selection of resistant individuals with ivermectin concentrations 10-fold higher than the $L.D._{95}$ produced a phenotype that involved reduced inhibition of both larval motility and development by the AM *in vitro*. This second scenario is thought to be most similar to the situation in the field and the White River II isolate was included in this type. The isotypes discussed by Blackhall et al. (1998) were selected under similar conditions to the TcR-1 and IVC isolates and are expected to have a different resistance phenotype to White River II. The differences in phenotype may well be reflected in the genotypes of isolates selected by different methods. Resistance in the Chiswick avermectin resistant *H.contortus* isolate (CAVR), which has a similar resistance phenotype to White River II isolates, is attributed to a single dominant trait (Le Jambre *et al.*, 2000), whereas in a laboratory-selected *T.columbriformis* resistant isolate, resistance appears a partially dominant trait and is not due to a single gene (Gill and Lacey, 1998). Resistance due to a single gene would rapidly spread through a population, as has been the case with the AM. The results of Gill and Lacey (1998) predict differences in resistance mechanisms both within and between species and further genetic studies on multiple resistant isolates are required to ascertain the usefulness of non-field strains as models.

Mutation studies in *C.elegans* have implicated a number of genes in high-level ivermectin resistance (Dent *et al.*, 2000). These include three GluCl genes, avr-14. avr-15 and glc-1, and a complicated parallel genetic pathway that is defined by these GluCl genes, but that also involves genes encoding innexins and amphid sensory neurons is suggested. Mutations in individual genes do not confer resistance. There is no evidence that these resistant mutants are analogous to the genotypes of ivermectin-resistant parasitic nematodes. Although AM resistance has been attributed to a single gene in the CAVR isolate, it is possible that multiple genes may be involved in AM

resistance, both in this and other isolates, but that they either have a modifying effect on and/or are linked to the major resistance gene. The observed variability in the nucleotide sequence of HG5 cDNA seen in this study confirms the observation by Blackhall *et al* (1998) that multiple HG5 alleles are present in the population. Further genetic and expression studies may implicate HG5, and other GluCl from parasitic nematodes, in the development of resistance.

4. Stable expression of inhibitory glutamate receptor subunits in a mammalian cell line

The successful cloning of four glutamate-gated chloride channel (GluCl) subunits from *H.contortus* paves the route for *in vitro* analysis of their function and for the development of an assay system to evaluate the efficacy of novel anthelmintics. Though there have been some studies on the pharmacology and physiology of the *C.elegans* GluCl subunits (Cully *et al.*, 1994; Laughton *et al.*, 1997; Dent *et al.*, 1997; Vassilatis *et al.*, 1997; Dent *et al.*, 2000; Horoszok *et al.*, in press) little is known about the function of these subunits in parasitic nematodes. The high sequence identity of the GluCls (appendix 1) and similar mode of action of the avermectins on *C.elegans* and *H.contortus* (Avery and Horvitz, 1990; Geary *et al.*, 1993; Paiement *et al.*, 1999; Gill *et al.*, 1995) predicts similar pharmacology for the GluCl subunits in these species, although adaptation to a parasitic life-style may have resulted in some modifications.

At present, the activity of novel avermectin analogues is primarily determined using whole organism fly and nematode assays. This is a time-consuming and inefficient process and the development of an assay system that could be easily maintained and used in high throughput screens is an attractive prospect. The industrial CASE sponsors of this PhD also viewed this as an important aspect of this project.

Gene transfer into mammalian cells is a powerful means of studying gene expression and allowing analysis of protein function (Spector *et al.*, 1998; Fernendez and Hoeffler, 1999). Relatively large amounts of target protein can be produced; reducing the time spent purifying protein and also removing the need for animal experimentation. Following the transfection of host cells a small percentage incorporate the foreign DNA into their genome and selection pressure can be applied to isolate these cells. If successful, this results in discrete colonies that can be isolated, expanded and analysed. These clonal cell lines are continually expressing the target gene, thereby producing a constant supply of the protein of interest.

A recipient cell line that grows in monolayers with a rapid doubling time increases the probability of successful gene transfer (Spector *et al.*, 1998). Mouse fibroblast L929 cells fit these criteria and were chosen for the production of cell lines stably expressing individual GluCl subunits. These cells do not naturally express ligand-gated ion channels thus reducing the likelihood of non-specific interactions and previous workers in our laboratory had used L929 cells for transient expression studies. Identification of cells with foreign DNA integrated into their genome requires the transfer of a selectable marker. A mammalian expression vector, pcDNA3, which contains a gene conferring drug resistance on transfected cells, was chosen as a vehicle for GluCl cDNA (appendix 6). The bacterial antibiotic neomycin affects the function of prokaryotic ribosomes and its analogue G418 blocks protein synthesis in mammalian cells by interfering with ribosomal function. The neomycin resistance gene (neo^r), included in the pcDNA3 genome, encodes a bacterial phosphotransferase that detoxifies G418. Eukaryotic cells expressing neo^r can survive in medium containing otherwise toxic concentrations of G418.

This chapter discusses the transfection of mammalian cells with recombinant plasmids containing GluCl cDNA and attempts to analyse the resulting cell lines using RT-PCR and radioligand binding. Two GluCl subunits, HG3 and HG4, were chosen for initial construction of cell lines as their *C.elegans* counterparts, ce-gbr2b and -gluclβ respectively, have physiological responses to ivermectin and/or glutamate when expressed in *Xenopus* oocytes (Cully *et al.*, 1994, Dent *et al.*, 2000).

4.1 Results

4.1.1 Attempted construction of an HG3 cell line

4.1.1.1 Sub-cloning HG3 for expression in mammalian cells

Jagannathan (1998) had previously cloned HG3 into the vector pBluescript II (appendix 3). A vector containing eukaryotic elements to control initiation of transcription and processing of DNA transcripts was required for expression of the subunit in mammalian cells. The HG3 cDNA was excised from

pBluescript II (figure 35) and sub-cloned into the mammalian expression vector pcDNA3 (appendix 6). Purified DNA from the resulting colonies was assessed for the presence of HG3 by restriction endonuclease digestion (figure 36).

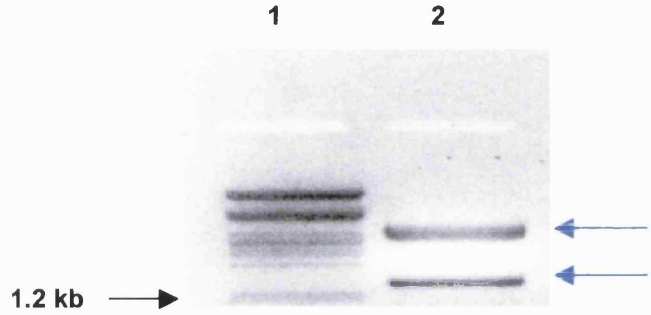

Figure 35 Restriction endonuclease digestion of recombinant pBluescript II. The enzymes Xba I and Hind III (20 units each) in buffer 2 were used to digest DNA (5 μg) for an hour at 37°C. The reaction was analysed by 1% (w/v) agarose gel electrophoresis in TAE buffer. Lane 1: λ pst I molecular weight marker. Lane 2: digested recombinant plasmid

A band of approximately the correct size for HG3 (1.3 kb) was cut from the gel and purified before ligation with Xba I/Hind III digested pcDNA3 DNA. Competent XL-1 Blue bacterial cells were transformed with the ligated DNA (5 μl).

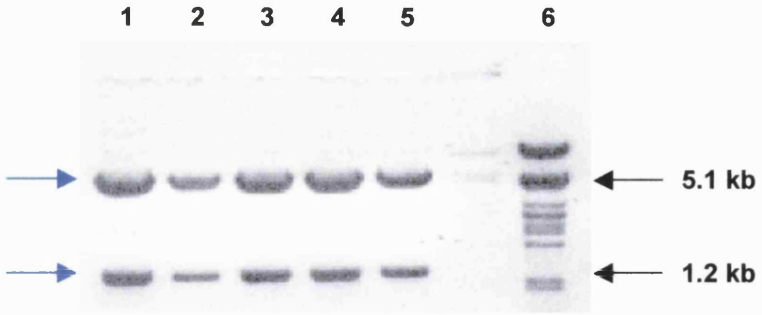

Figure 36 Analysis of recombinant pcDNA3 by restriction digestion. Plasmid DNAs (5 μg) were cut with Xba I and Hind III (20 units each) in buffer 2 for 2 hours at 37°C. The digested DNA was run on a 1% (w/v) agarose gel in TBE buffer and stained with ethidium bromide. Successful sub-cloning of HG3 was evident as digestion resulted in DNA bands of approximately 1.3 kb and 5.4 kb. Lanes 1-5: digested recombinant pcDNA3. Lane 6: λ pst I molecular weight marker.

HG3 cDNA was present in all recombinant plasmids analysed. The Qiagen Plasmid Maxikit was used to produce ultrapure recombinant DNA, as purity is a major determinant in the success of transfection. The resulting DNA was analysed by spectrophotometry ($O.D._{260}$), which indicated a concentration of 1.1 μg/μl and a purity ratio of 1.8 ($O.D._{260}/O.D._{280}$).

4.1.1.2 Sensitivity of L929 mouse fibroblast cells to the antibiotic G418

Selection of cells expressing foreign DNA on the basis of their antibiotic resistance requires toxicity of the antibiotic to untransfected cells. Cells exhibit varying sensitivities to G418 and therefore L929 cells were assayed to identify the minimum G418 lethal dose. Cells were incubated with a range of G418 concentrations and effects on viability were recorded (figure 37). All concentrations reduced cell confluence after 48 hours, but 450 μg/ml was the lowest concentration to entirely prevent cell division after 72 hours, although 35% confluence was observed. Control cells had reached 100% confluence at this time.

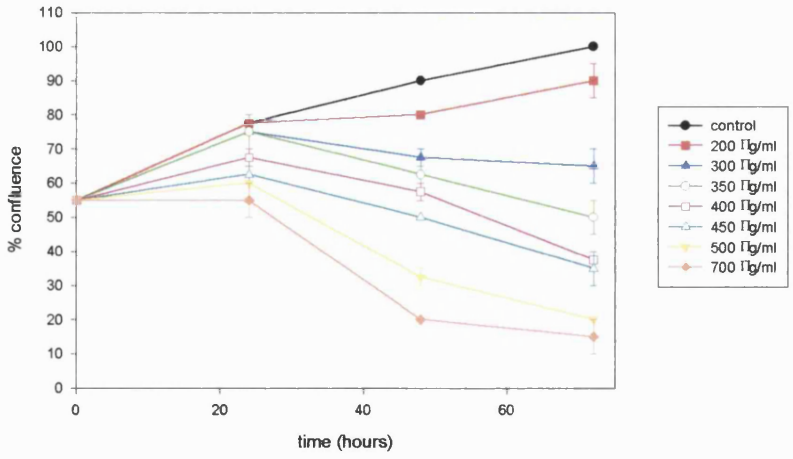

Figure 37 Sensitivity of L929 cells to the antibiotic G418. Cells were seeded at a concentration of 1 x 10^4 in 6 well plates containing minimal essential medium (3 ml) supplemented with 200-700 μg/ml G418. Cell viability was observed at 24 hour intervals for 72 hours and recorded as percentage confluence.

Cell viability was reduced more slowly by 400 μg/ml G418 but only 5% were still dividing 72 hours after treatment; confluence was reduced to 40% in this sample group. A concentration of 450 μg/ml was used for selection of cells expressing the neo^r gene and this was reduced to 400 μg/ml for maintenance of selection.

4.1.1.3 Transfection and selection of L929 cells

Transfected cells were selected approximately 48 hours post-transfection by the addition of 450 μg/ml G418 antibiotic to the growth media. Control (untransfected) cells were also treated with antibiotic and were all dead 7 days post-treatment. Clones were grown individually, as the plasmid may be inserted into the genome in a different position in each clone, thereby determining the level of protein expression of the transfected gene.

4.1.2 Analysis of HG3 transformed L929 cells

4.1.2.1 RT-PCR amplification of partial HG3 cDNA

Total RNA was extracted from each of 24 G418 resistant L929 colonies and run on an Rnase-free agarose gel to ensure degradation had not occurred (figure 38).

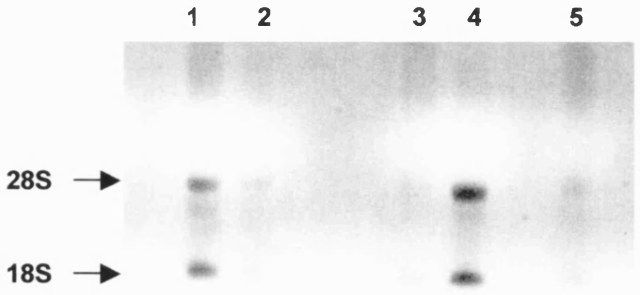

Figure 38 Total RNA from transformed L929 clones. RNA (3 μg) was run on a 1% (w/v) agarose TBE gel and stained with ethidium bromide to verify that extraction had been successful. RNA was observed in all 24 clones, but concentrations varied. Five representative clones are shown.

The low yield of RNA in some clones suggested that RT-PCR amplification would be the most efficient method for initial assessment of HG3 expression.

A positive control sample was produced for use in the RT-PCR amplification. Recombinant pcDNA3 expressing HG3 cDNA (10 μg) was linearised upstream of the HG3 sequence with the restriction enzyme Nru I and the T7 promoter was utilised to transcribe cRNA.

Primers were designed to internal regions of HG3 (5HG3part and 3HG3part. Appendix 4), as short lengths of cDNA should amplify more easily than full-length sequence. The access RT-PCR kit was used in conjunction with these primers to attempt detection of HG3 mRNA in the L929 clones (figure 39).

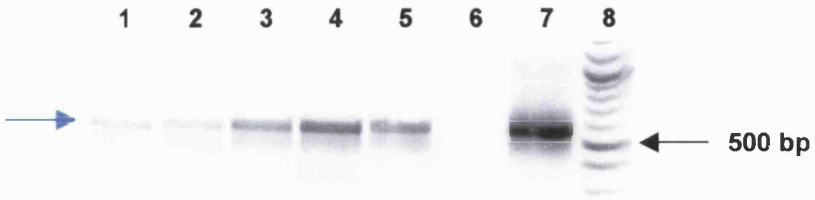

Figure 39 RT-PCR amplification of partial HG3 cDNA from transfected L929 cells. Sequence specific oligonucleotides 5HG3part and 3HG3part were used with the Access RT-PCR kit to amplify part of the HG3 subunit cDNA (approx. 550 bp) from total RNA. Positive and negative controls were included in the form of 200 ng HG3 cRNA and 1 μg total RNA from L929 cells transfected with pcDNA3 respectively. RT-PCR conditions were as follows: 45 min at 48°C, 2 min at 94°C and then 40 cycles of 95°C for 30 sec., 62°C for 30 sec., 72°C for 30 sec., followed by 72°C for 5 min. Amplification products were identified by electrophoresis through a 1.3% (w/v) agarose gel in TBE buffer and staining with ethidium bromide. Lanes 1-5: amplification products from transformed L929 cells. Lane 6: Negative control amplification. Lane 7: Positive control amplification. Lane 8: 100 bp molecular weight marker. cDNA of approximately the expected molecular weight was amplified from 20 clones. Five representative amplifications are shown.

RT-PCR amplification of partial HG3 RNA indicated that twenty L929 clones were expressing mRNA for this subunit.

4.1.2.2 Investigation of HG3 protein expression in transformed L929 cells

As HG3 mRNA was present in a number of the L929 clones, protein expression was looked for. Membranes were prepared from transformed

L929 cells of approximately 80% confluence and resuspended in 50 mM HEPES buffer at a concentration of 1 mg/ml.

4.1.2.2.1 Radioligand binding

Initial assessment of protein expression was attempted by measuring [^{3}H] ivermectin binding to membrane preparations. The *C.elegans* HG3 homologue forms channels that are gated by both ivermectin and glutamate, when expressed in *Xenopus* oocytes (Dent *et al.*, 2000), and the high sequence identity between the two subunits predicts similar pharmacology for HG3. Binding was determined by incubating varying concentrations of membranes (5-40 μg) with 0.5 nM [^{3}H] ivermectin for two hours at room temperature. No specific binding was observed to membrane preparations from any clone. Cells were grown at a reduced temperature (30°C), as this has previously been shown to up-regulate expression of recombinant LGIC subunits in mammalian cells (Cooper *et al.*, 1999). [^{3}H] ivermectin binding experiments were executed as at 37°C and no specific binding was observed to membranes from any clone.

4.1.2.2.2 Western blotting

The lack of specific binding to transformed L929 membranes demanded further investigation and Western analysis of expressed protein was attempted (figure 40). No candidate HG3 protein band (predicted to be approximately 48 kDa) could be detected in any of the clones.

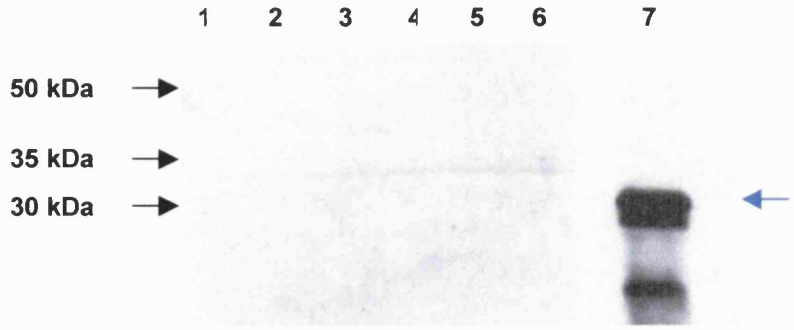

Figure 40 Western blot analysis of transformed L929 cell membranes. Membranes (20 μg) extracted from each transfected L929 clone were subjected to SDS-polyacrylamide gel electrophoresis and probing with an HG3 antibody (1/50 dilution) to the intracellular loop (designed and purified from rabbits by Virginia Portillo) before chemiluminescent detection. A positive control sample was included in the form of a recombinant plasmid with an inducible promoter (pGEX-GSTHG3) (32 kDa). No differences were observed between protein from untransfected and transfected cells. Lanes 1-5: transformed L929 cells. Lane 6: negative control. Lane 7: positive control.

4.1.3 Attempted construction of an HG4 cell line

Delany (1998) had previously cloned HG4 into the mammalian expression vector pcDNA3 and ultrapure DNA was extracted from XL-1 Blue cells expressing this recombinant plasmid. The DNA was analysed by spectrophotometry ($O.D._{260}$) and a concentration of 0.5 μg/μl and purity ratio of 1.7 were specified. Transfection and selection of colonies with the recombinant plasmid DNA incorporated into their genome proceeded as described for HG3.

4.1.4 Analysis of HG4 transformed L929 cells

4.1.4.1 RT-PCR amplification of partial HG4 cDNA

Total RNA was extracted from each of 36 L929 colonies selected for the presence of recombinant pcDNA3. Sequence-specific oligonucleotides (5HG4part and 3HG4part) (appendix 4) were designed to internal regions of HG4 and RT-PCR amplification was used for initial detection of clones expressing this subunit (figure 41). A positive control sample was produced for use in the RT-PCR amplification. Recombinant pcDNA3 expressing HG4

cDNA (10 μg) was linearised upstream of the HG4 sequence with the restriction enzyme Nru I and the T7 promoter was utilised to transcribe cRNA.

RT-PCR amplification of partial HG4 cDNA indicated that all 36 L929 clones were expressing HG4 message.

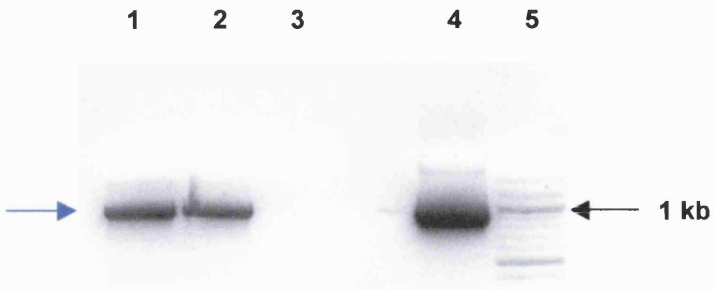

Figure 41 RT-PCR amplification of partial HG4 cDNA from transformed L929 cells. Sequence specific oligonucleotides 5HG4part and 3HG4part were used with the Access RT-PCR kit to amplify part of the HG4 subunit (approx. 900 bp) from total RNA. Positive and negative controls were included in the form of 200 ng HG4 cRNA and 1 μg total RNA from L929 cells transfected with pcDNA3 respectively. RT-PCR conditions were as follows: 45 min at 48°C, 2 min at 94°C and then 40 cycles of 94°C for 30 sec., 55°C for 30 sec., 72°C for 2 min, followed by 72°C for 5 min. Amplification products were identified by electrophoresis through a 1.2% (w/v) agarose gel in TBE buffer and staining with ethidium bromide. Lanes 1-2: amplification products from transformed L929 cells. Lane 3: Negative control amplification. Lane 4: Positive control amplification. Lane 5: molecular weight marker. cDNA of approximately the expected molecular weight was amplified from all clones. Two representative amplifications are shown.

4.1.4.2 Investigation of HG4 protein expression in transformed L929 cells

Membranes were prepared from all transformed L929 clones and binding of [^{3}H] ivermectin to the protein was measured as described for HG3. No specific ivermectin binding was seen to any clone. Attempts at Western blot analysis of expressed protein were obstructed by non-specific binding of the available HG4 antibody (Delany *et al.*, 1998) to untransfected L929 cells.

4.2 Discussion

Mammalian cell lines stably expressing HG3 and HG4 mRNA were successfully created. These clonal cell lines did not produce detectable protein encoded by the GluCl subunit gene. This suggests that the incorporation of recombinant plasmid DNA into the host cell genome was successful, but that incorrect processing occurred within the synthetic pathway.

It is probable that the lack of [^{3}H] ivermectin binding to HG3 transfected L929 clones was due to the non-existence of the HG3 protein. This is supported by the absence of this protein following Western blot analysis of transformed cells; the detection of the HG3 positive control sample suggested no problems with the experimental conditions. The *C.elegans* HG3 homologue, ce-gbr2b, has been shown to form homomeric channels that are gated by both ivermectin and glutamate when expressed in *Xenopus laevis* oocytes (Dent et al., 2000). The high sequence identity of this subunit between *H.contortus* and *C.elegans* (87%) predicts a similar pharmacology.

The absence of specific [^{3}H] ivermectin binding to the HG4 transfected L929 cells was not altogether surprising as homomeric expression of the *C.elegans* homologue, GluClβ, in *Xenopus* oocytes results in channels that are gated by glutamate but not ivermectin. A high level of sequence conservation is seen between these subunits (80%) and a comparable pharmacology is again probable. Binding experiments using radiolabelled glutamate were attempted, but the low affinity of this ligand for the GluCl receptor (Hejmadi *et al.*, 2000) coupled with the ubiquity of this amino acid and its binding sites in cells resulted in unmanageable levels of non-specific binding.

The reasons behind the observed lack of GluCl protein translation require further investigation beyond the scope of this project. Other workers have also attempted permanent expression of *C.elegans* (D. Cully, personal communication) and *H.contortus* (R. Prichard, personal communication) GluCl subunits in different mammalian cell lines and have obtained the same results. This suggests that the lack of protein expression is not due to the use of L929 cells. It is possible that permanent expression of the GluCl subunits

may be toxic to the mammalian cells. The transfer of GluCl genes to an insect cell line, or the development of a nematode cell line, may be more successful. It is probable that the functional GluCl receptor follows the pattern of expression observed in all LGIC in that a heteromeric pentamer of subunits is formed. The translation and processing of GluCl polypeptides may require signals from multiple subunits for completion, as is evident in mammalian $GABA_A$ receptors (Gorrie *et al.*, 1997, Taylor *et al.*, 2000).
Assessment of the ivermectin-binding properties of the *H.contortus* GluCl receptor subunits was therefore attempted using a transient gene expression system. Large quantities of foreign DNA can be expressed in such a system and, although the commercial application of this research may be reduced, this should determine which, if any, of the GluCl subunits form part of the ivermectin-binding site.

5. Pharmacology of glutamate-gated chloride channels

The avermectins bind to membrane preparations from parasitic nematodes with high affinity (Rohrer *et al.*, 1995; Hejmadi *et al.*, 2000), but their interaction with parasite recombinant GluCl is not known. Most *C.elegans* GluClα subunits form chloride channels gated by ivermectin (EC_{50} = 108-140 nM) (Cully *et al.*, 1994; Vassilatis *et al.*, 1997; Dent *et al.*, 2000; Horoszok *et al.*, in press).

The commercially available avermectins vary widely in their *in vivo* efficacy and their spectrum of activity. Studies in *C.elegans* comparing the activity of several avermectins and milbemycins have found strong correlation between the activation of glutamate-sensitive chloride currents, membrane binding and nematocidal activity (Arena *et al.*, 1995). The structure-activity relationships of the avermectins and their two modes of action, motility and development, have been investigated in parasitic nematodes (Gill and Lacey, 1998), but no data are available regarding their receptor-binding properties.

The absence of GluCl polypeptides in the HG3 and HG4 stable cell lines reduces the commercial potential of this study, but transient expression of the *H.contortus* GluCl subunits in a mammalian cell line should determine at least some of the components of the ivermectin-binding site. Following transfection of a mammalian cell line, approximately 5-50% of the cells will take up and express the foreign DNA (Spector *et al.*, 1998). A small percentage of these cells incorporate this DNA into their genome and if not selected, cells expressing the transfected protein will slowly be removed from the population. The plasmid DNA is transcribed within hours of transfection and cells can be assayed for gene products 24-72 hours post-transfection. Transient expression experiments preclude the effects of integration sites on expression and the possibility of harvesting cells that harbour mutations in the transfected DNA.

Cells vary in their transfection capacity, both in terms of DNA uptake and expression, and the most frequently used cell lines for transient expression are COS cells (Fernandez and Hoeffler, 1999). These are derived from African green monkey kidney cells by transformation with an origin defective simian virus 40 (SV40). High levels of the SV40 large tumour (T) antigen are

expressed by COS cells and this initiates viral DNA replication at the SV40 origin. Plasmids containing the SV40 origin of replication are thereby expressed at very high levels and copy numbers can be amplified to over 100,000. These cells cannot be used for stable expression of plasmids as a very high copy number is eventually lethal.

This chapter discusses the transient expression of each of the four cloned *H.contortus* GluCl subunits in the COS 7 cell line. Their potential role in the ivermectin-binding site was assessed and [^{3}H] ivermectin binding was characterised by saturation and competition studies. The structure-activity relationship of several avermectins and the recombinant GluCl subunits was analysed by competition against [^{3}H] ivermectin.

5.1 Results

5.1.1 Transient expression and analysis of HG2 in COS 7 cells

5.1.1.1 Subcloning HG2 cDNA for expression in mammalian cells

HG2 cDNA was previously cloned into the PCR cloning vector pCRBlunt (section 3.1.2.2), but expression in mammalian cells required the presence of the subunit in a mammalian expression vector. The vector pcDNA3 contains the SV40 origin of replication for high-level expression in COS cells. The HG2 cDNA was digested from pCRBlunt for subcloning into pcDNA3 (figure 42). The HG2 band (approximately 1.45 kb) was cut from the gel and purified before ligation with Xba I and Kpn I digested pcDNA3. Competent XL-1 Blue cells were transformed with the ligated DNA. Purified DNA from the resulting colonies was assessed for the presence of HG2 cDNA by restriction endonuclease digestion (figure 43).

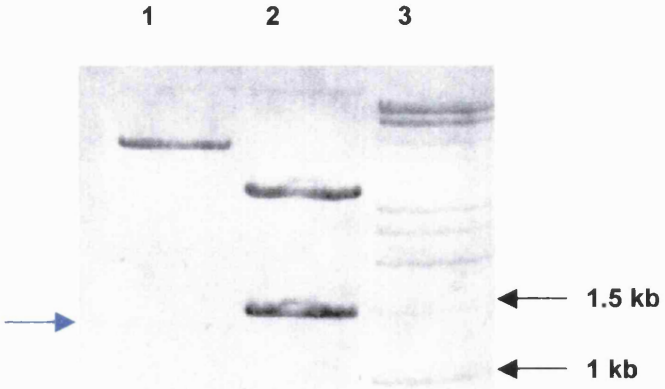

Figure 42 Restriction endonuclease digestion of recombinant pCRBlunt. DNA (5 μg) was cut with Xba I and Kpn I (10 units each) (in buffer 2) for 2 hours at 37°C. Samples were analysed by electrophoresis through a 1% (w/v) agarose gel in TAE buffer and staining with ethidium bromide. Lane 1: digested pcDNA3. Lane 2: digested recombinant pcrBlunt. Lane 3: 1 kb molecular weight marker.

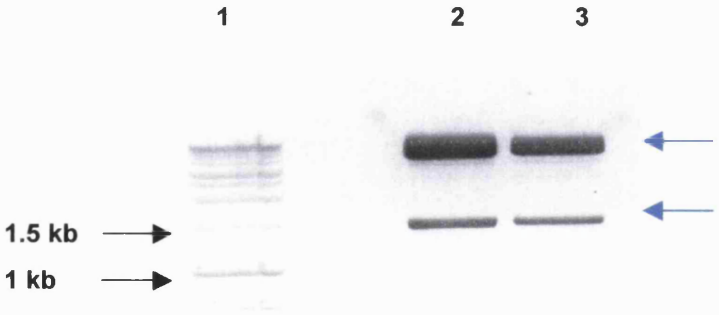

Figure 43 Restriction endonuclease digestion of recombinant pcDNA3. DNA (5 μg) was digested with Hind III and Apa I (10 units each) (in buffer 4) for 2 hours at 37°C. Digested DNA was run on a 1% (w/v) agarose gel in TBE buffer and stained with ethidium bromide. Successful subcloning of HG2 was evident as digestion resulted in DNA bands of approximately 1. 45 kb and 5.4 kb. Lane 1: 1 kb molecular weight marker. Lanes 2-3: digested recombinant pcDNA3.

HG2 cDNA was present in both pcDNA3 clones. Ultrapure DNA was extracted from one of these clones and its purity and concentration assessed by spectrophotometry. The DNA was at a concentration of 1.1 μg/μl ($O.D._{260}$) and had a purity ratio of 1.8 ($O.D._{260}/O.D._{280}$).

5.1.1.2 Transfection and harvesting of COS 7 cells

Cells were harvested approximately 48 hours post-transfection at which time they were approximately 85% confluent. Membranes were extracted and resuspended at a concentration of 1 mg/ml in ice-cold 50mM HEPES, pH 7.4.

5.1.1.3 Analysis of expressed protein

5.1.1.3.1 Radioligand binding

The role played by the HG2 polypeptide in the *H.contortus* ivermectin binding site was assessed by [^{3}H] ivermectin binding experiments. Binding conditions were a combination of those described previously for *H.contortus* and *Drosophila* membranes (Hejmadi *et al.*, 2000; Smith *et al.*, 2000). Binding was determined by incubating varying concentrations of transfected COS 7 cell membranes (5-40 μg) with 0.5 nM [^{3}H] ivermectin for two hours at room temperature. No specific binding was apparent (n = 3).

5.1.1.3.2 Western Blotting

The technique of immunoblotting can be used to determine the presence and quantity of an antigen. Western blotting of transfected COS 7 cell membranes was attempted to reveal if transfection had been successful, resulting in HG2 protein expression in the host cells (figure 44). Protein of approximately the predicted molecular weight of HG2 (predicted to be ~ 46 kDa) was detected in the HG2 transfected cells suggesting that HG2 protein was expressed in the transfected COS 7 cell membranes

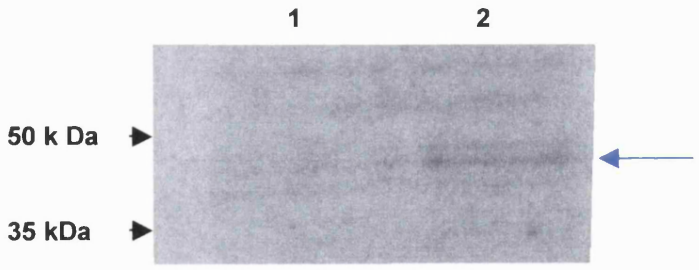

Figure 44 Western blot analysis of HG2 transfected COS 7 cell membranes. Protein (20 μg) was electrophoresed through an SDS polyacrylamide gel and probed with an HG2 antibody (1/50 dilution)(designed to the HG2 intracellular loop and purified from rabbits by Virginia Portillo) before chemiluminescent detection. Membranes were also analysed from pcDNA3 transfected COS 7 cells. Lane 1: negative control protein. Lane 2: HG2 transfected COS 7 cells.

5.1.2 Transient expression and analysis of HG3 in COS 7 cells

HG3 had previously been subcloned into the mammalian expression vector pcDNA3 (section 4.1.1.1) and this recombinant plasmid was used to transfect COS 7 cells. Cells were transfected and harvested as described for HG2.

5.1.2.1 Radioligand binding

Radiolabelled ivermectin was used to determine if HG3 forms part of the ivermectin-binding site. The *C.elegans* orthologue, gbr-2b, is included in the "alpha" subunit class of GluCl due to its relatively high level of homology to the other known alpha subunits (approx. 60%) (appendix 1) and its ability to form chloride channels that are gated by ivermectin (Dent *et al.*, 2000). Binding was determined by incubating varying concentrations of transfected COS 7 cell membranes (5-40 μg) with 0.5 nM [^{3}H] ivermectin for two hours at room temperature. Specific binding was easily measured to membrane preparations from COS 7 cells transfected with HG3 cDNA (figure 45). [^{3}H] ivermectin did not specifically bind to COS 7 cells transfected with pcDNA3. Binding was approximately linear over the range of protein used. No ligand depletion was apparent and a protein concentration of 10 μg was used in all further experiments.

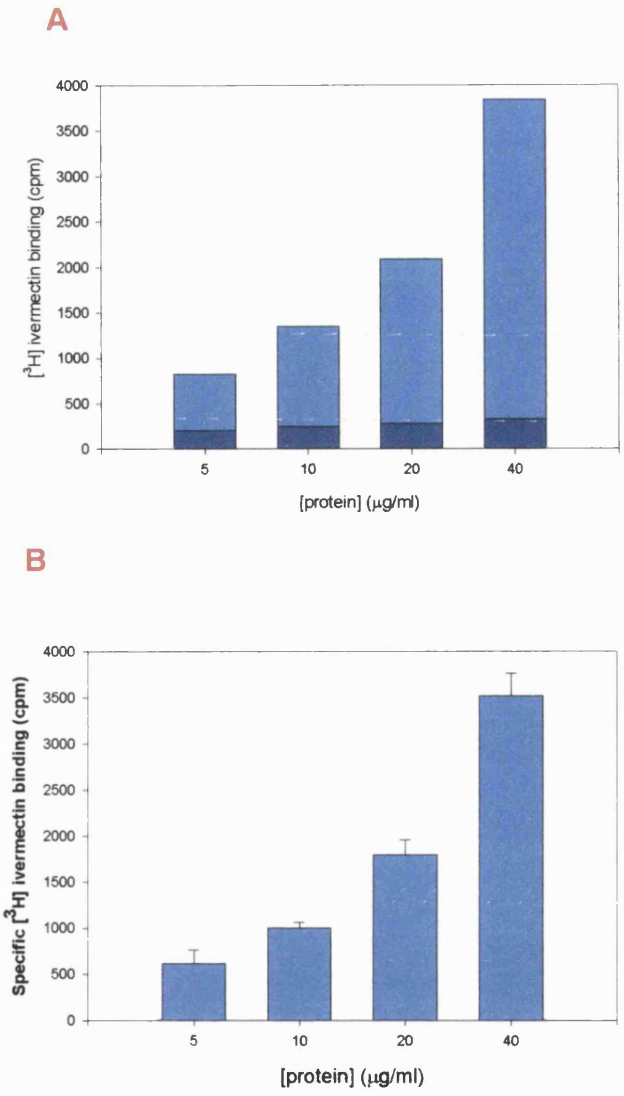

Figure 45 [^{3}H] ivermectin binding to membrane preparations from COS 7 cells transiently expressing HG3. Protein was incubated with 0.5 nM [^{3}H] ivermectin in a final assay volume of 1 ml for two hours at room temperature. Non-specific binding was determined by incubation in the presence of 10 µM unlabelled ivermectin. A shows total binding to membranes with ■ = non-specific binding and ■ = specific binding. B shows specific binding. n = 3.

5.1.2.1.1 Saturation and competition analysis of [^{3}H] ivermectin binding

Ivermectin binds with high affinity to membranes from *H.contortus* L3-stage larvae (reported K_d < 1 nM) (Rohrer *et al.*,1994; Hejmadi *et al.*, 2000) and

saturation studies were attempted to ascertain if recombinant HG3 showed similar binding properties.

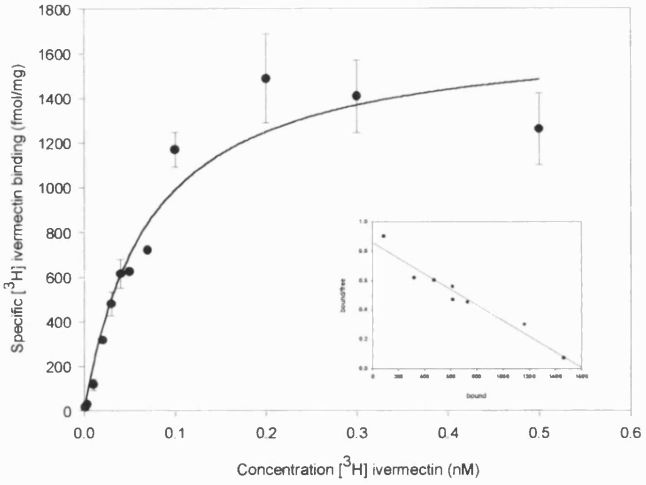

Figure 46 Saturation of membranes from COS 7 cells transiently expressing HG3 with [^{3}H] ivermectin. Protein (10 μg) was incubated with various concentrations of [^{3}H] ivermectin (1 pM – 1 nM) for 2 hours at room temperature. Non-specific binding was determined in the presence of 10 μM unlabelled ivermectin. Inset is the Scatchard plot. Replica experiments were carried out on membranes from the same transfection. n = 4.

Specific high-affinity [^{3}H] ivermectin binding was observed to membranes from HG3 transfected COS 7 cells (figure 46). This binding was saturable with a K_d of 70 +/- 16 pM and a B_{max} of 1.6 +/- 0.1 pmol/mg. Variation in B_{max} values between transfections was not significant.

Competition assays were also carried out, using various concentrations of unlabelled ivermectin to compete with [^{3}H] ivermectin for the binding site (figure 47). This is an additional means of confirming the estimated K_d value. High-affinity specific binding was measured and fitted to a one-site model with a Hill number of 0.7. The K_i was determined as 50 +/- 5pM.

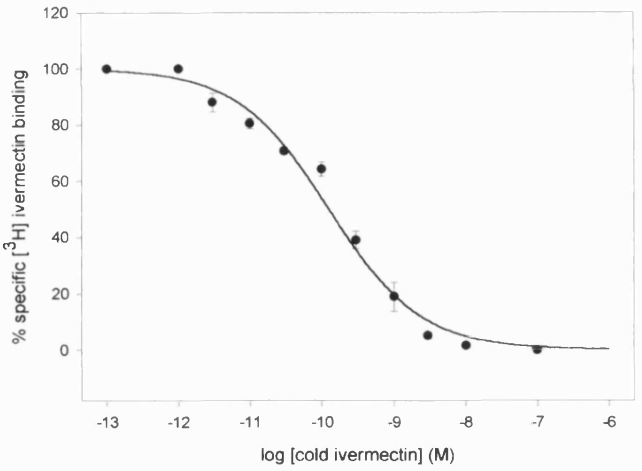

Figure 47 Competition between [^{3}H] ivermectin and unlabelled ivermectin for their binding sites on membranes from COS 7 cells transiently expressing HG3. Protein (10 μg) was incubated with 70 pM [^{3}H] ivermectin and various concentrations of unlabelled ivermectin (100 fM – 100 nM) for 2 hours at room temperature. n = 3.

5.1.2.1.2 Pharmacology of [^{3}H] ivermectin binding

There are no reported inhibitors of ivermectin binding in the literature except for other macrocyclic lactones and nodulisporic acid, a fungal product that binds with high affinity to insect, but not nematode, GluCl (Smith *et al.* 2000). Wide variation is seen between the macrocyclic lactones' spectra of activity and this is conserved in their ability to bind to membrane preparations from *C.elegans* (Arena *et al.*, 1995). The ability of a number of avermectin derivatives to compete for the ivermectin-binding site on COS 7 cell membranes expressing HG3 polypeptides was examined (figure 48). Structures are not shown due to intellectual property constraints.

All of the macrocylic lactones studied were able to compete for the ivermectin-binding site. Differences were observed in their binding affinities and none of them was as effective as ivermectin itself in this assay. Table 1 shows K_i values for the avermectins. The rank order of affinity was ivermectin >avm E > avm A > avm C + avm D > avm B.

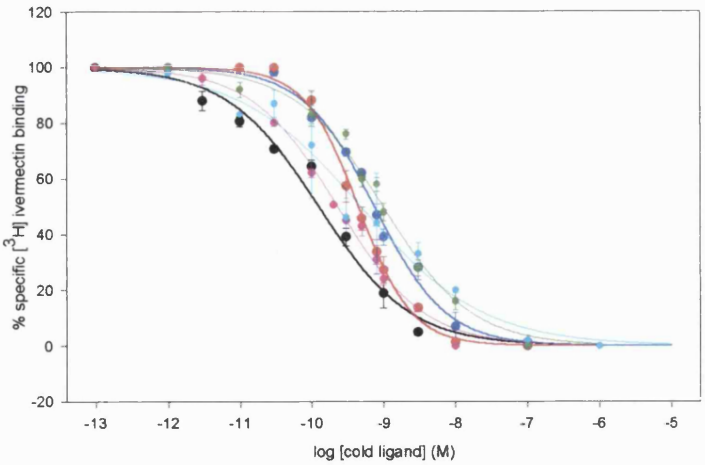

Figure 48 Competition for [^{3}H] ivermectin binding by different avermectins. P2 membranes (10 μg) from COS 7 cells expressing HG3 were incubated with 140 pM [^{3}H] ivermectin and various concentrations of each avermectin (100 fM – 1 μM) for 2 hours at room temperature. Competition with ivermectin (•), avm A (•), avm B (•), avm C (•), avm D (•) and avm E (•) was studied. n = 3 for each ligand.

Cold ligand	**K_i**	**Hill Number**
Ivermectin	50 +/- 5 pM	0.7
Avm A	182 +/- 30 pM	1.2
Avm B	334 +/- 60 pM	0.7
Avm C	233 +/- 18 pM	0.9
Avm D	233 +/- 64 pM	0.5
Avm E	75 +/-12 pM	0.7
GABA	No competition	
Glutamate	No competition	
Fipronil	No competition	
Picrotoxin	No competition	

Table 1 Affinity of various avermectins for the ivermectin-binding site of recombinant HG3 as measured by competition with [^{3}H] ivermectin.

The ivermectin-binding site was analysed with further competition assays (Table 1). Most of the ligands used had been shown to have some activity at *C.elegans* GluCl and/or interact with ivermectin. The amino acids glutamate and GABA (10 mM), picrotoxin (100 μM), a potent antagonist of vertebrate $GABA_A$ receptors and some GluCl receptors, and fipronil (100 μM), a phenylpyrazole insecticide, did not compete with [^{3}H] ivermectin binding (70 pM) under these conditions.

5.1.3 Transient expression and analysis of HG4 in COS 7 cells

Delany (1998) had subcloned HG4 into the mammalian expression vector pcDNA3 and this recombinant plasmid was used to transfect COS 7 cells.

5.1.3.1 Analysis of expressed protein

5.1.3.1.1 Radioligand binding

The HG4 *C.elegans* orthologue, GluClβ, forms channels that are gated by glutamate but not ivermectin (Cully *et al.*, 1994). Radiolabelled ivermectin studies were undertaken on membranes prepared from COS 7 cells transfected with HG4 cDNA to determine if this pattern was conserved. Binding was determined by incubating varying concentrations of transfected COS 7 cell membranes (5-40 μg) with 0.5 nM [^{3}H] ivermectin for two hours at room temperature. No specific binding could be detected (n = 3).

5.1.3.1.2 Immunofluorescence microscopy

Antibodies raised to a protein of interest can be used at the light microscopic level to detect and localise antigens within cells. Primary antibodies raised to HG4 (Delany, 1998) showed high non-specific binding to COS 7 cells, but an epitope-tagged form of HG4 cDNA (HG4pFLAG-CMV™-5c) was available (produced by Virginia Portillo) and could be used with commercial antibodies for detection. COS 7 cells were transfected with the tagged recombinant HG4 cDNA and expression was assessed by confocal microscopy (figure 49). Fluorescence was observed in HG4-flag transfected cells, but not in untransfected cells. A punctuate pattern of expression was observed in the cytoplasm. HG4 was not expressed at the plasma membrane.

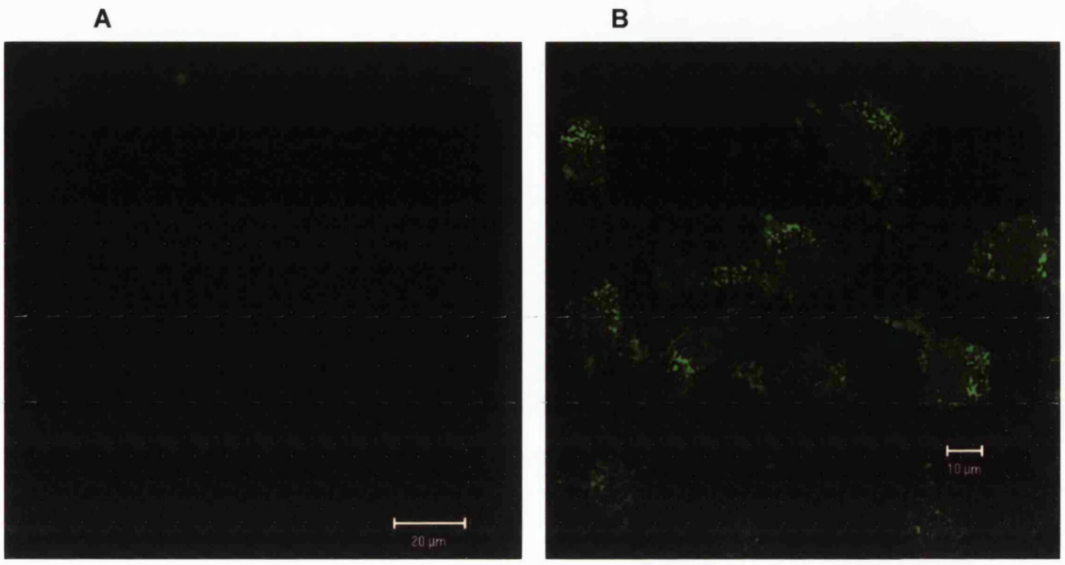

Figure 49 Expression of epitope-tagged HG4 in COS 7 cells. Forty eight hours after transfection, COS 7 cells were incubated with primary antibody (mouse anti-flag, 1/300 dilution) and secondary antibody (FITC-conjugated anti mouse, 1/200 dilution) before viewing on a confocal microscope. Negative control samples were included in the form of untransfected COS 7 cells. Antigen was detected in HG4-flag transfected cells but not untransfected cells. A: untransfected cells. B: HG4-flag transfected cells.

5.1.4 Transient expression and analysis of HG5 in COS 7 cells

5.1.4.1 Subcloning HG5 cDNA for expression in mammalian cells

The GluCl subunit HG5 was originally cloned into the bacterial expression vector pCRBlunt (section 3.1.3.2), but expression in COS 7 cells required transfer into a mammalian expression vector. HG5 cDNA was removed from pCRBlunt and subcloned into the plasmid pcDNA3 (figure 50). The resulting colonies were checked for the presence of HG5 by restriction endonuclease digestion (figure 51). The observed band of approximately the size of HG5 (1.45 kb) was purified and ligated with Kpn I/Xho I digested pcDNA3. Competent XL-1 blue cells were transformed with the ligated DNA (5 µl).

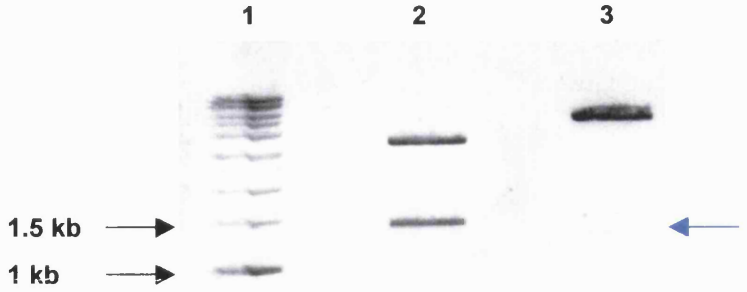

Figure 50 Removal of HG5 cDNA from the plasmid pCRBlunt. The restriction enzymes Kpn I and Xho I (10 units each) in buffer 2 were used to cut the recombinant plasmid (5 μg) for 2 hours at 37°C. The digested DNA was electrophoresed through a 1% (w/v) agarose gel in TAE buffer before staining with ethidium bromide. Lane 1: 1 kb molecular weight marker. Lane 2: digested recombinant pCRBlunt. Lane 3: digested pcDNA3.

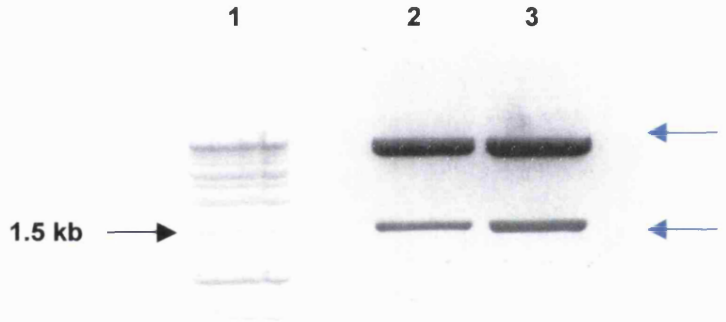

Figure 51 Restriction endonuclease digestion of recombinant pcDNA3. Plasmid DNA (5 μg) was cut with the enzymes Xba I and Hind III (10 units each) in buffer 2 for 2 hours at 37°C to verify successful subcloning of HG5 cDNA. Digested samples were run on a 1% (w/v) agarose gel in TBE buffer before staining with ethidium bromide. The presence of HG5 cDNA in the recombinant plasmid was confirmed as DNA bands of approximately 1.5 kb and 5.4 kb were apparent on the gel. Lane 1: 1 kb molecular weight marker. Lane 2-3: digested recombinant pcDNA3.

5.1.4.2 Radioligand binding

HG5 shows the highest identity to GluClα2 and the gbr-2 subunits (appendices 1 and 2). However, it does not appear to be orthologous with any of the *C.elegans* alpha subunits, as it is less similar to them than the *Hc-gluclβ* (HG4) or *Hc-gbr2* (HG2 and HG3) genes are to their orthologues. The alpha class of GluCl subunits form part of the *C.elegans* ivermectin binding site and it seemed interesting to investigate whether this novel gene played a role in the interaction with ivermectin in a parasitic nematode. Binding was determined by incubating varying concentrations of transfected COS 7 cell membranes (5-40 μg) with 0.5 nM [^{3}H] ivermectin for two hours at room temperature. Specific binding to recombinant HG5 protein was measured and was approximately linear over the range of protein concentrations tested (figure 52). No ligand depletion was apparent and a concentration of 20 μg was used in all further experiments.

A

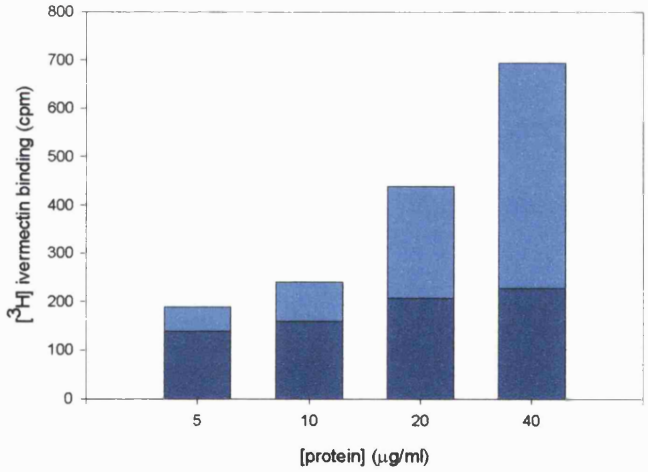

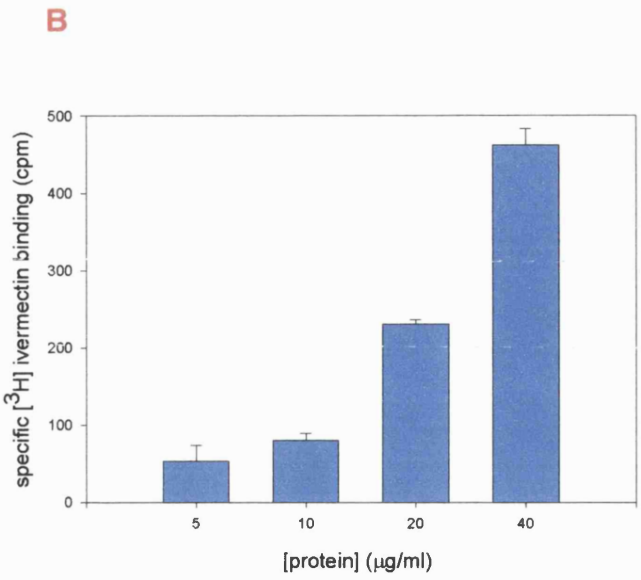

Figure 52 [^{3}H] ivermectin binding to membrane preparations from COS 7 cells transiently expressing HG5. Protein was incubated with 0.5 nM [^{3}H] ivermectin in a final assay volume of 1 ml for two hours at room temperature. Non-specific binding was determined by incubation in the presence of 10 µM unlabelled ivermectin. A shows total binding to membranes with ■ = non-specific binding and ■ = specific binding. B shows specific binding. n = 3.

5.1.4.2.1 Saturation and competition analysis of [^{3}H] ivermectin binding

The observed binding to recombinant HG5 was characterised further, both for comparison with ivermectin binding to HG3 and to *H.contortus* membranes (figure 53). Specific high-affinity binding was measured to HG5 transfected COS 7 cell membranes. This binding was saturable with a K_d of 26 +/- 12 pM and a B_{max} of 0.08 +/- 0.01 fmol/mg. Competition of unlabelled ivermectin for the ivermectin-binding site was determined as confimation of the calculated K_d (figure 54). High-affinity specific binding was observed and fitted to a one-site model with a Hill number of 0.98. The K_i was calculated as 9 +/- 0.7 pM.

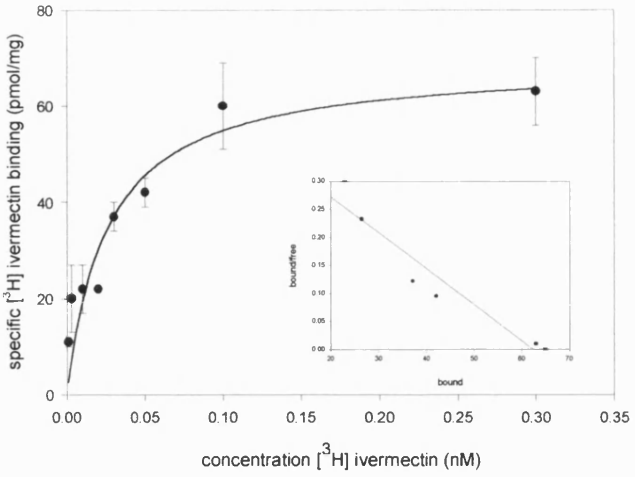

Figure 53 Saturation of membranes from COS 7 cells transiently expressing HG5 with [^{3}H] ivermectin. Protein (15 μg) was incubated with various concentrations of [^{3}H] ivermectin (1 pM – 1 nM) for 2 hours at room temperature. Non-specific binding was determined in the presence of 10 μM unlabelled ivermectin. Inset is the Scatchard plot. n = 3.

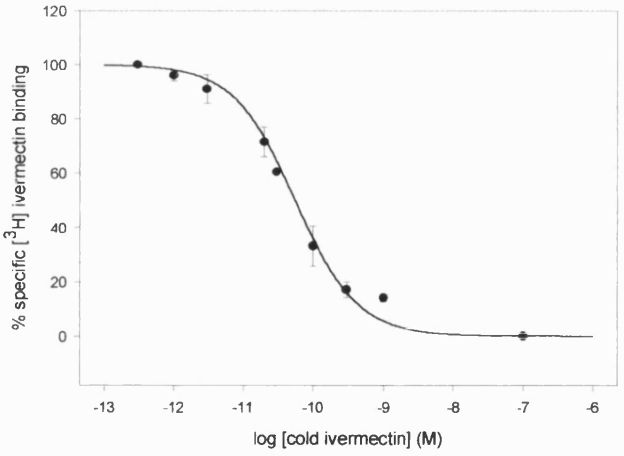

Figure 54 Competition between [^{3}H] ivermectin and unlabelled ivermectin for their binding sites on membranes from COS 7 cells transiently expressing HG5. Protein (15 μg) was incubated with 100 pM [^{3}H] ivermectin and various concentrations of unlabelled ivermectin (100 fM – 100 nM) for 2 hours at room temperature. n = 3.

5.1.4.2.2 Pharmacology of the recombinant HG5 ivermectin-binding site

The ability of a number of avermectin derivatives to compete for the ivermectin-binding site on COS 7 cell membranes transiently expressing HG5 was examined (figure 55). This allowed further characterisation of the ivermectin-binding site and direct comparison with binding to HG3.

All avermectins studied competed with [^{3}H] ivermectin binding, but with varying affinities. Ivermectin had the highest affinity for its binding site and the rank order was ivermectin > avm A = avm B > avm E > avm D > avm C. K_i values for competition studies with the avermectins on recombinant HG3 and HG5 are shown in table 2. Differences are seen between the two subunits, but all avermectins studied show higher affinity for COS 7 cells expressing HG5.

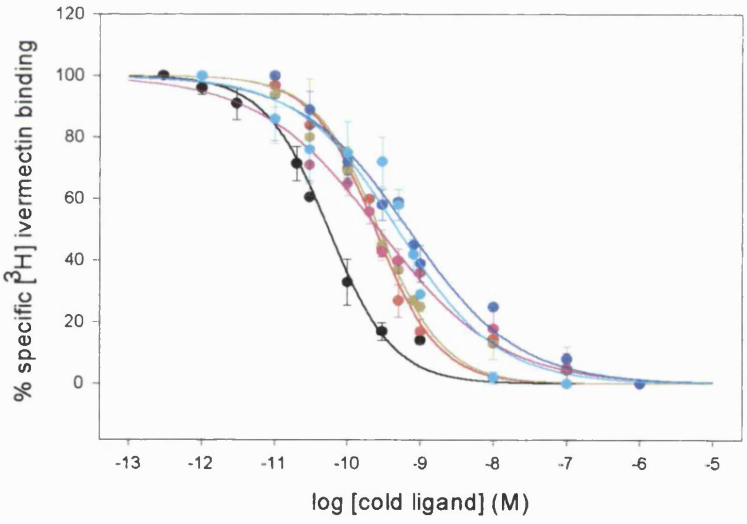

Figure 55 Competition for [^{3}H]ivermectin binding by different avermectins. P2 membranes (15 μg) from COS 7 cells expressing HG5 were incubated with 150 pM [^{3}H] ivermectin and various concentrations of each avermectin (100 fM – 1 μM) for 2 hours at room temperature. Competition with ivermectin (•), avm A (•), avm B (•), avm C (•), avm D (•) and avm E (•) was studied. n = 3 for each ligand.

Cold ligand	K_i HG5	Hill Number
Ivermectin	9 +/- 0.7 pM	1
Avm A	37 +/- 3 pM	1
Avm B	37 +/- 7 pM	1
Avm C	110 +/- 9 pM	0.58
Avm D	64 +/- 6 pM	0.64
Avm E	40 +/- 7 pM	0.52
GABA	No competition	
Glutamate	No competition	
Fipronil	No competition	
Picrotoxin	No competition	

Table 2 Affinity of various avermectins for the ivermectin-binding site of recombinant HG5 as measured by competition with [^{3}H] ivermectin.

Ivermectin binding to recombinant HG5 was further characterised using ligands that had previously been described to have some interaction with ivermectin and/or the *C.elegans* GluCl. Glutamate, GABA (10 mM each), picrotoxin and fipronil (100 μM each) did not compete with [^{3}H] ivermectin binding (150 pM) under these conditions (table 2).

5.1.5 Ivermectin binding to *H.contortus* membranes

The affinity of [^{3}H] ivermectin binding to the recombinant *H.contortus* GluCl subunits was slightly higher than was reported in the literature for *H.contortus* L3 membrane preparations (0.16-0.6 nM) (Rohrer *et al.*, 1994; Hejmadi *et al.*, 2000). Research on larval membranes had been carried out under different experimental conditions. We examined the binding of ivermectin to P2 membrane preparations from *H.contortus* L3 larvae under similar conditions to those used for experiments with the recombinant subunits (figure 56). Under these conditions, [^{3}H] ivermectin bound to larval membranes with a K_d of 70 +/- 7 pM. Additional binding sites may be present that were not detected in these experiments. A comparison of [^{3}H] ivermectin binding to *H.contortus* L3 membranes and recombinant GluCl subunits is shown in table 3.

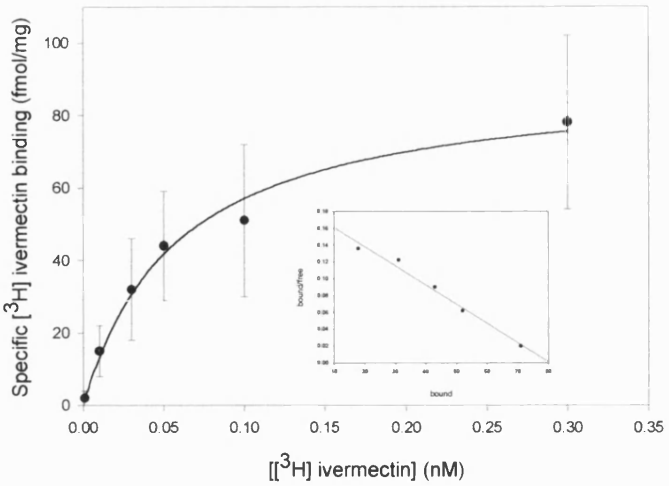

Figure 56 Saturation curve of [^{3}H] ivermectin binding to P2 membranes from *H.contortus* L3 stage larvae. Protein (15 μg) was incubated with various concentrations of [^{3}H] ivermectin (1 pM – 1 nM) for 2 hours at room temperature. Non-specific binding was determined by the presence of 10 μM unlabelled ivermectin. Inset is the Scatchard plot. n = 3.

Substrate	**K_d**	**K_i**
H.contortus L3	70 +/- 7 pM	N.D.
HG2	No binding	
HG3	70 +/- 16 pM	50 +/- 5 pM
HG4	No binding	
HG5	26 +/- 12 pM	9 +/- 0.7 pM

Table 3 [^{3}H] ivermectin binding to recombinant GluCl subunits and *H.contortus* L3 larvae. N.D. not determined.

The highest affinity [^{3}H]ivermectin binding was to recombinant HG5. Ivermectin had very similar affinity for L3 membranes and recombinant HG3.

5.2 Discussion

The four known glutamate-gated chloride channel subunits from *H.contortus* have been successfully expressed in a mammalian cell line. The subunits

show differences in their pharmacology with respect to their interaction with ivermectin. No [^{3}H] ivermectin binding was observed to cells transfected with HG2 or HG4, but western hybridisation and epitope-tagged confocal imaging respectively demonstrated that the subunit polypeptides were present. The lack of [^{3}H] ivermectin binding to HG4 is not unexpected as its orthologue in *C.elegans*, GluClβ, forms channels gated by L-glutamate but not ivermectin (Cully *et al.*, 1994). The high sequence identity between these subunits is reflected in their pharmacology, at least in terms of ivermectin (appendix 1) (table 4). The *C.elegans* orthologues of HG3 and HG4 form channels gated by glutamate (Cully *et al.*, 1994; Dent *et al.*, 2000). Attempts to investigate the binding capacity of radiolabelled glutamate to HG3 and HG4 polypeptides were hampered by the low affinity of this ligand for the GluCl receptor (Hejmadi *et al.*, 2000) and the ubiquity of glutamate and its binding sites within the host cell. This resulted in very high levels of non-specific binding.

The alternatively spliced gene, *gbr-2*, appears to encode two subunits with different pharmacology. The HG2 polypeptide was expressed in transfected COS 7 cell membranes, but did not specifically bind [^{3}H] ivermectin. In contrast, specific [^{3}H] ivermectin binding was easily measured to the HG3 variant. The *H.contortus* subunits HG2 and HG3 have clear orthologues in *C.elegans*, GBR-2A and GBR-2B, based on a very high level of sequence identity and conservation of alternative splicing (Laughton *et al.*, 1997; Jagannathan *et al.*, 1999). Gating of GBR-2B channels but not GBR-2A channels with ivermectin has recently been reported (Dent *et al.*, 2000) suggesting that the interaction of these subunits with ivermectin is also conserved between species. The observed difference in ivermectin binding between the *gbr-2* encoded polypeptides from both *H.contortus* and *C.elegans* is somewhat surprising as the N-terminal regions of the spliced variants, which are thought to contain most of the ligand binding sites, are identical. It is apparent that sequences in the C-terminal half of the GluCl receptor are important in the formation of the ivermectin-binding site

The subunits HG3 and HG5 specifically bind [^{3}H] ivermectin with very high affinity. Binding to both recombinant subunits was saturable and K_ds were calculated as 70 +/- 16pM for HG3 and 26 +/-12 pM for HG5. These figures

were supported by competition assays with unlabelled ivermectin as measured K_i values were very similar at 50 +/- 5 pM for HG3 and 9 +/- 0.7 pM for HG5. Although ivermectin showed higher affinity for recombinant HG5 than HG3, the quantity of bound radioligand (fmol/mg) was much lower to HG5 suggesting a reduced number of binding sites. Co-workers in the laboratory have identified HG5 expression both intracellularly and at the plasma membrane of transfected mammalian cells (Virginia Portillo, personal communication) and co-expression studies may result in enhanced transport of HG5 to the plasma membrane. It is possible that HG3 is able to form a functional receptor without the need for additional subunits.

Electrophysiological investigations of *C.elegans* GluCl have intimated that only GluCl α-subunits form channels that are gated by ivermectin. Table 4 illustrates the pharmacology of the known GluCl subunits from *H.contortus* and *C.elegans*. Channels formed by the *C.elegans* β-subunit are gated by L-glutamate and require co-expression with an α-subunit for ivermectin activation (Cully *et al.*, 1994). Horoszok *et al.* (in press) report the formation of an ivermectin- and glutamate-sensitive channel on expression of the GluCl subunit GLC-3 in *Xenopus laevis* oocytes. This subunit shows highest identity to GluClα2 (66%), which also forms channels gated by both ivermectin and glutamate (Vassilatis *et al.*, 1997). The *C.elegans gbr-2* (*avr-14*) encoded subunits are also suggested to be α-subunits due to the gating of GBR-2B channels by ivermectin and the high identity of both variants to the other alpha subunits (appendix 1). GBR-2A is apparently the only *C.elegans* α-subunit that does not possess an ivermectin binding site. HG5 does not have a clear orthologue in *C.elegans* (appendices 1 and 5), although it has high sequence identity to gluclα2 and is most similar to the *gbr-2* genes of both *C.elegans* and *H.contortus.* If this is coupled with its ivermectin-binding capacity, the inclusion of HG5 in the α class of GluCl subunits, as suggested by Forrester *et al.* (1999), is not unreasonable. The ability to interact with ivermectin is therefore proposed as a distinguishing feature of GluCl α-subunits from both free-living and parasitic nematodes.

Analysis of the ivermectin-binding site of *H.contortus* L3 larvae was repeated under the conditions used for ivermectin binding to the recombinant subunits

for direct comparison. The affinity of [^{3}H] ivermectin binding to L3 membranes (70 +/- 7 pM) was higher under these conditions than had originally been reported (0.16-0.6 nM) (Rohrer *et al.*, 1994; Hejmadi *et al.*, 2000) and was very similar to that measured for recombinant HG3 (table 2). Reports that HG5 is predominantly expressed in adult *H.contortus* (Forrester *et al.*, 1999); and the apparent lack of further α-subunits in this species, allow supposition that HG3 represents the major ivermectin-binding site in the free-living larval stages and that this is reflected in the similar affinity of ivermectin for larval membranes. Recently it was reported that the K_d of [^{35}S] sulphonamide-ivermectin binding to *C.elegans* membranes could be modelled at 3 pM, but that the GBR-2 (AVR-14) subunits contributed a relatively small proportion of the total binding (Dent *et al.*, 2000). It is clear that the drug binds with very high affinity to the native nematode receptor, but it is possible that the importance of the individual subunits to the overall binding may differ between species and/or at different stages of the life cycle. It would be interesting to assess the ivermectin-binding site of the other stages of the *H.contortus* life cycle to determine any changes in affinity which may represent the dominance of alternative subunits, but it is not as simple to isolate the large quantities of membrane required for these experiments from adults or eggs; isolation of adult *H.contortus* would require the sacrifice of a number of hosts.

The interaction of the amino acids L-glutamate and GABA with the ivermectin-binding site was investigated. Ivermectin has low affinity for nematode (Holden-Dye et al., 1988; Holden-Dye and Walker, 1990) and mammalian ($GABA_A$) GABA receptors (Pong and Wang, 1980; Sigel and Baur, 1987; Adelsberger *et al.*, 2000) but GABA does not activate GluCl (Dent *et al.*, 1997; Cully *et al.*, 1996; Horoszok, *et al.*, in press).L-glutamate gates native and some recombinant nematode GluCl channels and ivermectin potentiates the glutamate response (Arena *et al.*, 1992; Martin, 1995; Cully *et al.*, 1994; Dent *et al.*, 1997; Vassilatis *et al.*, 1997; Dent *et al.*, 2000; Horoszok *et al.*, in press). Neither amino acid competed for the

C.elegans		*H.contortus*	
GluClα	Forms ivermectin-gated, but not L-glutamate-gated channels. Binds L-glutamate (Cully *et al.*, 1994; Etter *et al.*, 1996)		
GluClα2 (*avr-15*)	Forms L-glutamate- and ivermectin-gated channels (Dent *et al.*, 1997;Vassilatis *et al.*, 1997)		
GLC-3	Forms L-glutamate- and ivermectin-gated channels (Horoszok *et al.*,in press)		
		HG5 (HcGluClα)	High affinity ivermectin binding
GBR-2A (*avr-14*)	Does not form L-glutamate- or ivermectin-gated channels (Dent *et al.*, 2000)	HG2 (Hcgbr-2A)	Does not bind ivermectin
GBR-2B (*avr-14*)	Forms L-glutamate and ivermectin-gated channels (Dent *et al.*, 2000)	HG3 (Hcgbr-2B)	High affinity ivermectin binding
GluClβ	Forms L-glutamate-gated, but not ivermectin-gated channels (Cully *et al.*, 1994)	HG4 (Hc GluCl-β)	Does not bind ivermectin
C27H5.5	Does not form functional channels (Cully et al., 1996)		

Table 4 Pharmacology of *C.elegans* and *H.contortus* GluCl subunits

ivermectin-binding site under these conditions at concentrations up to 10 mM.

The plant-derived convulsant, picrotoxin, blocks most *C.elegans* recombinant GluCl subunits (Arena *et al.*, 1991; Arena *et al.*, 1992; Cully *et al.*, 1994) and its binding site has been localised by point mutation to the second transmembrane region (Etter *et al.*, 1999). The position of the ivermectin-binding site is not known, but HG2/HG3 binding data indicates that it may be in the C-terminal half of the receptor. Interactions between these two ligands were assessed. Picrotoxin did not block channels formed by the *C.elegans* GluCl subunit GLC-3, but fipronil, an insecticide which blocks GABA-gated chloride channels (Bloomquist, 1996) showed dose-dependent inhibition of the response to L-glutamate. A point mutation in the TM2 of the *Drosophila* GABA receptor subunit, RDL, has been shown to reduce fipronil potency (Hosie *et al.*, 1995). Neither of these ligands competed with [^{3}H] ivermectin for its binding site on recombinant HG3 and HG5. It is evident from these results that these four ligands either do not interact with these GluCl subunits, or that they have a different binding site to ivermectin. Electrophysiological studies would help to resolve this matter.

The success of the avermectin and milbemycin class of anthelmintics is shown by their financial dominance of the market (Witty, 1999). The vast cost of discovering new anthelmintics coupled with the triumph of the avermectins currently in use has made the development of avermectin analogues the most lucrative commercial prospect. The interaction of a number of avermectins with their biologically relevant site of action has been studied in *C.elegans* and binding, electrophysiology and nematocidal activity correlate well (Arena *et al.*, 1995). The capability of five structural analogues of ivermectin to compete for the ivermectin-binding site of recombinant *H.contortus* GluCl subunits was analysed. All compounds tested competed with [^{3}H]ivermectin for its binding site. Varying levels of affinity were measured and none was as effective as ivermectin on either recombinant HG3 or HG5. All of the avermectins showed higher affinity for COS 7 cell membranes expressing the HG5 polypeptide and differences in the rank order of affinity were observed between the two subunits. This suggests that there are differences in the composition of the ivermectin-binding site

between subunits. Differences in Hill coefficients were also observed between avermectins. This suggests that allosteric modulation, whereby binding of a molecule alters the conformation of a receptor and its binding sites and therefore the binding parameters of a second molecule, of receptors by these compounds may be present. As discussed, [^{3}H]ivermectin shows very similar affinity for *H.contortus* L3 membranes and recombinant HG3 implying that this subunit may be a major constituent of the binding site in this stage of the life cycle. It would be interesting to compare the ability of these avermectin derivatives to compete for the native ivermectin-binding site with the results shown for HG3 and HG5.

The efficacy and spectra of activity of the avermectins shows wide variation and it is probable that metabolism of the drugs by the nematode impacts on their efficacy *in vivo*. In *C.elegans*, metabolism of the avermectins does not seem to destroy the correlation between their biological activity and their action at the recombinant GluCl subunits (Arena *et al.*, 1995), but this may not be the case with all nematodes. An additional element is introduced when the interaction of anthelmintics with parasitic nematodes is considered. Host metabolism of the avermectins has been studied and it is apparent that the majority of the drug is excreted, largely unchanged, in the bile or faeces (Steel, 1993; McKellar and Benchaoui, 1996). The formulation, route of administration and bioavailability of avermectins will also have an impact on anthelmintic activity in the host.

Studies to ascertain the *in vitro* nematocidal activity of these compounds on *H.contortus* could be undertaken and compared with their effects on the recombinant GluCl subunits to discover if the results obtained in this research are indicative of the potency of these avermectins against *H.contortus*. This investigation may also demonstrate which subunits predominate in each life cycle stage. Gill and Lacey (1998) found differences in the major effect of ivermectin depending on whether *in vivo* or *in vitro* analysis was used. It is probable that the *in vivo* situation will differ to some extent from experiments on individual recombinant subunits and the data presented here does not reflect clinical usefulness. Data pertaining to the activity of these avermectins against *H.contortus* in their host would be an interesting comparison with the research on recombinant GluCl subunits.

The similarity of the GluCl to the other members of the cys-loop ligand-gated ion channel superfamily (cLGIC) predicts that the native receptor will be heteromeric. Interactions between co-expressed subunits are observed in other cLGIC both in terms of their synthesis and ligand-binding site (Gorrie et al., 1997; Taylor *et al.*, 2000; Miles and Huganir, 1998; Blount *et al.*, 1990; Gu *et al.*, 1991; Saedi *et al.*, 1991). It is probable that all GluCl receptor subunits play some role in the native receptor and that their co-expression may result in different pharmacology; as is seen with the *C.elegans* GluClα and -β subunits (Cully *et al.*, 1994; Vassilatis *et al.*, 1997). Localisation studies have supported the hypothesis of a heteromeric native receptor in both *C.elegans* and *H.contortus*. The pattern of expression of the *C.elegans* subunits GluClα2 and GluClβ is similar, with both being expressed in the pharyngeal muscle pm4 (Laughton *et al.*, 1997; Dent *et al.*, 1997). These subunits co-assemble to form channels gated by both ivermectin and glutamate (Vassilatis *et al.*, 1997). Antibodies have localised the expression of the *H.contortus* HG4 and HG5 polypeptides to the motor neuron commissures from both the ventral and dorsal nerve cords (Delany *et al.*, 1997; Portillo *et al.*, 2000). The expression pattern of these subunits is identical to the non-pharyngeal regions inhibited by the avermectins, suggesting that they may co-assemble to form the target of these drugs (Geary *et al.*, 1993). It is possible that HG2 and HG4 require co-expression with other GluCl subunits for the formation of a functional receptor. The reduced number of binding sites in COS 7 cell membranes expressing recombinant HG5, as opposed to HG3, may be indicative of a requirement for co-expression with additional GluCl subunits; co-localisation studies highlight HG4 as the probable candidate. Electrophysiological investigations would be useful to determine if functional receptors are formed by each of the cloned *H.contortus* GluCl subunits and if co-assembly alters their channel properties. Comparison of the genes encoding GluCl in *C.elegans* and *H.contortus* suggests that further GluCl subunits may be present in *H.contortus*. Studies contrasting the pharmacology of known GluCl subunits with the native receptor may result in the identification of novel polypeptides.

6. Conclusions

This research aimed to assess the pharmacology of the glutamate-gated chloride channel receptor subunits from the parasitic nematode *Haemonchus contortus* with respect to the anthelmintic ivermectin. Prior to this study, two of the four known GluCl subunits from *H.contortus* were available as full-length cDNAs. HG2 and HG5 cDNAs were therefore RT-PCR amplified to allow *in vitro* analysis of the interaction of all four GluCl subunits with ivermectin. Gene transfer into mammalian cells allowed analysis of protein expression and radiolabelled ivermectin was used to study its binding site. This was the first study to demonstrate an interaction between recombinant GluCl from parasitic nematodes and ivermectin. The involvement of HG5 cDNA in ivermectin resistance was also assessed.

- No coding differences were apparent between HG5 cDNA from the ivermectin-resistant White River II *H.contortus* field isolate (IVR) and HG5 cDNA from an ivermectin-sensitive *H.contortus* isolate (IVS). Amplification of this subunit was more difficult from IVR and only achieved from adults, which have the highest levels of HG5 expression in IVS (Forrester *et al.*, 1999). It is possible that HG5 is down regulated as part of the ivermectin-resistance mechanism.

- Stable expression of the GluCl subunits in a mammalian cell line is very problematic. Following selection for integration of recombinant HG3 and HG4 into the host cell genome, subunit mRNA, but not protein, was detected.

- Transient expression of GluCl subunits in the COS 7 cell line resulted in high affinity ivermectin binding to recombinant HG3 and HG5. HG2 and HG4 polypeptides did not bind ivermectin.

- The affinity of ivermectin for recombinant HG3 and membrane preparations from *H.contortus* L3 larvae is very similar. HG5 is differentially expressed with maximal expression in the adult stage

(Forrester *et al.*, 1999). HG3 may be the major component of the ivermectin-binding site in L3 larvae.

- The ivermectin-binding capacity and alternative splicing of orthologous GluCl subunits from parasitic and free-living nematodes appear to be conserved, but differences in the number and importance of the individual subunits to the overall binding between species and/or at different stages of the life-cycle are probable.

- All avermectins tested competed for the ivermectin-binding site of recombinant HG3 and HG5 with high affinity (K_i < 0.5 nM), though none was as effective as ivermectin itself. All compounds showed higher affinity for HG5 than HG3 and differences were observed in the rank order of affinity for the two subunits suggesting variation in the composition of the ivermectin-binding site.

- GABA, glutamate, fipronil and picrotoxin did not compete for the ivermectin-binding site on either recombinant GluCl subunit. These ligands either do not bind to these polypeptides or they have a different binding-site to ivermectin.

It is probable that native GluCl receptors are heteromeric and that the co-expression of subunits will alter the observed pharmacology. Future work should include electrophysiological or fluorescent chloride imaging investigations to investigate the co-expression of subunits, to ascertain whether functional receptors are formed by the individual subunits and to allow the pharmacological profile to be extended. Further binding studies could incorporate adult and egg *H.contortus* membranes to look for correlations between ivermectin receptor affinity for recombinant GluCl subunits and each life cycle stage. Comparison of the avermectin profile demonstrated in this study with the potency of the same avermectins against *H.contortus* both in culture and in the host may yield further information with regard to the clinical usefulness of such research.

7. References

Adelsberger, H., Scheuer, T., Dudel, J. (1997). A patch clamp study of a glutamatergic chloride channel on pharyngeal muscle of the nematode *Ascaris suum*. Neuroscience Letters *230*, 183-86.

Alfonso, A., Grundahl, K., Duerr, J.S., Han, H.P., Rand, J.B. (1993). The *C.elegans* unc-17 gene: A putative vesicular acetylcholine transporter. Science *261*, 617-19.

Alfonso, A., Grundahl, K., McManus, J.R., Rand, J.B., (1994). Cloning and characterisation of the choline acetyltransferase structural gene (cha-1) from *C.elegans*. The Journal of Neuroscience *14*, 2290-300.

Andrews S, J., Hole, N.J.K., Munn, E.A., Rolph, T.P., (1995). Vaccination for sheep against haemonchosis with H11 - prevention of the periparturient rise and colstral transfer of protective immunity. International Journal for Parasitology *25*.

Arena, J. P., Liu, K.K., Paress, P.S., Cully, D.F., (1991). Avermectin-sensitive chloride currents induced by *Caenorhabditis elegans* RNA in *Xenopus* oocytes. Molecular Pharmacology *40*, 368-74.

Arena, J. P., Liu., K.K., Paress., P.S., Schaeffer, J.M., Cully, D. F. (1992). Expression of a glutamate-activated chloride current in *Xenopus* oocytes injected with *Caenorhabditis elegans* RNA: evidence for modulation by avermectin. Molecular Brain Research *15*, 339-48.

Arena, J. P., Liu, K.K., Paress, P.S., Frazier, E.G., Cully, D.F., Mrozik, H., Schaeffer, J.M., (1995). The mechanism of action of avermectins in *Caenorhabditis elegans*: correlation between activation of glutamate-sensitive chloride current, membrane binding and biological activity. Journal of Parasitology *81*, 286-94.

Armour, J., Bairden, K., Preston, J.M., (1980). Anthelmintic activity of ivermectin against naturally acquired bovine gastrointestinal nematodes. The Veterinary Record *107*, 226-227.

Aubry, M. L., Cowell, P., Davey, M.J., Shevde, S., (1970). Aspects fo the pharmacology of new anthelmintics: pyrantel. British Journal of Pharmacology *38*, 332-344.

Avery, L., Horvitz, H.R., (1990). Effects of starvation and neuroactive drugs on feeding in *Caenorhabditis elegans*. Journal of Experimental Zoology *253*, 263-70.

Baldwin, E., Moyle, V. (1949). A contribution to the physiology and pharmacology of *Ascaris lumbricoides* from the pig. British Journal of Pharmacology *4*, 145-52.

Ballivet, M., Alliod, C., Bertrand, S., Bertrand, D., (1996). Nicotinic acetycholine receptors in the nematode *Caenorhabditis elegans*. Journal of Molecular Biology *258*, 261-69.

Bamber, B. A., Beg, A.A., Twyman, R.E., Jorgensen, E.M., (1999). The *Caenorhabditis elegans* unc-49 locus encodes multiple subunits of a heteromultimeric GABA receptor. The Journal of Neuroscience *19*, 5348-59.

Bargmann, C. I. (1998). Neurobiology of the *Caenorhabditis elegans* genome. Science *282*, 2028-33.

Barnard, E. A. (1992). Receptor classes and the transmitter-gated ion channels. Trends in Biochemical Sciences *17*, 368-74.

Baylis, H. A., Matsuda, K., Squire, M.D., Fleming, J.T., Harvey, R.J., Darlison, M.G., Barnard, E.A., Sattelle, D.B. (1997). ACR-3, a *Caenorhabditis elegans* nicotinic acetycholine receptor subunit. Receptors and Channels *5*, 149-58.

Bernt, U., Junkersdorf, B., Londershausen, M., Harder, A., Schierenberg, E. (1998). Effects of anthelmintics with different modes of action on the behaviour and development of *Caenorhabditis elegans*. Fundamentals of applied Nematology *21*, 251-263.

Beugnet, F., Kerboeuf, D., Nicolle, J.C., Soubieux, D., (1996). Use of free-living larval stages to study the effects of thiabendazole, levamisole, pyrantel and ivermectin on the fine structure of *Haemonchus contortus* and *Heligmosomoides polygyrus*. Veterinary Parasitology *63*, 83-94.

Blackhall, W. J., Pouliot, J-F., Prichard, R.K., Beech, R.N. (1998). Haemonchus Contortus:Selection at a glutamate-gated chloride channel gene in ivermectin- and moxidectin-selected strains. Experimental Parasitology *90*, 42-48.

Blaxter, M. (1998). *Caenorhabditis elegans* is a nematode. Science *282*, 2041-2046.

Blaxter, M., De Ley, P., Garey, J. R., Liu, L. X., Scheldeman, P., Vierstraete, A., Vanfleteren, J.R., Mackey, L.Y., Dorris, M., Frisse, L. M., Vida, J.D., Thomas, W. K, (1998). A molecular evolutionary framework for the phylum Nematoda. Nature *392*, 71-75.

Bloomquist, J.R. (1996) Ion channels as targets for insecticides. Annual Reviews in Entomology. *41*, 163-90.

Blount, P., Smith, M.M., Merlie, J.P. (1990). Assembly intermediates of the mouse muscle nicotinic acetylcholine receptor in stably transfected fibroblasts. Journal of Cell Biology *6*, 2601-11.

Blount, P., Merlie, J.P. (1990). Mutational analysis of muscle nicotinic acetycholine receptor subunit assembly. Journal of Cell Biology *111*, 1125-32.

Bradford, M. M. (1976). A rapid and sensitive method for the quantitation of microgram quantites of protein utilizing the principle of protein-dye binding. Annals in Biochemistry *72*, 248-54.

Brandon, N. J., Uren, J.M., Kittler, J.F., Wang, H., Olsen, R., Parker,P.J., Moss, S.J. (1999). Subunit-specific association of protein kinase C and the receptor for activated C kinase with GABA type A receptors. The Journal of Neuroscience *19*, 9228-9234.

Brownlee, D. J. A., Holden-Dye, L., Walker, R.J., (1997). Actions of the anthelmintic ivermectin on the pharyngeal muscle of the parasitic nematode *Ascaris suum.* Parasitology *115*, 553-61.

Brownlee, D., Holden-Dye, L., Walker, R (2000). The range and biological activity of FMRFamide-related peptides and classical neurotransimitters in nematodes. Advances in Parasitology *45*, 109-80.

Brownlee, D., Holden-Dye, L., Walker, R. (2000). The range and biological activity of FMRFamide-related peptides and classical neurotransmitters in nematodes. Advances in Parasitology *45*, 109-180.

Burkhart, C. N. (2000). Ivermectin: An assessment of its pharmacology, microbiology and safety. Veterinary and Human Toxicology *42*, 30-35.

Campbell, W. C. (1981). An introduction to the avermectins. New Zealand Veterinary Journal *29*, 174-78.

Campbell, W. C., Benz, G.W., (1984). Ivermectin: a review of efficacy and safety. Journal of Veterinary Pharmacology and Therapy *7*, 1-16.

Chabala, J. C., Mrozik, H., Tolman, R.L., Eskola, P., Lusi, A., Peterson, L.H., Woods, M.F., Fisher, M.H., Campbell, W.C., Egerton, J.R., Ostlind, D.A. (1980). Ivermectin, a new broad-spectrum antiparasitic agent. Journal of Medicinal Chemistry *23*, 1134-36.

Chandrawathani, P., Adnan, M., Waller, P.J., (1999). Anthelmintic resistance in sheep and goat farms on Peninsular Malaysia. Veterinary Parasitology *82*, 305-10.

Changeux, J.-P. (1993). Chemical Signalling in the brain. Scientific American, 30-37.

Chappell, L. H. (1993). Physiology and Nutrition. In Modern Parasitology, F. E. G. Cox, ed., pp. 157-192.

Chomczynski, P., Sacchi, N. (1987). Single-step method of RNA isolation by acid guanidinium thiocyanate phenol-chloroform extraction. Annals in Biochemistry *162*, 156-9.

Colditz, I. G., Watson, D.L., Gray, G.D., Eady, S.J., (1996). Some relationships between age, immune responsiveness and resistance to parasites in ruminants. International Journal for Parasitology *26.*

Colquhoun, L., Hoden-Dye, L., Walker, R.J. (1991). The pharmacology of cholinoceptors on the somatic muscle cells of the parasitic nematode *Ascaris suum.* Journal of Experimental Biology *158*, 509-30.

Colquhoun, L. M., Holden-Dye, L., Walker, R.J. (1993). The action of nicotinic receptor specific toxins on the somatic muscle cells of the parasitic nematode *Ascaris suum*. Molecular Neuropharmacology *3*, 11-16.

Cooper, S. T., Harkness, P.C., Baker, E.R., Millar, N.S. (1999). Up-regulation of cell-surface alpha4beta2 neuronal nicotinic receptors by lower temperatures and expression of chimeric subunits. Journal of Biological Chemistry *274*, 27145-52.

Corringer, P-J., Le Novere, N., Changeux, J-P. (2000). Nicotinic receptors at the amino acid level. Annual reviews in Pharmacology and Toxicology *40*, 431-58.

Cully, D. F., Paress, P.S., (1991). Solubilization and characterization of a high affinity ivermectin binding site from *Caenorhabditis elegans.* Molecular Pharmacology *40.*

Cully, D. F., Vassilatis, D.K., Liu, K.K., Paress, P.S., Van der Ploeg, L.H.T., Schaeffer, J.M., Arena, J.P. (1994). Cloning of an avermectin-sensitive glutamate-gated chloride channel from *Caenorhabditis elegans.* Nature *371*, 707-11.

Cully, D. F., Wilkinson, H., Vassilatis, D.K., Etter, A., Arena, J.P., (1996). Molecular biology and electrophysiology of glutamate-gated chloride channels. Parasitology *113*, S191-200.

Culotti, J. G., Von Ehrenstein, G., Culoti, M.R., Russell, R.L., (1981). A second class of acetylcholinesterase-deficient mutants of the nematode *Caenorhabditis elegans.* Genetics *97*, 281-305.

Dale, V. M. E., Martin, R.J., (1995). Oxantel-activated single channel currents in the muscle membrane of *Ascaris suum*. Parasitology *110*, 437-48.

Davis, R. E. (1998). Action of excitatory amino acids on hypodermis and the motornervous system of *Ascaris suum*: pharmacological evidence for a glutamate transporter. Parasitology *116*, 487-500.

Davis, R. E., Stretton, A.O.W., (1996). The motornervous system of *Ascaris*: electrophysiology and anatomy of the neurons and their control by neuromodulators. Parasitology *113*, S97-117.

de Silva, N., Guyatt, H., Bundy, D., (1997). Anthelmintics. A comparative review of their clinical pharmacology. Drugs *53*, 769-788.

Del Castillo, J., de Mello, W.C., Morales, T. (1963). The physiological role of acetylcholine in the neruomuscular system of *Ascaris lumbricoides*. Archives Internationales de Physiologie et de Biochimie *71*, 741-57.

Del Castillo, J., De Mello, W.C., Morales, T. (1964). Inhibitory action of g-aminobutyric acid (GABA) on *Ascaris* muscle. Experientia *20*, 141-43.

Delany, N. S. (1998). Glutamate-gated chloride chloride ion channels in the parasitic nematode *Haemonchus contortus*. PhD thesis.

Delany, N. S., Laughton, D.L., Wolstenholme, A.J., (1998). Cloning and localisation of an avermectin receptor-related subunit from *Haemonchus contortus*. Molecular and Biochemical Parasitology *97*, 177-87.

Dent, J. A., Davis., M.W., Avery., L. (1997). avr-15 encodes a chloride channel subunit that mediates inhibitory glutamatergic neurotransmission and ivermectin sensitivity in *Caenorhabditis elegans*. The EMBO Journal *16*, 5867-79.

Dent, J. A., Smith, M.M., Vassilatis, D.K., Avery, L., (2000). The genetics of ivermectin resistance in *Caenorhabditis elegans*. Proceedings of the National Academy of Science *97*, 2674-79.

Donelson, J. E., Duke, B.O.L., Moser, D., Zeng, W., Erondu, N.E., Lucius, R., Renz, A., Kjaram, M., Flores, G.Z., (1988). Construction of *Onchocerca volvulus* cDNA libraries and partial characterisation of the cDNA for a major antigen. Molecular and Biochemical Parasitology *31*, 241-50.

Dorris, M., De Ley, P., Blaxter, M.L. (1999). Molecular analysis of nematode diversity and the evolution of parasitism. Parasitology Today *15*, 188-193.

Duke, B. O., Zea-Flores, G., Munoz, B. (1991). The embryogenesis of *Onchocerca volvulus* over the first year after a single dose of ivermectin. Tropical Medicine and Parasitology *42*, 175-80.

Elard, L., Comes, A.M., Humbert, J.F., (1996). Sequences of b-tubulin cDNA from benzamidazole-susceptible and -resistant strains of *Teladorsagia circumcincta*, a nematode parasite of small ruminants. Molecular and Biochemical Parasitology *79*, 249-53.

Enos, A., Coles, G.C., (1990). Effect of benzamidazole drugs on tubulin in benzamidazole resistant and susceptible strains of *Caenorhabditis elegans*. International Journal for Parasitology *20*, 161-167.

Etter, A., Cully, D.F., Schaeffer, J.M., Liu, K.K., Arena, J.P., (1996). An amino acid substitution in the pore region of a glutamate-gated chloride channel enables the coupling of ligand binding to channel gating. The Journal of Biological Chemistry *271*, 16035-39.

Etter, A., Cully, D.F., Liu, K.K., Reiss, B., Vassilatis, D.K., Schaeffer, J.M., Arena, J.P. (1999). Picrotoxin blockade of invertebrate glutamate-gated chloride channels: subunit dependence and evidence for binding within the pore. Journal of Neurochemistry *72*, 318-26.

Evans, A. M., Martin, R.J. (1996). Activation and cooperative multi-ion block of single nicotinic-acetylcholine channel currents of *Ascaris* muscle by the tetrahydropyrimidine anthhelmintic, morantel. British Journal of Pharmacology *118*, 1127-40.

Fellowes, R. A., Maule, A.G., Martin, R.J., Geary, T.G., Thompson, D.P., Kimber, M.J., Marks, N.J., Halton, D.W. (2000). Classical neurotransmitters in the ovijector of *Ascaris suum*: localization and modulation of muscle activity. Parasitology *121*, 325-36.

Fernandez, J. M., Hoeffler, J.P. (1999). Gene expression systems - using nature for the art of expression: Academic Press.

Fleming , J. T. B., H.A., Sattelle, D.B., Lewis, J.A., (1996). Molecular Cloning and in vitro expression of *C.elegans* and parasitic nematode ionotropic receptors. Parasitology *113*, S175-90.

Fleming, J. T., Squire, M.D., Barnes, T.M., Tornoe, C., Matsuda, K., Ahnn, J., Fire, A., Sulston, J.E., Barnard, E.A., Sattelle, D.B., Lewis, J.A., (1997). *Caenorhabditis elegans* levamisole resistance genes lev-1, unc-29 and unc-38 encode functional nicotinic acetylcholine receptor subunits. Journal of Neuroscience *17*, 5843-57.

Forrester, S. G., Hamdan, F.F., Prichard, R.K., Beech, R.N. (1999). Cloning, sequencing, and developmental expression levles of a novel glutamate-gated chloride channel homologue in the parasitic nematode *Haemonchus contortus*. Biochemical and Biophysical Research Communications *254*, 529-34.

Fujimura, M., Oeda, K., Inoue, H., Kato, T. (1992). A single amino acid substitution in the b-tubulin gene of Neurospora confers both carbendazim resistance and diethofencarb sensitivity. Current Genetics *21*, 399-404.

Galzi, J.-L., Bertrand, D., Devillers-Thiery, A., Revah, F., Bertrand, S., Changeux, J-P. (1991). Functional significance of aromatic amino acids from

three peptide loops of the a7 neuronal nicotinic receptor site investigated by site-directed mutagenesis. FEBS Letters *294*, 198-202.

Galzi, J.-L., Devillers-Theiry, A., HUssy, N., Bertrand, S., Changeux, J.P., Bertrand, D. (1992). Mutations in the channel domain of a neuronal nicotinic receptor convert ion selectivity from cationic to anionic. Nature *359*, 500-05.

Galzi, J. L., Changeux, J-P. (1994). Neurotransmitter-gated ion channels as unconventional allosteric proteins. Current Opinion in Structural Biology *4*, 554-565.

Geary, T. G., Klein, R.D., Vanover, L., Bowman, J.W., Thompson, D.P., (1992). The nervous system of nematodes as targets for drugs. Journal of Parasitology *78*, 215-230.

Geary, T. G., Sims, S.M., Thomas, E.M., Vanover, L., Davis. J.P., Winterrowd, C.A., Klein, R.D., Ho., N..H., Thompson, D.P., (1993). *Haemonchus contortus*: ivermectin-induced paralysis of the pharynx. Experimental Parasitology *77*, 88-96.

Geary, T. G., Sangster, N.C., Thompson, D.P., (1999). Frontiers in anthelmintic pharmacology. Veterinary Parasitology *84*, 275-95.

Gill, H. S., Watson, D.L., Brandon, M.R., (1993). Monoclonal antibody to CD4+ T cells abrogates genetic resistance to *Haemonchus contortus* in sheep. Immunology *78*, 43-49.

Gill, J. H., Redwin, J.M., Van Wyk., J.A., Lacey, E., (1995). Avermectin inhibition of larval development in *Haemonchus contortus* - effects of ivermectin resistance. International Journal for Parasitology *25*, 463-70.

Gill, J. H., Lacey, E. (1998). Avermectin/milbemycin resistance in tristrongyloid nematodes. International Journal for Parasitology *28*, 863-77.

Gill, J. H., Kerr, C.A., Shoop, W.L., Lacey, E. (1998). Evidence of multiple mechanisms of avermectin resistance in *Haemonchus contortus* - comparison of selection protocols. International Journal for Parasitology *28*, 783-9.

Githegia, S. M. T., S.M., Larsen, M., Kyvsgaard, N., Nansen, P., (1997). The preventative effect of the fungus *Duddington flagrans* on tristrongyle infections of lambs on pasture. International Journal for Parasitology *27*, 931-939.

Gorrie, G.H., Vallis, Y., Stephenson, A., Whitfield, J., Browning, B., Smart, T.G., Moss, S.J. (1997) Assembly of $GABA_A$ receptors composed of α1 and β2 subunits in both cultured neurons and fibroblasts. The Journal of Neuroscience *17*, 6587-96

Gottesman, M. M., Pastan, I. (1993). Biochemistry of multidrug resistance mediated by the multidrug transporter. Annual Reviews in Biochemistry *62*, 385-427.

Grant, W. (2000). What is the real target for ivermectin resistance selection in *Onchocerca volvulus*? Parasitology Today *16*, 458-59.

Gronvold, J., Wolstrup, J., Larsen, M., Henriksen, S.A., Nansen, P. (1993). Biological control of *Ostertagia ostertagi* by feeding selected nematode-trapping fungi to calves. Journal of Helminthology *67*, 31-36.

Gu, Y., Forsayeth, J.,Verrall, S., Yu, X., Hall, Z., (1991). Assembly of the mammalian muscle acetylcholine receptor in transfected COS cells. Journal of Cell Biology *114*, 799-807.

Guastella, J., Johnson, C.D., Stretton, A.O.W., (1991). GABA-immunoreactive neurons in the nematode *Ascaris.* Journal of Comparative Neurology *307*, 598-608.

Harrow, I. D., Gration, K.A.F., (1985). Mode of action of the anthelmintics morantel, pyrantel and levamisole in the muscle cell membrane of the nematode *Ascaris suum*. Pesticide Science *16*, 662-72.

Hart, A. C., Sims, S., Kaplan, J.M., (1995). Synaptic code for sensory modalities revealed by *C.elegans* GLR-1 glutamate receptor. Nature *378*, 82-85.

Hay, F. S., Niezen, J.H., Miller, C., Bateson, L., Robertson, H., (1997). Infestation of sheep dung by nematophagous fungi and implications for the control of free-living stages of gastrointestinal nematodes. Veterinary Parasitology *70*, 247-254.

Hejmadi, M. V., Jagannathan, S., Delany, N.S., Coles., G.C., Wolstenholme, A.J., (2000). L-glutamate binding sites of parasitic nematodes: an association with ivermectin resistance. Parasitology *120*, 535-45.

Higgins, C. F. (1995). The ABC of Channel Regulation. Cell *82*, 693-96.

Hoekstra, R., Visser, A., Wiley, L.J., Weiss, A.S., Sangster, N.C., Roos., M.H. (1997). Characterisation of an acetylcholine receptor gene of *Haemonchus contortus* in relation to levamisole resistance. Molecular and Biochemical Parasitology *84*, 179-87.

Holden-Dye, L., Hewitt, G.M., Wann, K.T., Krogsgaard-Larsen, P., Walker, R.J., (1988). Studies involving avermectin and the 4-aminobutyric acid (GABA) receptor of *Ascaris suum* muscle. Pesticide Science *24*, 231-45.

Holden-Dye, L., Walker, R.J., (1990). Avermectin and avermectin derivatives are antagonists at the 4-aminobutyric acid (GABA) receptor on the somatic

muscle cells of *Ascaris*; is this the site of anthelmintic action? Parasitology *101*, 265-71.

Hope, I. A. (1999). Background on *Caenorhabditis elegans*. In *C.elegans*: A practical approach, I. A. Hope, ed.: Oxford University Press), pp. 1-15.

Horoszok, L., Raymond, V., Sattelle, D.B., Wolstenholme, A.J. GLC-3: A novel fipronil and BIDN-sensitive, but picrotoxin-insensitive, L-glutamate-gated chloride channel subunit from *Caenorhabditis elegans*. In press.

Hosie, A. M., Baylis, H.A., Buckingham, S.D., Sattelle, D.B. (1995). Actions of the insecticide fipronil, on dieldrin-sensitive and -resistant GABA receptors of *Drosophila melanogaster*. British Journal of Pharmacology *115*, 909-12.

Huganir, R., Grungard, P., (1990). Regulation of neurotransmitter receptor desensitization by protein phosphorylation. Neuron *5*, 555-567.

Jackson, F., Coop, R.L., (2000). The development of anthelmintic resistance in sheep nematodes. Parasitology *120*, S95-S107.

Jacobs, H. J., Ashman, K., Bowles, V., Meeusen, E.N.T., (1999). Vaccination against the gastrointestinal nematode *Haemonchus contortus* using a purified larval surface antigen. vaccine *17*, 362-368.

Jagannathan, S. (1998). Nematode inhibitory glutamate-gated chloride ion channel receptors. PhD thesis.

Jagannathan, S., Laughton, D.L., Critten, C.L., Skinner, T.M., Horoszok, L., Wolstenholme, A.J., (1999). Ligand-gated chloride channel subunits encoded by the *Haemonchus contortus* and *Ascaris suum* orthologues of the *Caenorhabditis elegans* gbr-2 (avr-14 gene). Molecular and Biochemical Parasitology *103*, 129-40.

Jarrett, W. F. H., Jennings, F.W., Martin, B., McIntyre, W.I.M., Mulligan, W., Sharp, N.C.C., Urquhart, G.M. (1958). A field trial of a parasitic bronchitis vaccine. Veterinary Record *70*, 451-454.

Jasmer, D. P., Yao, C., Rehman, A., Johnson, S. (2000). Multiple lethal effects induced by a benzimidazole anthelmintic in the anterior intestine of the nematode *Haemonchus contortus*. Molecular and Biochemical Parasitology *105*, 81-90.

Johnson, C. D., Duckett, J.G., Culotti, J.G., Herman, R.K., Meneely, P.M., Russell, R.L. (1981). An acetycholinesterase-deficient mutant of the nematode *Caenorhabditis elegans*. Genetics *97*, 261-79.

Johnson, C. D., Stretton, A.O.W. (1985). Localization of choline acetyltransferase within identified motorneurons of the nematode *Ascaris*. The Journal of Neuroscience *5*, 1984-92.

Johnson, C. D., Stretton, A.O.W. (1987). GABA-immunoreactivity in inhibitory motor neurons of the nematode *Ascaris*. The Journal of Neuroscience *7*, 223-35.

Kass, I. S., Wang, C.C., Walrond, J.P., Stretton, O.W., (1980). Avermectin B_{1a}, a paralyzing anthelmintic that affects interneurons and inhibitory motorneurons in *Ascaris.* Proceedings of the National Academy of Sciences USA *77*, 6211-15.

Kass, I. S., Stretton, A.O.W., Wang, C.C. (1984). The effects of avermectin and drugs related to acetylcholine and 4-aminobutyric acid on neurotransmission in *Ascaris suum*. Molecular and Biochemical Parasitology *13*, 213-25.

Knox, D. P. (2000). Development of vaccines against gastrointestinal nematodes. Parasitology *120*, S43-S61.

Kolson, D. L., Russell, R.L (1985a). A novel class of acetycholine esterase, revealed by mutations, in the nematode *Caenorhabditis elegans*. Journal of Neurogenetics *2*, 93-110.

Kolson, D. L., Russell, R.L., (1985b). New acetylcholinesterase-deficient mutants of the nematode *Caenorhabditis elegans*. Journal of Neurogenetics *2*, 69-91.

Kotze, A. C. (1998). Effects of macrocyclic lactones on ingestion in susceptible and resistant *Haemonchus contortus* larvae. Journal of Parasitology *84*, 631-35.

Krause, R. M., Buisson, B., Bertrand, S., Corringer, P-J., Galzi. J-L., Changeux, J-P., Bertrand, D. (1998). Ivermectin: a positive allosteric effector at the a7 neuronal nicotinic acetylcholine receptor. Molecular Pharmacology *53*, 283-94.

Krishek, B. J., Xie, X., Blackstone, C., Huganir, R.L., Moss, S.J., Smart, T.G. (1994). Regulation of $GABA_A$ receptor function by protein kinase C phosphorylation. Neuron *12*, 1081-95.

Kuwabara, P., Coulson, A. (2000). RNAi - Prospects for a general technique for determining gene function. Parasitology Today *16*, 347-349.

Kwa, M. S. G., Veenstra, J.G., Roos, M.H. (1993). Molecular characterisation of b-tubulin genes present in benzamidazole-resistant populations of *Haemonchus contortus*. Molecular and Biochemical Parasitology *60*, 133-44.

Kwa, M. S. G., Veenstra, J.G., Van Dijk, M., Roos, M.H. (1995). b-tubulin genes from the parasitic nematode *Haemonchus contortus* modulate drug resistance in *Caenorhabditis elegans.* Journal of Molecular Biology *246*, 500-10.

Kwa, M. S. G., Okoli, M.N., Schulz-Key, H., Okongkwo, P.O., Roos., M.H., (1998). use of P-glycoprotein gene probes to investigate anthelmintic resistance in Haemonchus contortus and comparison with *Onchocerca volvulus*. International Journal for Parasitology *28*, 1235-40.

Lacey, E. (1990). Mode of action of benzamidazoles. Parasitology today *6*, 115-116.

Larsen, M. (1999). Biological Conrtol of Helminths. International Journal for Parasitology *29*, 139-146.

Laughton, D. L. (1993). A characterisation of nematode receptors. PhD thesis.

Laughton, D. L., Lunt, G.G., Wolstenholme, A.J., (1997a). Alternative splicing of a *Caenorhabditis elegans* gene produces two novel inhibitory amino acid receptor subunits with identical ligand binding domains but different ion channels. Gene *201*, 119-25.

Laughton, D. L., Lunt, G.G., Wolstenholme, A.J., (1997b). Reporter gene contructs suggest that the *Caenorhabditis elegans* avermectin receptor b-subunit is expressed solely in the pharynx. Journal of Experimental Biology *200*, 1509-14.

Le Jambre, L. F. (1995). Relationship of blood loss to worm number, biomass and egg production in *Haemonchus* infected sheep. International Journal for Parasitology *25*, 269-73.

Le Jambre, L.F., Gill, J.H., Lenane, I.J., Baker, P. (2000) Inheritance of avermectin resistance in H*aemonchus contortus*. International Journal for Parasitology *30*, 105-11

Lee, D. L. (1962). The distribution of esterase enzymes in *Ascaris lumbricoides*. Parasitology *52*, 241-60.

Lewis, J. A., Wu, C.H., Levine, J.H., Berg, H. (1980). Levamisole-resistant mutants of the nematode *Caenorhabditis elegans* appear to lack pharmacological acetylcholine receptors. Neuroscience *5*, 967-89.

Lewis, S., Lee, M.G-S., Cowen, N.J., (1985). Five mouse tubulin genes and their regulated expression during development. Journal of Cell Biology *101*, 852-861.

Lewis, J. A., Fleming, J.T., McLafferty, S., Murphy, H., Wu, C. (1987a). The levamisole receptor, a cholinergic receptor of the nematode *Caenorhabditis elegans*. Molecular Pharmacology *31*, 185-193.

Lewis, J. A., Elmer, J.S., skimming, J., McLafferty, S., Fleming, J., McGee, T., (1987b). Cholinergic receptor mutants of the nematode *Caenorhabditis elegans.* The Journal of Neuroscience *7*, 3059-71.

Li, H., Avery, L., Denk, W., Hess, G.P., (1997). Identification of chemical synapses in the pharynx of *Caenorhabditis elegans.* Proceedings of the National Academy of Science USA *94*, 5912-16.

Lilley, C. J., Devlin, P., Urwin, P.E., Atkinson, H.J. (1999). Parasitic nematodes, proteinases and transgenic plants. Parasitology Today *15*, 414-417.

Lowe, T., Sharefkin, J., Yang, S.Q., Dieffenbach, C.W. (1990). A computer program for selection of oligonucleotide primers for polymerase chain reactions. Nucleic Acids Research *18*, 1757-61.

Lubega, G. W., Prichard, R.K., (1991a). Interaction of benzamidazole anthelmintics with *Haemonchus contortus* tubulin, binding affinity and anthelmintic efficacy. Experimental Parastiology *73*, 203-213.

Lubega, G. W., Prichard, R.K., (1991b). Specific interaction of benzamidazole anthelmintics with tubulin: Comparison of developing stages of thiabendazole-susceptible and thiabendazole-resistant strains of *Haemonchus contortus*. Biochemical Pharmacology *41*, 93-101.

Lubega, G. W., Klein, R.D., Geary, T.G., Prichard, R.K., (1994). *Haemonchus contortus*: the role of two b-tubulin gene subfamilies in the resistance to benzamidazole anthelmintics. Biochemical Pharmacology *47*, 1705-15.

MacDonald, R. L., Olsen, R.W. (1994). $GABA_A$ receptor channels. Annual Reviews in Neuroscience *17*, 569-602.

Manton, V. J. A., Peacock, B., Poynter, D., Silvermann, P.H., Terry, R.J., (1962). The influence of age on naturally acquired resistance to *Haemonchus contortus* in lambs. Research in Veterinary Science *3*, 308-314.

Maricq, A. V., Peckol, E., Driscoll, M., Bargmann, C.I. (1995). Mechanosensory signalling in *C.elegans* mediated by the GLR-1 glutamate receptor. Nature *378*, 78-81.

Martin, R. J. (1980). The effect of g-aminobutyric acid on the input conductance and membrane potential of *Ascaris* muscle. British journal of Pharmacology *71*, 99-106.

Martin, R. J. (1982). Electrophysiological effects of piperazine and diethylcarbamine on *Ascaris suum* somatic muscle. British Journal of Pharmacology *77*, 255-265.

Martin, R. J. (1985). g-Aminobutyric acid- and piperazine-activated single-channel currents from *Ascaris suum* body muscle. British Journal of Pharmacology *84*, 445-461.

Martin, R. J., Pennington, A., (1989). A patch clamp study of effects of dihydroavermectin on Ascaris muscle. British Journal of Pharmacology *98*, 747-56.

Martin, R. J. (1996). An electrophysiological preparation of *Ascaris suum* pharyngeal muscle reveals a glutamate-gated chloride channel sensitive to the avermectin analogue, milbemycin D. Parasitology *112*, 247-52.

Martin, R. J., Valkanov, M.A., Dale, V.M.E., Robertson, A.P., Murray, I. (1996). Electrophysiology of *Ascaris* muscle and anti-nematodal drug action. Parasitology *113*, S137-S156.

Martin, R. J., Robertson, A.P., Bjorn, H., Sangster, N.C., (1997). Heterogenous levamisole receptors: a single channel study of acetylcholine receptors from *Oesophagostomum dendatum*. European Journal of Pharmacology *322*, 249-57.

Martin, R. J., Murray, I., Robertson, A.P., Bjorn, H., Sangster, N., (1998). Anthelmintics and ion-channels: after a puncture use a patch. International Journal for Parasitology *28*, 849-62.

Martin, R. J., Robertson, A.P., (2000). Electrophysiological investigation of anthelmintic resistance. Parasitology *120*, S87-94.

McCracken, R. O., Sillwell, W.H., (1991). A possible biochemical mode of action for benzamidazole anthelmintics. International Journal for Parasitology *21*, 99-104.

McDonald, B. J., Moss, S.J. (1994). Differential phosphorylation of intracellular domains of g-aminobutyric acid type A receptor subunits by calcium/calmodulin type 2-dependent protein kinase and cGMP-dependent protein kinase. The Journal of Biological Chemistry *269*, 18111-17.

McDonald, B. J., Amato, A., Connolly, C.N., Benke, D., Moss, S.J., Smart, T.G. (1998). Adjacent phosphorylation sites on $GABA_A$ receptor b subunits determine regulation by cAMP-dependent protein kinase. Nature Neuroscience *1*, 23-28.

McIntire, S. L., Jorgensen, E., Horvitz, H.R. (1993a). Genes required for GABA function in *Caenorhabditis elegans*. Nature *364*, 334-37.

McIntire, S. L., Jorgensen, E., Kaplan, J., Horvitz, R. (1993b). The GABAergic nervous system of *Caenorhabditis elegans*. Nature *364*, 337-341.

McIntire, S. L., Reimer, R.J., Schuske, K., Edwards, R.H., Jorgensen, E.M. (1997). Identification and characterization of the vesicular GABA transporter. Nature *389*, 870-76.

McKeand, J., Bairden, K., Ibarra-Silva, A.M., (1988). The degradation of bovine faecal pats containing ivermectin. Veterinary Record *122*, 587-88.

McKellar, Q. A., Benchaoui, H.A., (1996). Avermectins and Milbemycins. Journal of Veterinary Pharmacology and Therapy *19*, 331-5.

McLeod, R. S. (1995). Costs of major parasites to the Australian livestock industry. International Journal for Parasitology *25*, 1363-1367.

Meeusen, E. N. T. (1996). Rational design of nematode vaccines: natural antigens. International Journal for Parasitology *26*, 813-818.

Meeusen, E. N. T. (1999). Immunology of helminth infections, with special reference to immunopathology. Veterinary Parasitology *84*, 259-273.

Mellanby, H. (1955). Identification and estimation of acetylcholine in three parasitic nematodes (*Ascaris lumbicoides, Litomosoides carinii* and the microfilatiae of *Dirofilaria repens*). Parasitology *45*, 287-94.

Miles, K., Huganir, R., (1988). Regulation of nicotinic acetylcholine receptors by protein phosphorylation. Molecular Neurobiology *2*, 91-124.

Miller, H. R. P. (1984). The protective mucosal response against gastrointestinal nematodes in ruminants and laboratory animals. Veterinary Immunology and Immunopathology *6*, 167-259.

Miller, H. R. P. (1996). Prospects for the immunological control of ruminant gastrointestinal nematodes: natural immunity, can it be harnessed? International Journal for Parasitology *26*, 801-811.

Molento, M. B., Prichard, R.K., (1999). Effects of the multidrug-resistance-reversing agents verapamil and CL 347,099 on the efficacy of ivermectin or moxidectin against unselected and drug-selected strains of *Haemonchus contortus* in jirds (*Meriones unguiculatus*). Parasitology Research *85*, 1007-11.

Mongan, N. P., Baylis, H.A., Adcock, C., Smith, G.R., Sansom, M.S., Sattelle, D.B. (1998). An extensive and diverse gene family of nicotinic acetycholine receptor alpha subunits in *Caenorhabditis elegans*. Receptors and Channels *6*, 213-28.

Moreno-Guzman, M. J., Coles, G.C., Jimenez-Gonzales, A., Criado-Fornelio, A., Ros-Moreno, R.M., Rodriguez-Caabeiro, F. (1998). Levamisole binding sites in *Haemonchus contortus*. International Journal for Parasitology *28*, 413-18.

Munn, E. A., Smith, T.S., Smith, H., Smith, F., Andrews, S.J., (1997). Vaccination against *Haemonchus contortus* with denatured forms of the protective antigen H11. Parasite Immunology *19*, 243-248.

Newton, S. E., Munn, E.A., (1999). The development of vaccines against gastrointestinal nematodes, particularly *Haemonchus contortus*. Parasitology Today *15*, 116-122.

Nielsen, C. (1998). Sequence leads to tree of worms. Nature *392*, 25-26.

Norton, S., de Beer, E.J. (1957). Investigations on the action of piperazine on *Ascaris lumbricoides*. American Journal of Tropical Medicine *6*, 898-905.

Ottesen, E. A., Campbell., W.C. (1993). Ivermectin in human medicine. Journal of Antimicrobial Chemotherapy *?*, 195-203.

Paiement, J.-P., Leger, C., Ribeiro, P., Prichard, R.K. (1999). *Haemonchus contortus*:effects of glutamate, ivermectin and moxidectin on inulin uptake activity in unselected and ivermectin-selected adults. Experimental Parasitology *92*, 193-8.

Pong, S. S., Wang, C.C., (1980). The specificity of high affinity binding of avermectin B1a to mammalian brain. Neuropharmacology *19*, 311-17.

Portillo, V., Jagannathan, S., Samson-Himmelstjerna, G., Wolstenholme, A.J. (2000). Expression pattern of ivermectin receptor subunits. Oxford 2000. 18-22 September.

Pouliot, J.-F., L'Heureux, F., Liu, Z., Prichard, R.K., Georges, E. (1997). Reversal of p-glycoprotein-associated multidrug resistance by ivermectin. Biochemical Pharmacology *53*, 17-25.

Raizen D.M., L. R. Y., Avery L. (1995). Interacting genes required for pharyngeal excitation by motor neuron MC in *Caenorhabditis elegans*. Genetics *141*, 1365-82.

Rand, J. R., Nonet, M.L. (1997). Synaptic transmission. In C. ELEGANS II, D. L. Riddle, Blumenthal, T., Meyer, B.J., Priess, J.R., ed.: Cold Spring Harbour Laboratory Press), pp. 611-43.

Reiner, D. J., Thomas, J.H., (1995). Reversal of a muscle response to GABA during *C.elegans* male development. The Journal of Neuroscience *15*, 6094-102.

Richmond, J. E., Jorgensen, E.M. (1999). One GABA and two acetylcholine receptors function at the *C.elegans* neuromuscular junction. Nature Neuroscience *2*, 791-797.

Riddle, D. L., Blumenthal, T., Meyer, B.J., Priess, J.R.,. (1997). Introduction to *C.elegans*. In C.elegans II, D. L. Riddle, Blumenthal, T., Meyer, B.J., Priess, J.R.,, ed.: Cold Spring Harbour Laboratory Press), pp. 1-22.

Robertson, A. P., Martin, R.J., (1993). Levamisole activated single-channel currents from muscle of the nematode parasite *Ascaris suum*. British Journal of Pharmacology *108*, 170-8.

Robertson, S. J., Pennington, A.J., Evans, A.M., Martin, R.J., (1994). The action of pyrantel as an agonist and an open channel blocker at acetylcholine receptors in isolated *Ascaris suum* muscel vesicles. European Journal of Pharmacology *271*, 273-82.

Robertson, A. P., Bjorn, H.E., Martin, R.J., (1999). Resistance to levamisole resolved at the single-channel level. The FASEB Journal *13*, 749-60.

Rohrer, S. P., Birzin, E.T., Eary, C.H., Schaeffer, J.M., Shoop, W.L., (1994). Ivermectin binding in sensitive and resistant *Haemonchus contortus*. Journal of Parasitology *80*, 493-97.

Roos, M. H., Kwa, M.S.G., Grant, W.N. (1995). New genetic and practical implications of selection for anthelmintic resistance in parasitic nematodes. Parasitology Today *11*, 148-50.

Saedi, M., Conroy, W.G., Lindstrom, J. (1991). Assembly of Torpedo acetycholine receptor in *Xenopus* oocytes. Journal of Cell Biology *112*, 1007-15.

Sangster, N. C., Prichard, R.K., Lacey, E. (1985). Tubulin and benzamidazole resistancein *Trichstrogylus colubriformis* (Nematoda). Journal of Parasitology *71*, 645-51.

Sangster, N. C., Davis, C.W., Collins, G.H., (1991). Effect of cholinergic drugs on longitudinal contraction on levamisole-susceptible and -resistant *Haemonchus contortus*. International Journal for Parasitology *21*, 689-95.

Sangster, N. (1996). Pharmacology of anthelmintic resistance. Parasitology *113*, S201-16.

Sangster, N. C., Bannan, .C., Weiss, A.S., Nulf, S.C., Klein, R.D., Geary, T.G., (1999). *Haemonchus contortus*: sequence heterogeneity of internucleotide binding domains from P-glycoproteins and an association with avermectin/milbemycin resistance. Experimental Parasitology *91*, 250-57.

Sangster, N. C., Gill, J., (1999). Pharmacology of anthelmintic resistance. Parasitology Today *15*, 141-46.

Sasaki, Y., Kitagawa, H. (1993). Effects of milbrmycin D on microfilarial number and reproduction of *Dirofilaria immitis* in dogs. Journal of Veterinary Medical Science *55*, 763-9.

Schaeffer, J. M., Haines, H.W., (1989). Avermectin binding in *Caenorhabditis elegans*. A two state model for the avermectin binding site. Biochemical Pharmacology *38*, 2329-38.

Schallig, H. D. F. H., Van Leeuwen, M.A.W, Cornelisen, A.W.C.A. (1997). Protective immunity induced by vaccination with two *Haemonchus contortus* excretory secretory proteins in sheep. Parasite Immunology *19*, 447-453.

Schallig, H. D. F. H. (2000). Immunological responses of sheep to *Haemonchus contortus*. Parasitology *120*, S63-S72.

Sharma, R. L., Bhat, T.K., Dhar, D.N., (1988). Control of sheep lungworm in India. Parasitology Today *4*, 33-36.

Shoop, W. L. (1993). Ivermectin Resistance. Parasitology Today *9*, 154-59.

Sigel, E., Baur, R., (1987). Effect of avermectin B1a on chick neuronal γ-aminobutyrate receptor channels expressed in *Xenopus* oocytes. Molecular Pharmacology *32*, 749-752.

Smith, G. B., Olsen, R.W., (1995). Functional domains of $GABA_A$ receptors. Trends in Pharmacological Sciences *16*.

Smith, M.M., Warren, V.A., Thomas, B.S., Brochu, R.M., Ertel, E.A., Rohrer, S., Schaeffer, J., Schmatz, D., Petuch, B.R., Tang, Y.S., Meinke, P.T., Kaczorowski, G.J., Cohen, C.J. (2000) Nodulosporic acid opens insect glutamate-gated chloride channels: identification of a new high affinity modulator. Biochemistry *39*, 5543-5554

Smyth, J. D. (1994). Introduction to animal parasitology, 3rd Edition.

Spector, D. L., Goldman, R.D., Leinwand, L.A. (1998). Gene expression systems - using nature for the art of expression, Volume 1: Coldspring Harbor Laboratory Press.

Squire, M. D., Tornoe, C., Baylis, H.A., Fleming, J.T., Barnard, E.A., Sattelle, D.B., (1995). Molecular cloning and functional co-expression of a *Caenorhabditis elegans* nicotinic acetylcholine receptor subunit (acr-2). Receptors and Channels *3*, 107-115.

Stephenson, F. A. (1995). The $GABA_A$ receptor. Biochemical Journal *310*, 13-21.

Steel, J.W. (1993) Pharmacokinetics and metabolism of avermectin in livestock. Veterinary Parasitology *48*, 45-57

Sutherland, I. H., Campbell., W.C. (1990). Development, pharmacokinetics and mode of action of ivermectin. Acta Leidensia *59*.

Taylor, P.M., Connolly, C.N., Kittler, J.T., Gorrie, G.H., Hosie, A., Smart, T.G., Moss, S.J. (2000) Identification of residues within $GABA_A$ receptor α subunits that mediate specific assembly with receptor β subunits. The Journal of Neuroscience *20* 1297-1306

Thamsborg, S. M., Roepstorff, A., Larsen, M., (1999). Integrated and biological control of parasites in organic and conventional production systems. Veterinary Parasitology *84*, 169-186.

Thomas, J. H., Lockery, S. (1999). Neurobiology. In *C.elegans*: A practical approach, I. A. Hope, ed.: Oxford University Press), pp. 143-179.

Treinin, M., Chalfie, M. (1995). A mutated acetylcholine receptor subunit causes neuronal degeneration in *C.elegans.* Neuron *14*, 871-77.

Unwin, N. (1993). Nicotinic acetylcholine receptor at 9 A resolution. Journal of Molecular Biology *229*, 1101-24.

Unwin, N. (1995). Acetylcholine receptor channel imaged in the open state. Nature *373*, 37-43.

Urquhart, G. M., Jarrett, W.F.H., Jennings, F.W., MacIntyre, W.I.M., Mulligan, W., (1966). Immunity to *Haemonchus contortus* infection. Relationship between age and successful vaccination. American Journal of Veterinary Research *27*, 1645-1648.

van den Bossche, H., Roshette, F., Horig, C., (1982). Mebendazole and related anthelmintics. Advances in Pharmacology and Chemotherapy *19*, 67-128.

van Wyk, J. A., Malan, F.S. (1988). Resistance of field strains of Haemonchus contortus to ivermectin, closantel, rafoxanide and the benzamidazoles in South Africa. Veterinary Research *123*, 226-8.

van Wyk, J. A., Malan, F.S., Randles, J.L., (1997). How long before resistance makes it impossible to control some field strains of *Haemonchus contortus* in South Africa with any of the modern anthelmintics? Veterinary Parasitology *70*, 111-122.

van Wyk, J. A., Stenson, M.O., Van der Merwe, J.S., Vorster, R.J., Viljoen, P.G. (1999). Anthelmintic resistance in South Africa: surveys indicate an extremely serious situation in sheep and goat farming. Onderstepoort journal of Veterinary Research *66*, 273-84.

Vassilatis, D. K., Elliston, K.O., Paress, P.S., Hamelin, M., Arena, J.P., Schaeffer, J.M., Van Der Ploeg, L.H.T., Cully, D.F. (1997a). Evolutionary

relationship of the ligand-gated ion channels and the avermectin-sensitive glutamate-gated chloride channels. Journal of Molecular Evolution *44*, 501-08.

Vassilatis, D. K., Arena, J.P., Plasterk, R.H.A., Wilkinson, H.A., Schaeffer, J.M., Cully, D.F., Van der Ploeg, L.H.T. (1997b). Genetic and biochemical evidence for a novel avermectin-sensitive chloride channel in *Caenorhabditis elegans*. The Journal of Biological Chemistry *272*, 33167-74.

Wall, R., Strong, L., (1987). Environmental consequences of treating cattle with the antiparasitic drug ivermectin. Nature *327*, 418-421.

Wallace, B., Qu, Z., Huganir, R., (1991). Agrin induces phosphorylation of the nicotinic acetylcholine receptor. Neuron *6*, 869-78.
Waller, P. J. (1997). Anthelmintic resistance. Veterinary Parasitology *72*, 391-412.

Waruiru, R. M., Kogi, J.K., Weda, E.H., Ngotho, J.W., (1998). Multiple anthelmintic resistance on a goat farm in Kenya. Veterinary Parasitology *75*, 191-97.

Watson, D. L., Colditz, I.G., Andrew, M., Gill, H.S., Altmann, K.G., (1994). Age-dependent immune response in Merino sheep. Research in Veterinary Science *57*, 152-158.

Whitfield, P. J. (1993). Parasitic helminths. In Modern Parasitology, F. E. G. Cox, ed.: Blackwell Scientific Publications), pp. 24-52.

W.H.O. (1998). Dracunculus eradication: W.H.O., pp. 1-3.

W.H.O. (1999). Lyphatic Filariasis: W.H.O., pp. 1-5.

W.H.O. (2000). Onchocerciasis (River Blindness): W.H.O., pp. 1-6.

Wiley, L. J., Weiss, A.S., Sangster, N.C., Qun Li (1996). Cloning and sequence analysis of the candidate nicotinic acetylcholine receptor alpha subunit receptor gene tar1 from *Trichostrongylus colubriformis*. Gene *182*, 97-100.

Withers, P. C. (1992). Comparative Animal Physiology, International Edition: Saunders College Publishing).

Witty, M. J. (1999). Current strategies in the search for novel antiparasitic agents. International Journal for Parasitology *29*, 95-103.

Xu, M., Molento, M., Blackhall, W., Ribeiro, P., Beech, R., Prichard, R. (1998). Ivermectin resistance in nematodes may be caused by alteration of P-glycoprotein homolog. Molecular and Biochemical Parasitology *91*, 327-35.

Zheng, Y., Brockie, P.J., Mellem, J.E., Madsen, D.M., Maricq, A.V. (1999). Neuronal Control of locomotion. Neuron *24*, 347-361.

Appendix 1

Amino acid identities of GluCl receptor subunits (%)

	GluCl β	HG4	Gbr2a	Gbr2b	HG2	HG3	GluCl X	HG5	C27h5.5	GluCl α1	GluCl α2s	GluCl α2l	GluCl α3	GluCl α
GluCl β		80	48	47	46	48	57	43	39	45	47	47	50	44
HG4			48	47	45	48	53	43	38	47	46	46	47	42
Gbr2a				79	79	74	81	62	41	57	57	57	60	52
Gbr2b					72	87	88	57	40	54	54	55	58	50
HG2						75	81	55	37	52	53	54	55	45
HG3							88	56	40	54	55	55	59	49
GluCl X								66	55	63	63	68	68	55
HG5									44	56	65	55	53	48
C27h5.5										38	38	38	40	37
GluCl α1											77	77	60	46
GluCl α2s												96	66	48
GluCl α2l													67	50
GluCl α3														47

Key: H.contortus C.elegans O.volvulus D.immitis

Appendix 2

Map of pCRBlunt II TOPO vector

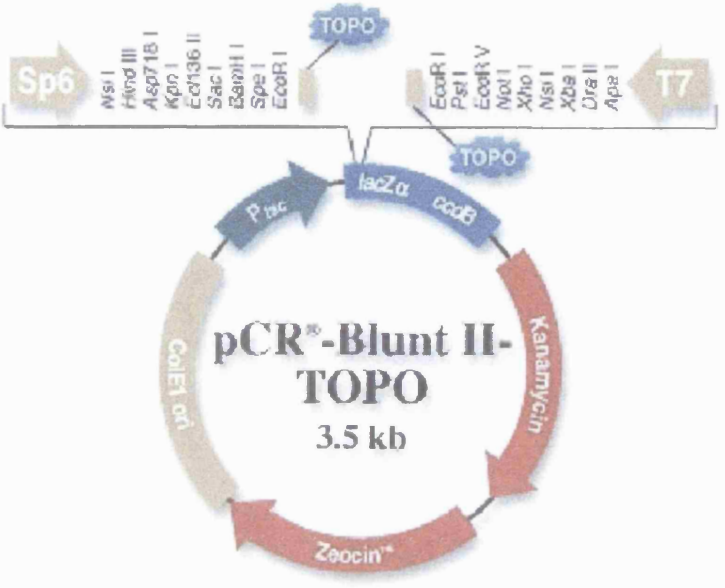

Appendix 3

Map of pBluescript II vector

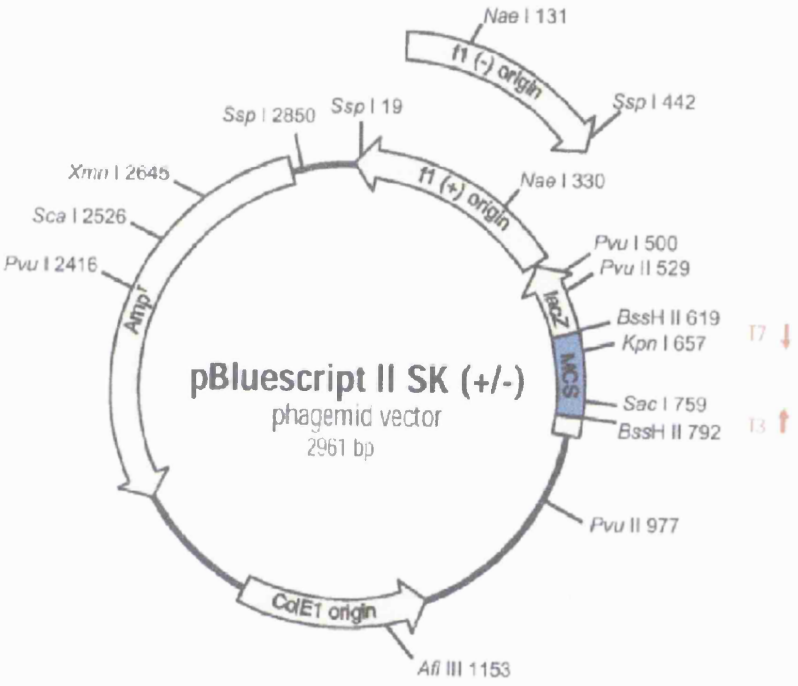

Appendix 4

RT-PCR and sequencing primer sequences and melting temperatures

Primer	Sequence	Calculated Tm °C
5HG2full	5' GCATGCGCAATTCC GTCCCTC 3'	55
3HG2full	5' GCTTCACATCAAGTA GACAGCC 3'	52
5HG5full	5' GACACTAATGTTCG CCTTAATTCTGC 3'	53
3HG5full	5' TCATTCCAACTGCG CTTGbAC 3'	50
M13 forward	5' GTAAAACGACGGCC AG 3'	50
M13 reverse	5' CAGGAAACAGCTAT GAC 3'	50
HG2seq	5' CGCCAGACATACGC CAATC 3'	53
5HG5seq	5' GATATCGATACTCC GAACAT 3'	48
3HG5seq	5' CTGACGTACAATTAC CGGTT 3'	50
5IVRseq	5' CGATTATCCGCTTGA TGTACAGAC 3'	56
3IVRseq	5' CATCCGTATTCTAT GTCTTTCG 3'	51
5HG3part	5' AGTTGTGCTCGGGT CAAACTTC 3'	55
3HG3part	5' ATACGCATTTCGACC CAACATATC 3'	54
5HG4part	5' GTCATAGCGGCCGC GATCTTGAATGTCACAGT ATA 3'	65
3HG4part	5' ACCGGTGGCAGTTT AGCATTGA 3'	55

Appendix 5

Neighbour-joining tree illustrating the relationship between the *C.elegans* and *H.contortus* GluCl subunits

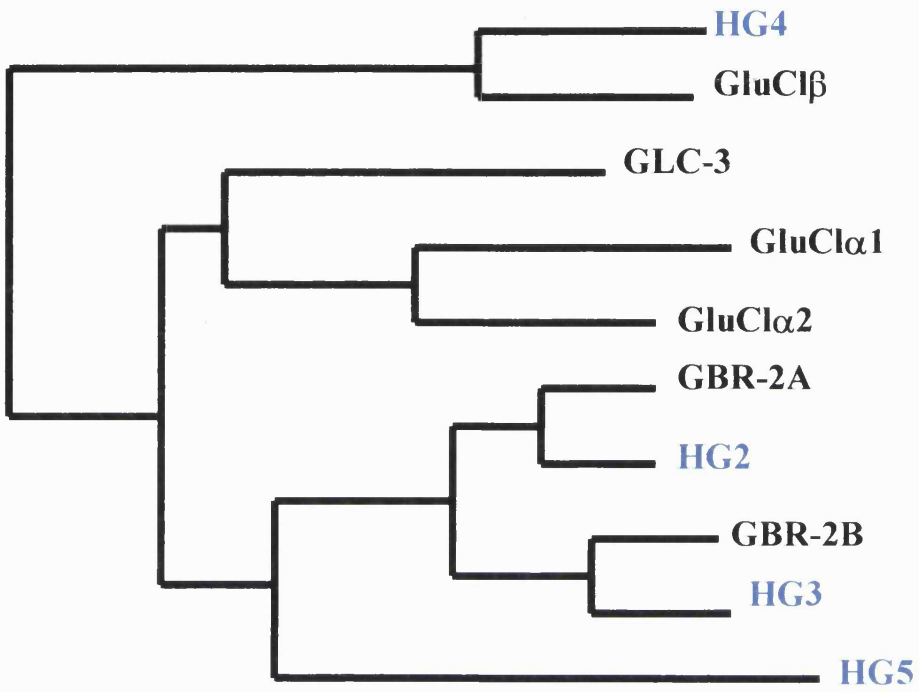

Appendix 6

Map of the mammalian expression vector pcDNA3

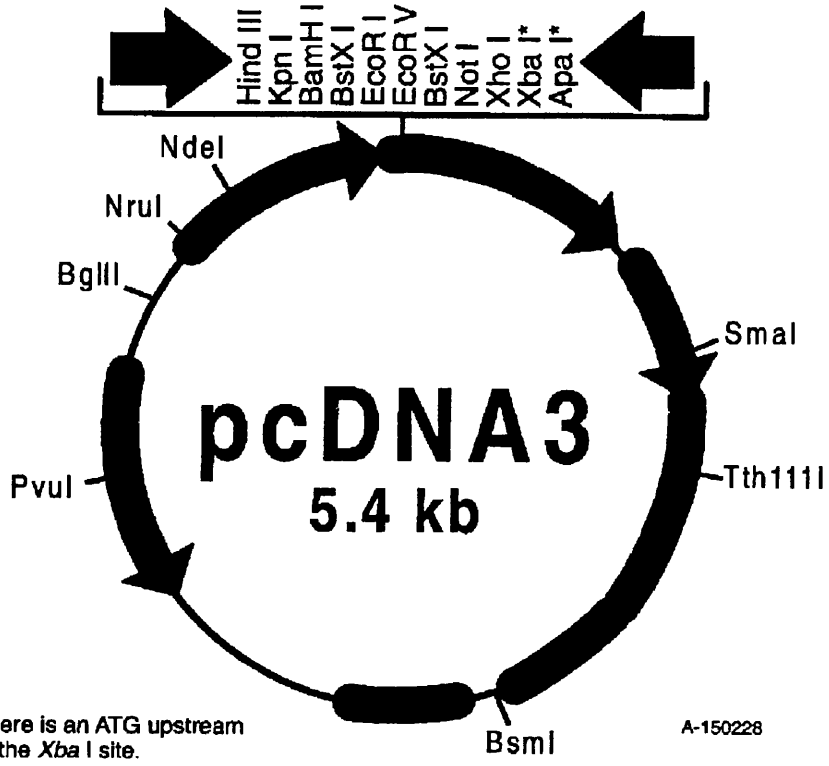

I would like to thank my supervisor Dr. Adrian Wolstenholme for his help and support throughout my PhD. Also, thank you to my industrial supervisors Dr. Ken Gration and Dr. Debra Woods for their help above and beyond the call of duty. Huge thanks also go to Dr. Jane Eastlake and Dr. Momna Hejmadi, whose knowledge and patience got me through those first rocky months! To all members of lab 0.47 past and present, I first have to apologise for my incredible capacity to talk and then thank you all for putting up with me and helping me along the way. To all the friends I have made in Bath, especially Samantha Jarrold, Sarah Backen and Alison Gibbard, thanks for your friendship, sympathetic ear and party spirit!
To my parents, an invaluable source of strength and inspiration, and to my husband, Michael, who supported me through the agonies and ecstasies of postgraduate life and still married me at the end, words are not enough!

This research was funded by a BBSRC-CASE award with Pfizer Global Research and Development.

Abbreviations

AM	Avermectins/Milbemycins
bp	base pairs
B.C.	Biological Control
BSA	Bovine Serum Albumin
CMV	Cytomegalovirus
cDNA	Copy Deoxyribonucleic acid
DEPC	diethyl pyrocarbonate
DIG	Digoxygenin
DMEM	Dulbecco's Modified Essential Medium
DNA	Deoxyribonucleic Acid
DNase	Deoxyribonuclease
dNTP	Deoxyribonucleoside triphosphate
DTT	Dithiothreitol
DYT	Double Yeast Tryptone
EDTA	Ethylenediaminetetracetic acid
EMBL	European Molecular Biology Laboratory
FBS	Foetal Bovine Serum
FITC	Fluorescein isothiocyanate
GABA	γ-aminobutyric acid
GFP	Green Fluorescent Protein
GluCl	Glutamate-gated chloride channel receptor
HEPES	N-[2-Hydroxyethyl] piperazine-N'-[2-ethanesulfonic acid]
IVR	Ivermectin Resistant
IVS	Ivermectin Sensitive
kb	kilobase pairs
kDa	kilo Daltons
LB	Luria Bertani
LGIC	Ligand-gated ion Channel
MEM	Minimal Essential Medium
MOPS	(N-morpholino)propanesulfonic acid
mRNA	messanger ribonucleic acid
nAChR	nicotinic Acetylcholine receptor
O.D.	Optical Density
PBS	Phosphate-buffered saline
PCR	Polymerase Chain Reaction
PMSF	(4-bromo) phenylmethylsuphonyl fluoride
Pwo	*Pyrococcus wosei*
RACE	Rapid Amplification of cDNA Ends
RT-PCR	Reverse Transcription-Polymerase Chain Reaction

RNA	Ribonucleic Acid
RNase	Ribonuclease
SDS	Sodium Dodecyl Sulphate
Taq	*Thermus aquaticus*
TAE	Tris Acetate EDTA
TBE	Tris Borate EDTA
TEMED	N, N, N', tetramethylethylenediamine
TM	Transmembrane domain
Unc	uncoordinated
UV	Ultraviolet
Tfl	*Thermus flavus*

Publications

Cheeseman, C.L., Delany, N.S., Woods, D.J., Wolstenholme, A.J., (2001) High-affinity ivermectin binding to recombinant subunits of the *Haemonchus contortus* glutamate-gated chloride channel. Molecular and Biochemical Parasitology *114* (2): 161-68

Jagannathan, S., Laughton, D.L., Critten, C.L., Skinner, T.M., Horoszok, L., Wolstenholme, A.J., (1999) Ligand-gated chloride channel subunits encoded by the *Haemonchus contortus* and *Ascaris suum* orthologues of the *Caenorhabditis elegans gbr-2 (avr-14)* gene. Molecular and Biochemical Parasitology *103*: 129-40.

Critten C.L., and Wolstenholme, A.J., (2000) Ivermectin binds to recombinant nematode glutamate-gated chloride channels with high affinity. European Journal of Neuroscience *12* (S11):44.

Critten C.L., and Wolstenholme, A.J., (2000) High affinity ivermectin binding to recombinant nematode glutamate-gated chloride channels. Oxford 2000. 18-22 September.